

# **Development of a Rotational Shear Vane for use in Avalanche Safety Work**

**M. Halsegger**

**Department of Mechanical Engineering  
University of Canterbury  
New Zealand**

**2007**

**For Matthew Davies**

## Acknowledgements

There are many people who deserve mention for adding to this project and helping me with my work. However, I am particularly grateful to my Supervisor, Keith Alexander for his calm thoughtful guidance and innovative design expertise. Your input has been truly valuable to me.

Thankyou to Arthur Tyndall and Sonia Mellish who have been excellent sources of motivation and ideas. Many thanks to the workshop team, in particular Julian Murphy for putting together a fine prototype and putting up with my constant time pressure. Without his efforts the project would not have been a success.

Thanks to Broken River and the many staff who supported me. A particular thanks to Lorrie Frankcom for allowing me to test during work hours and Henriette Beikirch for helping me with testing.

Finally thanks to Ed Evans and Matthew Davies for the work they completed on this project. Your work has been an invaluable resource to me.

## **Abstract**

This Masters Thesis describes the continuation of the Snow Probe development. The focus of this project was to establish the rotational shear vane as a useful tool in avalanche safety work as well as develop a robust method for measuring the applied torque.

A new and novel way of measuring the torque on a rotational shear vane has been developed to illustrate its effectiveness. The new system measures the power supplied to a cordless drill to get an indication of the applied torque. This was done because it was found that the earlier method of using a strain gauge/cantilever system repeatedly failed to work, largely due to complexity.

The snow probe in its present embodiment has been shown to provide a good clear indication of the snow profile under easily repeated circumstances. Shear strength results are at this stage not sufficiently for reliable quantitative results. However the probe in its present form is able to give pictorial impressions of the snow pack that compare well to current hand hardness profiles derived from snow pit methods. Even in its current form the snow probe is able to collect useful snow profile data in a matter of minutes, much quicker than conventional snow pit methods.

A loose relationship was found to exist between the approach angle of a shear vane blade and the clarity of the snow profile. These relationships are relatively inaccurate at present due to lack of rotational velocity data and therefore approach angle data. It is believed that the addition of a rotation counter would greatly increase the accuracy of the probe results and enable a shear strength profile to be quantified.

Further developments and testing are underway with a view to forming a company around the snow probe.

## Table of Contents

1	Introduction .....	8
1.1	Project Motivation.....	8
1.2	Project History .....	9
1.2.1	Initially.....	10
1.2.2	Prototype 1 .....	10
1.2.3	Project Status March 2006 .....	11
1.2.4	Project Overview .....	12
1.3	Scope of Masters Thesis .....	12
2	Avalanches.....	13
2.1	Avalanche Types .....	13
2.1.1	Dry Slab Avalanches .....	13
2.1.2	Wet Slab Avalanches .....	13
2.1.3	Loose Snow Avalanches .....	14
2.2	Snow .....	14
2.2.1	Crystal Formation.....	14
2.2.2	Crystal Morphology.....	15
2.2.3	Surface Hoar Formation.....	15
2.2.4	Temperature Gradients.....	16
2.3	Snow Stability .....	16
2.3.1	Spatial variability of shear strength.....	17
2.4	Shear strength tests.....	18
2.4.1	Shear frame test.....	18
2.4.2	Quantified Loaded Column Stability Test (QLCT).....	19
2.4.3	Rotary Shear Vane.....	19
2.5	Current Snow Probes.....	19
2.5.1	Snow Micro Pen (SMP).....	19
2.5.2	Capacitec Snow Sonde.....	20
3	Initial Design Developments 2006.....	22
3.1	Prototype 1 Developments.....	22

3.1.1	Amplifier Insert.....	23
3.1.2	Modified Vane Placement .....	25
3.1.3	Addition of Bluetooth.....	25
3.2	Prototype 2.....	26
3.2.1	Batteries .....	26
3.2.2	Electrical Configuration.....	27
4	Testing 2006.....	29
4.1	Testing Sites .....	29
4.2	Preliminary Testing.....	30
4.2.1	Prototype 2 Results.....	31
4.2.2	Prototype 1 Results.....	33
4.2.3	Problems Encountered.....	34
5	Design Developments on Prototype 2 between November 2006 and June 2007	38
5.1	Electrical Modifications .....	38
5.2	Mechanical Modification .....	40
6	Calibration.....	41
6.1	Voltage and Current Calibration.....	41
6.2	Power to Torque Calibration Method .....	44
6.2.1	Test Variable Combinations .....	47
6.3	Torque to Shear Strength Calculation.....	48
7	Testing 2007.....	50
7.1	Testing Methods: 2007.....	50
7.1.1	Snow Profile.....	50
7.1.2	Shear Frame Test.....	51
7.1.3	Shear Vane Test .....	51
7.2	Austrian Test Results .....	54
7.3	New Zealand Test Results.....	58
7.3.1	Snow Pack Characteristics.....	58
7.3.2	Test Sites.....	59
7.3.3	Layer Identification .....	60
7.3.4	Range Finder.....	63
7.3.5	Minimum Shear Strength Lines .....	65
7.3.6	Results .....	65

7.3.7	Discussion .....	87
8	Conclusions .....	91
9	Future Research and Developments.....	92
9.1	Rotation Counter .....	92
9.2	Depth Sensor .....	92
9.3	Calibration .....	93
9.4	Industrial Design Aspects .....	93
10	References.....	1
11	Appendix A: Prototype 1 Modification Drawings .....	97
12	Appendix B: Electrical Diagrams .....	105

# 1 Introduction

## 1.1 *Project Motivation*

The idea of a rotational shear vane to measure shear strength is not a new one. A simple device was tested by Keeler and Weeks, U.S. Army Cold Regions Research and Engineering Laboratory in the 60's (Keeler and Weeks 1967; Keeler and Weeks 1968). However since then no significant progress had been made on a rotational type shear measurement device.

In 1992 a large avalanche on Broken Rover Ski Area took the life of one staff member. This prompted Arthur Tyndall, a structural engineer to take an interest. Current snow stability assessment methods require a huge amount of operator knowledge and experience to interpret test results. Arthur's initial goal was to create a way of recording more precise data, to remove some of the guess work from snow stability assessments. Civil engineers have been using a simple shear vane for decades to sample soil strengths. Shear strength is also one of the main factors contributing to slab avalanche release. Therefore it was a logical step for Arthur to attempt to build a rotational shear vane.



## 1.2 Project History

This project has been through 3 main development stages which are summarised in Figure 1.1 below.

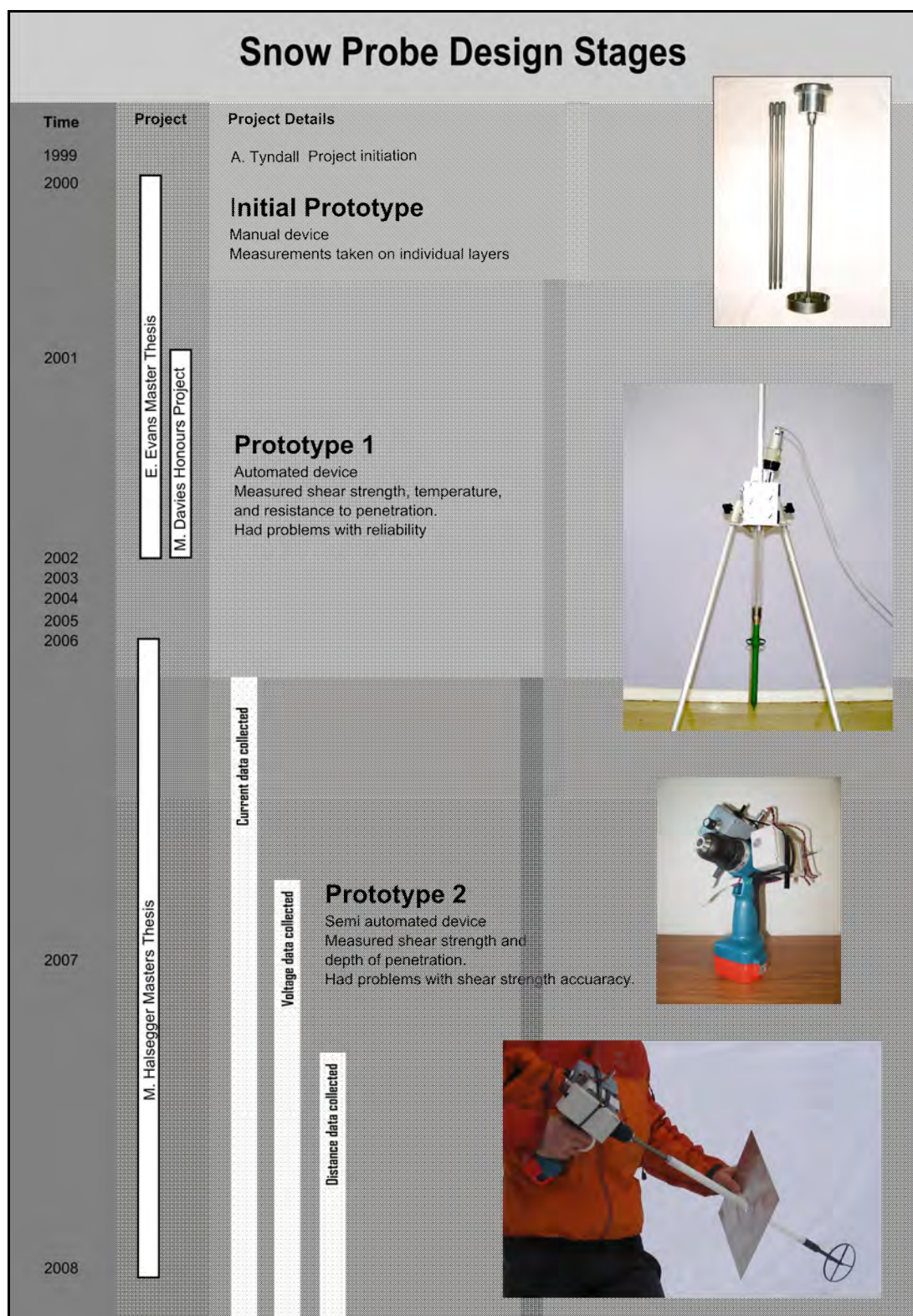


Figure 1.1 Overall probe time frame showing the 3 stages of development between 2000 and 2008.

### **1.2.1 Initially**

Initially Arthur Tyndall used a simple modified soil sampler (Figure 1.2) attempting to determine its viability as a snow measurement device. The project was then passed on to the University of Canterbury's engineering department in 2000 where Edward Evans completed a Masters project on the topic (Evans 2002).

The initial prototype had some problems. It was often difficult to locate the desired layer in the snow pack. There were also a host of difficulties associated with the instrument head and measuring device. However some good data was obtained, providing the justification for a new prototype.



**Figure 1.2 The Initial Snow Probe.**

### **1.2.2 Prototype 1**

This was a much more complex snow probe. The probe attempted to measure, resistance to penetration, temperature and shear strength (Figure 1.3, Figure 1.4). This was an ambitious task for an early prototype of a single probe.

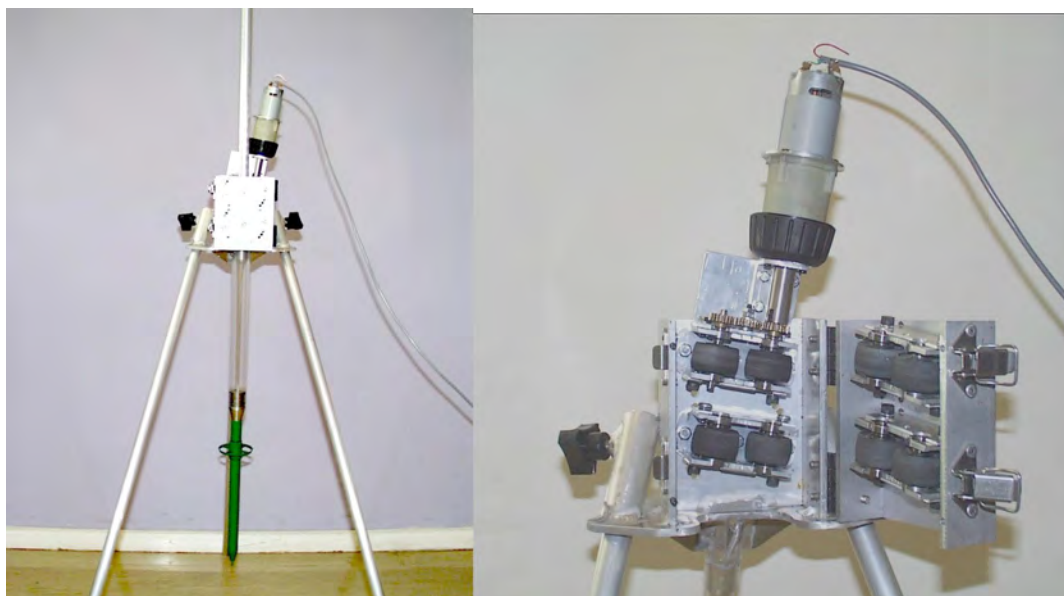


**Figure 1.3 the complete 1<sup>st</sup> prototype (left) and the drive mechanism (right).**

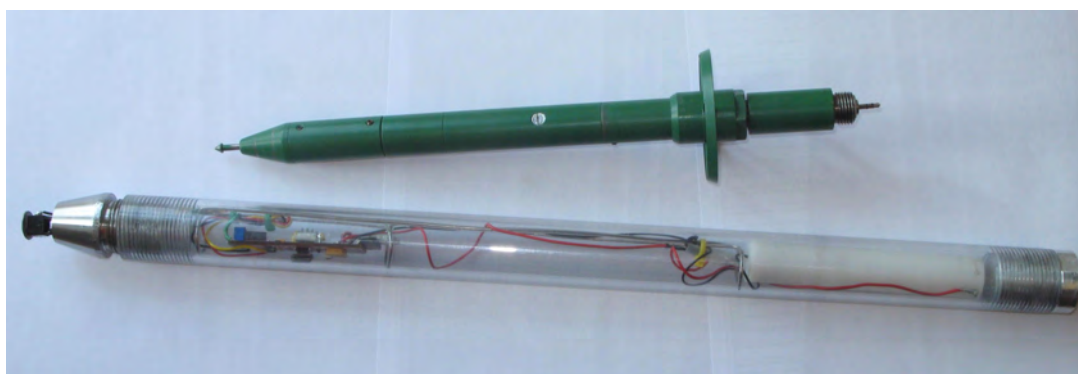


**Figure 1.4 Prototype 1, Shear penetrometer system.**

The shear module used a cantilever strain gauge system to measure the applied torque. The temperature module used two thermocouples embedded in silicon to measure the temperature. The force module used a highly sensitive Honeywell piezoelectric force sensor. The transmitter module contained a control module, a radio transmitter and two AA batteries. The drive mechanism used a cordless drill motor driving a set of rubber rollers to rotate and push the probe into the snow.

### **1.2.3 Project Status March 2006**

No significant testing was done on the first prototype before the end of the project. The snow probe was subsequently handed to Matthew Davies as part of his Honours degree. The probe underwent some modification, calibration and testing during 2002 with Matthew Davies. The testing was however made difficult with frequent breakages and electrical failures. Results from these tests were not conclusive.



#### **1.2.4 Project Overview**

The present project went through 3 development phases over 3 winters. This has been illustrated in the lower 3<sup>rd</sup> of Figure 1.1. Prototype 2 is a drill where power input properties are measured to determine a measure of the output torque and hence enable an estimation of snow shear strength.

Prototype 1 was investigated in the early stages of this project but was then set aside in favour of prototype 2. The focus of this project and report is therefore on prototype 2 which went through 3 stages of development. In each stage another stream of data is added.

Initially only current data was collected from prototype 2. This was tested in New Zealand between July and September 2006. A voltage measurement was then added for testing completed in Austria during February and March 2007. Finally the depth of penetration was measured in tests done between June and September 2007 in New Zealand.

Each stage gives more insight to the actual snow properties than the last. The reader will therefore note that data display methods develop over the course of the project.

### **1.3 Scope of Masters Thesis**

This project focuses on providing evidence that the rotational shear vane in a probe form, can provide a sufficiently accurate shear strength profile to be useful in avalanche safety work. The probe will be evaluated against an industry standard method for measuring shear strength, namely the manual shear frame test and a standard hand hardness snow profile.

The project endeavours to find and test a simple and robust method for measuring the torque applied by the shear frame.

## **2 Avalanches**

The aim of this chapter is to provide a brief outline of avalanche failure mechanisms focussing primarily on shear strength aspects of avalanche release. A basic knowledge of Avalanches is assumed. More information can be obtained from texts such as McClung and Schaerer (2006) and Perla and Martinelli (1976).

### **2.1 Avalanche Types**

#### **2.1.1 Dry Slab Avalanches**

The dry slab avalanche is the single most dangerous form of avalanche in the alpine region. It is characterised by a thick, largely cohesive layer over a weak layer or interface. Instability develops when the downward component of weight exceeds the shear strength of the weak layer. A dry slab avalanche also requires a high rate of deformation in the weak layer which allows rapid fracture propagation in the crown wall and shear layer. It is therefore extremely useful to know the shear strength of the weak layer as it is a fundamental condition for dry slab avalanches.

#### **2.1.2 Wet Slab Avalanches**

Wet slab avalanches are particularly relevant for New Zealand conditions. A wet slab avalanche will generally form due to one of 3 factors:

1. increased weight of the overlying snow pack due to rain,
  2. a change in the strength of the weak layer due to increased water content,
  3. or lubrication of the weak layer by water running down the layer surface
- (Figure 2.1).

This type of avalanche can be particularly dangerous as it is extremely heavy. The kinetic energy of the avalanche melts the snow during the fall allowing it to move rapidly but once stationary it is likely to re-freeze making rescue difficult.

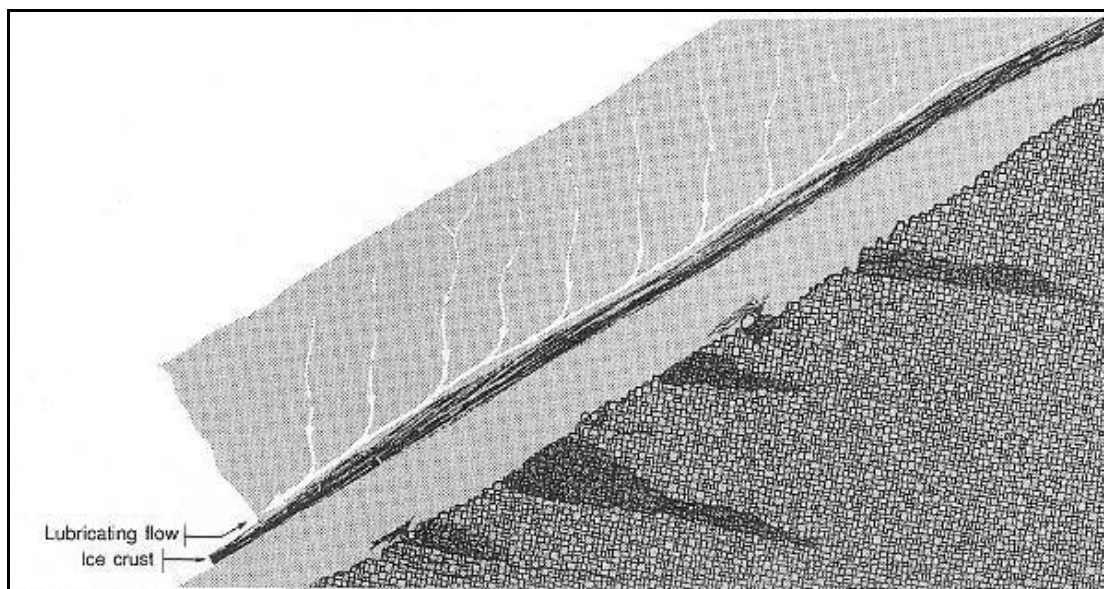


Figure 2.1 Wet snow lubrication (McClung and Schaerer 1993)

### 2.1.3 Loose Snow Avalanches

As with slab avalanches loose snow avalanches can be dry or wet. They are easily recognisable because of the point release initiation. They are triggered by metamorphism in the snow near the surface due to sun or rain. Local loss of cohesion results from deterioration of the snow properties, decreasing the static friction angle necessary to cause motion. This will often occur near rocky outcrops where the snow temperature is likely to increase rapidly under direct sun light. Wet loose snow avalanches are generally slow moving but can cause significant damage to roads or building. There is considerable force behind a wet avalanche and once motion stops crystals re-freeze making excavation difficult.

## 2.2 Snow

### 2.2.1 Crystal Formation

When the water vapour in a cloud is high enough the air becomes supersaturated and water tries to condense into water droplets. The water vapour is able to condense out on so called condensation nuclei (salt, dust, or soil) to form water droplets. For water droplets to freeze, freezing nuclei (dust, soil and other chemical particles) are necessary. These have a slightly different chemical composition to condensation nuclei. Only at very low temperatures ( $-40^{\circ}\text{C}$ ) do water droplets freeze without

freezing nuclei. Without freezing nuclei water droplets can remain in a super cooled state.

Once an ice crystal forms it can grow in one of two ways:

- Direct transfer of water vapour from supercooled water droplets to the ice crystal. This happens as a result of the vapour pressure around the water droplet being higher than that around the ice crystal, causing diffusion of the water vapour to the ice crystal.
- As crystals move in the atmosphere (due to wind currents or gravity), the crystals inevitably collide with water droplets which then freeze on the crystal. This is called riming. Via this method the crystal becomes heavier without increasing its air resistance because the ice freezes in a much denser manner. The end effect, depending on temperature, the time and distance the crystal travelled through the cloud is graupel, or in the case of a melt freezing process hail.

### **2.2.2 Crystal Morphology**

Newly fallen crystals vary in shape largely depending on the temperature and moisture content of the surrounding air. These range from column like crystals to dendritic star like crystals to warmer ball shaped corns. In general crystals degrade over time, increasing inter crystal bond strength. Warmer temperatures will cause finer dendritic type crystals to melt starting at the extremities. Freed water vapour and liquid causes rounding of crystals. This is also associated with a reduction in snow pack depth and an increase in snow hardness. Crystal degradation is associated with increased snow stability until too much water is freed, at which point the free water acts as a lubricant destabilising the snow pack.

Old snow crystals can also grow under certain conditions. Re-growth crystals grow in leafy planar type shapes, destroying inter crystalline bonding. Crystal growth in the snow pack is always associated with a decrease in stability. This type of re-growth is often present at the earth snow interface when a temperature gradient is present (ground warm, snow cold).

### **2.2.3 Surface Hoar Formation**

Surface hoar is particularly relevant to this project as it forms particularly weak layers when buried. Surface hoar is a type of re-growth crystal which forms when the

snow surface temperature drops below the dew point temperature of the surrounding air. Favourable conditions for crystal growth are predominantly at night in the absence of solar radiation and when the air humidity is high. Crystals grow vertically and remain upright making them prone to collapse with small disturbances. Crystals often take the form of a fan shape, two dimensional crystals, feathery trees, regular plates or slender spikes depending on atmospheric conditions (Foehn 2001). Crystals can grow up to 10cm in length and remain in a snow pack for several weeks or even months.

Surface hoar layers provide ideal slip plains due to the planar shape of the crystals. When a layer collapses, energy is released creating a large and rapidly spreading slab avalanche.

#### **2.2.4 Temperature Gradients**

On most ski fields snow is only present during the winter. The ground will therefore warm up during summer and store heat over the winter. The snow is bounded by the ground underneath and by the air above. The ground will generally stay at or close to 0°C while the air will generally have a lower average temperature. This creates a temperature gradient which can cause re-growth crystals to form near the base of the snow pack. As the snow close to the base warms and degrades water vapour is released which subsequently rises and re-freezes on colder higher up crystals. This process is similar to that of surface hoar. The crystals form large leaf-like crystals with very low cohesion. This significantly decreases the strength of the snow and can often be the cause of an avalanche initiation. Even a low level of crystal re-growth can cause deeply buried layers to turn into a coarse sandy consistency which easily falls out when disturbed.

### **2.3 Snow Stability**

Snow stability refers to the likelihood of an avalanche initiation given current snow conditions. “Stability is defined as the ratio of resistance to failure versus the forces acting toward a failure...” (McClung and Schaerer 1993). Snow failure can occur when the slope parallel downward forces exceed the resisting shear forces of the snow. In dry loose snow avalanches the gravitational forces on the grains and the frictional forces between the grains determine the stability of the snow. In slab avalanches the critical shear strength is in the weakest layer interface. The stability of



the snow pack is then largely a function of the weight of the overlying snow and the strength of the weakest layer interface.

Determination of snow stability is best done by loading the snow pack of interest until failure occurs. Due the inherent danger, high variability of snow characteristics and limited time available it is often difficult to obtain accurate results. Several studies have concluded a single pit not to be representative of an entire slope (Conway and Abrahamson 1984; Jamieson and Johnston 2001; Birkeland, Kronholm et al. 2004; Logan, Birkland et al. 2005), More indirect methods are used such as knowledge of the snow pack history, weather, and terrain as well as empirical relationships relating various slopes or snow characteristics.

All information on snow characteristics can be useful but some types of information are more useful than others. Information types have been categorised into 3 classes (McClung and Schaerer 1993).

Class 3: Meteorological Factors refers to information collected from outside the snow pack and includes the amount of new snow, wind speed, wind direction, air temperature, solar radiation, humidity and condition of the snow surface.

Class 2: Snow Pack Factors refer to information obtained from within the snow pack such as snow pack depth; previous slope use; past avalanches; and snow pack structure such as hardness, texture, layering, crystal forms and free water content. This type of data is useful but it does not directly test the stability of the snow pack.

Class 1: Stability Factors are data that are directly related to the current snow stability. For example current avalanches, loading tests and fracture propagation and cracking of the snow cover.

It is often difficult to obtain class 1 information, particularly over a wide area and renowned start zones. An assessment of the snow stability is then made on information gathered from class 2 and 3 information. Stability estimates therefore rely on experience and generally include significant factors of safety.

### **2.3.1 Spatial variability of shear strength**

The spatial variability of the shear strength over a layer can be significant depending on the type of terrain is in question. Changes in angle, aspect or exposure will have a significant effect on the shear strength. It has also been shown that an even slope with no significant surrounding features or changes in angle can have significant spatial variability in snow shear strength (Conway and Abrahamson 1984). Several

studies have attempted to quantify spatial variability in shear strength and general snow stability (Birkeland 1995; Landry, Birkeland et al. 2004; Logan, Birkeland et al. 2005; Schweizer, Kronholm et al. 2006). So far these studies have been unable to determine why some times single pits or tests are representative of a slope and at other times not. From this one must conclude that the spatial variability of snow shear strength and stability is not completely understood. However from previous tests it is apparent that significant strength and stability variations can occur over short distances.

## **2.4 Shear strength tests**

A number of shear strength tests provide a qualitative estimate of the shear strength where the tester assigns a rating often between 1 and 5 to the shear strength of the weakest layer. These tests include the rutschblock, stuffblock and shovel shear tests. These tests are a valuable tool but for the purpose of this project a quantitative test is required. The shear frame test and the quantified loaded column stability test (QLCT) are currently the most widely accepted methods for obtaining a quantitative shear strength.

### **2.4.1 Shear frame test**

The shear frame test (Jamieson and Johnston 2001) is a widely accepted method for testing the shear strength of weak snow pack layers. The test uses a metal frame of between 0.1 and 0.5m<sup>2</sup> and generally 25mm high. The snow above the layer is removed, leaving 40-50mm of snow (See Figure 5.2). The frame is then placed in the snow, 2-5mm above the layer. Using a spring balance with a maximum force indicator, a smooth short pull is applied to the frame (usually <1s). The shear strength is calculated by dividing the pull force by the area of the frame. Due to the variability of the snow shear strength several tests (generally about 12 tests) are required to get the required confidence level.

A downside of this method is that it does not take into account the effect of the overlying snow burden and is therefore not an exact representation of the actual shear strength.

### **2.4.2 Quantified Loaded Column Stability Test (QLCT)**

A more recent method for testing the stability of weak layers in a snowpack is the QLCT which is explained in detail by Landry, Borkowski and Brown (2001). The advantage of this test is that it takes into account the overburden snow and should therefore theoretically give a more accurate representation of the snow stability. The test is however more complicated to carry out than the shear frame test.

### **2.4.3 Rotary Shear Vane**

The first thorough shear vane tests were carried out by Keeler and Weeks (1968). These tests used a simple vane based on a similar device used to measure soil shear strengths. Tests were done by inserting the vane vertically and in some cases horizontally into place above a snow layer of interest. The vane was then rotated at an approximate rate of 0.25Hz. A torque reading was obtained from a torque wrench used to apply the rotation.

Shear strength results appeared to be directly proportional to the variance of shear strength. A comparison between the shear vane and shear frame results suggested good correlation.

Problems existed with shear vane placement above the layer of interest. A layer in which shear strength varied significantly with depth was therefore susceptible to significant variability.

## **2.5 *Current Snow Probes***

### **2.5.1 Snow Micro Pen (SMP)**

The SMP was developed by Martin Schneebeli of the Swiss Federal Institute for Snow and Avalanche Research (SFISAR) and Jerry Johnson of the US Army Cold Regions Research and Engineering Laboratory.



**Figure 2.2 the SMP being tested.**

This is a vertically motor driven force penetrometer (Figure 2.2). The instrument records the resistance to penetration of a small conical tip. It has a high vertical resolution ( $4\mu\text{m}$ ) and high force resolution ( $0.005\text{N}$ ) (Johnson and Schneebeli 1997; Schneebeli and Johnson 1998; Schneebeli, Pielmeier et al. 1999; Birkeland, Kronholm et al. 2004).

The SMP provides a good digital hardness profile which theoretically can be used in a similar manner as a standard manual snow profile.

Its main drawbacks are that it has a small tip (60 degree cone with a 5mm diameter) which can fail to detect very thin weak layers.

### **2.5.2 Capacitec Snow Sonde**

The Capacitec snow sonde (Cognar 2007) was developed by Capacitec, a micro capacitor production company. The basic theory behind the probe is that snow has a capacitance which the probe is able to measure. Simply put this is done by using a small set of electrodes which put an electric field through the snow. Output voltages are measured and related back to density through an empirical relationship. This means that hardness values are gained by relating manually measured hardness in the snow profile to the output voltages. Currently accurate results require frequent calibration.

The Capacitec snow sonde (Cognar 2007) was developed by Capacitec, a micro capacitor production company. The basic theory behind the probe is that snow has a capacitance which the probe is able to measure. Simply put this is done by using a small set of electrodes which put an electric field through the snow. Output voltages

are measured and related back to density through an empirical relationship. This means that hardness values are gained by relating manually measured hardness in the snow profile to the output voltages. Currently accurate results require frequent calibration.

### **3 Initial Design Developments 2006**

Due to the unreliable nature of prototype 1 it was decided that a second concept would be designed and tested in parallel to the original. This would provide some redundancy to the testing program in case one of the concepts failed. The second concept, prototype 2 was largely independent of the first decreasing the possibility of wasting a winter season due to failures.

#### **3.1 Prototype 1 Developments**

Significant changes were necessary to the 1<sup>st</sup> prototype, considering that no conclusive data had been obtained due to frequent failures. It was decided from the outset to concentrate solely on the verification of the shear vane part of the snow probe. To do this the probe was made significantly simpler, reducing the likelihood of a technical failure. The thermocouple segment and the penetrometer segment were removed. Reasons for this are as follows:

- A penetrometer type device has in the past and still is undergoing research in other parts of the world. The most advanced of these is the SMP (Johnson and Schneebeli 1997; Schneebeli and Johnson 1998; Schneebeli, Pielmeier et al. 1999; Birkeland, Kronholm et al. 2004). The efforts of this project are therefore better spent on the shear vane.
- The thermo couples would present a further project and was deemed out side of the scope of this project.

The support frame and drive was also removed. At first it would seem that this would greatly decrease the accuracy of the probe. The penetrometer is heavily influenced by the rate of penetration and therefore required the support frame and guide. The rotational shear vane is more dependant on the rate of rotation than the rate of penetration. The need for the support frame and drive was therefore reduced. The reasons for its removal are:

- The probe will be easier to transport without the frame and therefore be more marketable.
- The reduction in accuracy this change brought about was not believed to be significant or detrimental to the usability of the data.

- Problems had been encountered associated with the frame and drive mechanism so it was believed that its removal would reduce the probability of technical failures in the field.

With these changes the probe now had only one function, the shear vane. Further changes needed to use as much of the remaining parts as possible to save on manufacturing time and expenses and also make the probe more reliable in the snow.

### 3.1.1 Amplifier Insert

One of the problems associated with the 1<sup>st</sup> prototype was the twisting of wires while assembling each section. Modules were connected via 2.5mm stereo plugs to allow modules to screw together. However assembling of the modules themselves still twisted the wires and left little room for extra wire. The shear vane module contains an amplifier circuit board to amplify the signal coming from the strain gauges (Figure 3.1). Initially the 2.5mm stereo plug was mounted in the amplifier housing so when the amplifier housing was screwed on to the shear vane, the wires connecting the amplifier and strain gauges twisted.

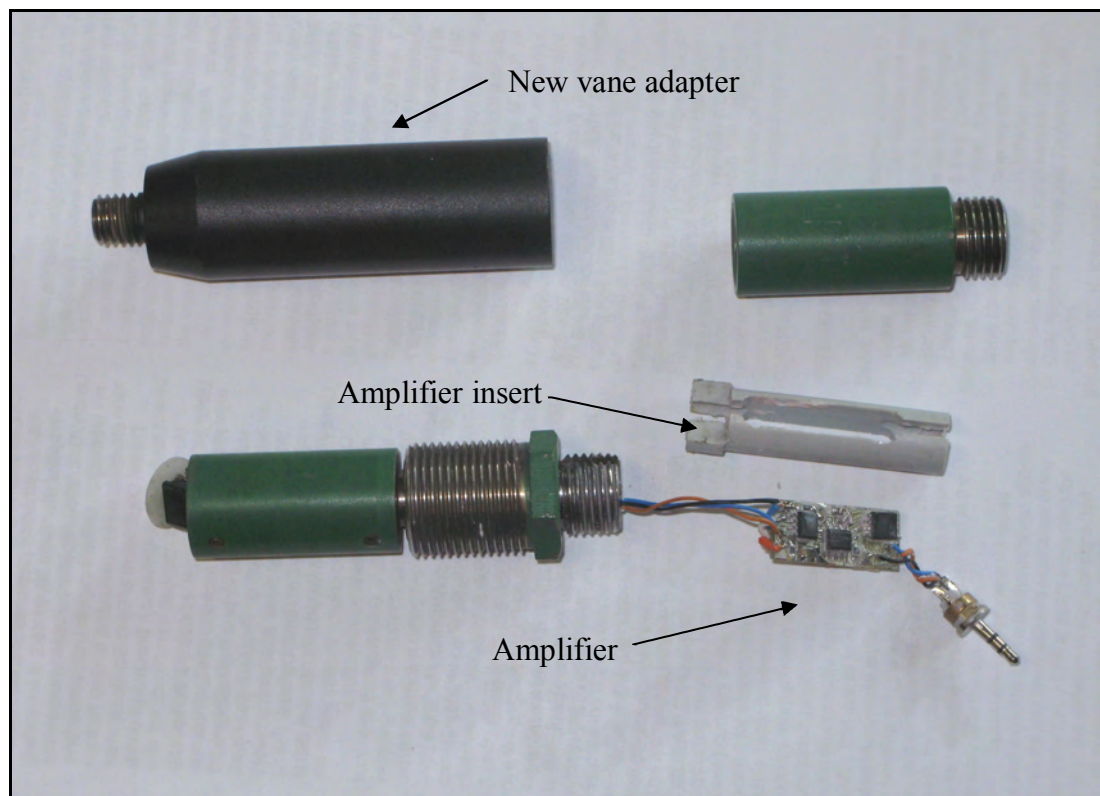
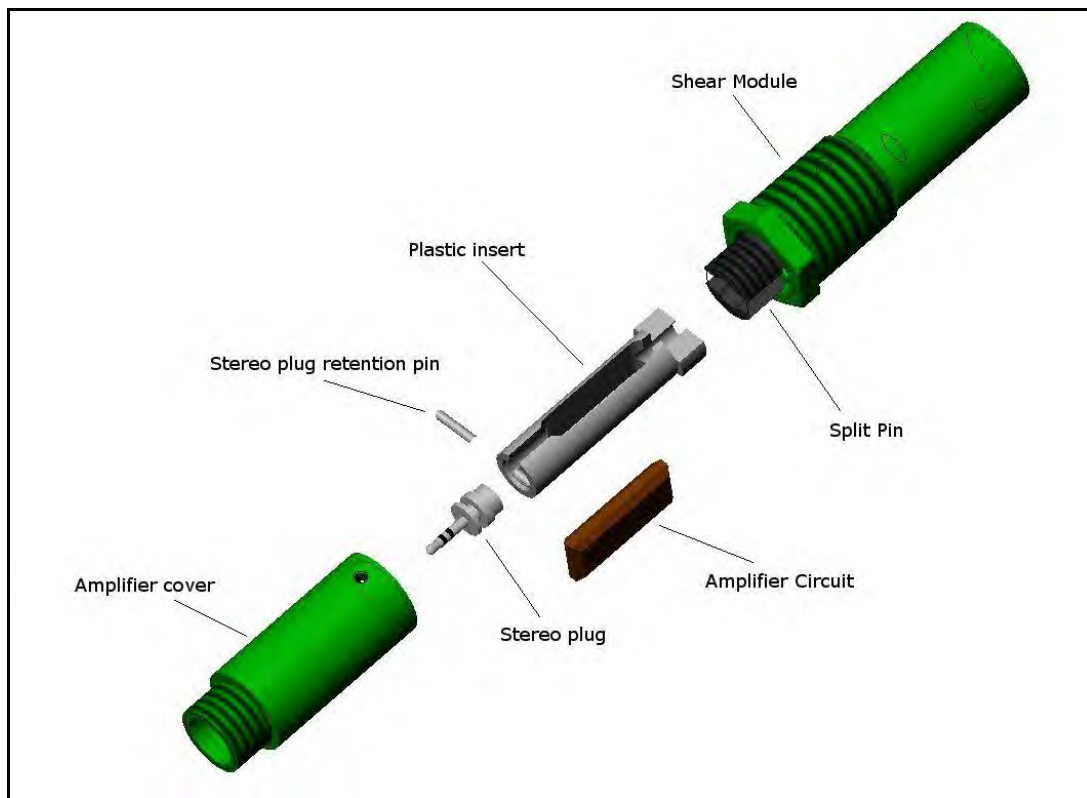


Figure 3.1 Shear vane module

Frequent problems with the strain gauges and amplifier unit meant that the housing needed to be removed often. Consequently the wires did not last long.

Another problem with this section was that the male side thread section on the split pin which connected to the amplifier cover (Figure 3.1). The two sides of the split pin were forced together when a moment or torque was applied to the probe. After a time the connection became loose, allowing the lower half of the probe to wobble.

To overcome these problems a plastic insert was designed and machined out of PETP Ertalyte TX (Figure 3.2).



**Figure 3.2 An expanded view of the shear module including the plastic insert.**

The plastic insert achieves several functions:

- To provide a fixture point independent of the amplifier cover for the 2.5mm stereo plug.
- To house and protect the amplifier circuit during disassembly and re-assembly.
- To keep the split pin from bending out of shape.

The flat surfaces depicted in Figure 3.2 near the shear module fit neatly between the two split pin surfaces, ensuring that the split pin is not pressed together under load. The stereo plug is held in place using a plastic pin. The gaps at the top and bottom of the plastic insert allow the stereo plug and amplifier circuit to be removed with out



needing to cut any wires. Finally the plastic insert can be filled with wax to protect the amplifier circuit from water. The wax can easily be melted out when repairs are required.

### 3.1.2 Modified Vane Placement

One of the problems with prototype 1 was that its shear vane was not located at the bottom of the probe, meaning that:

- Measurements could not be made all the way to the ground.
- Snow was disturbed due to the thicker shaft at the centre of the vane.

A new set of attachments were manufactured to bring the vane to the bottom of the probe (Figure 3.3). The attachments were made so that the same vane could be used for either prototype or both at the same time.

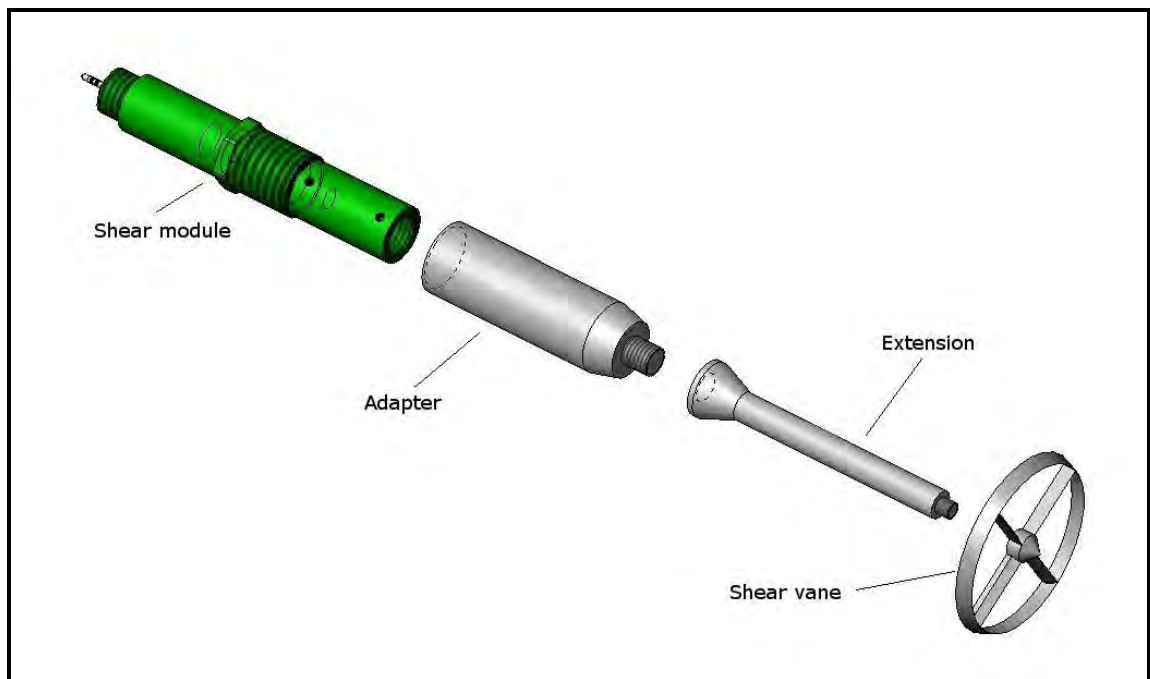


Figure 3.3 Shear module with new extension and vane.

### 3.1.3 Addition of Bluetooth

It was found that the original radio transmitter was unreliable and tended to transmit errors. The connection could not be made using conventional cables since the vane rotates. The radio transmitter was therefore replaced with a Bluetooth transmitter.

The original laptop (Tough Book “Rocky”) was also replaced with a conventional modern laptop (Figure 3.5). Problems had existed with battery charge in the cold and the absence of any USB ports in the old machine. The draw back to this conversion

was that the new laptop was sensitive to knocks and water unlike the older “Rocky”. The replacement laptop was covered in closed cell foam and duck tape in an attempt to make it more robust. During field testing the screen icons were made larger and a high contrast colour scheme was chosen to facilitate use in bright sunlight. No significant problems were encountered with the use of this laptop in the field.

This brought the snow probe up to current technological standards and increased the reliability of the transmission.

### **3.2 Prototype 2**

The second prototype obtained a measure of the applied torque by reading the current being drawn from the battery. This had some obvious drawbacks which limited its accuracy but it was far simpler and more robust than the 1<sup>st</sup> prototype. It was thought that the decreased accuracy would not significantly reduce the value of the results. Snow shear strength has been observed to be variable over short distances (Conway and Abrahamson, 1984). So a decrease in the probe accuracy should not significantly decrease the significance of the shear strength obtained for a small area in relation to its surroundings because the actual variability of the shear strength is likely to be far greater than the snow probes uncertainty and the associated variability caused by this uncertainty.

This prototype used the extension rod and vane pictured in Figure 3.3 and allowed for the possibility of using both prototypes at the same time. Prototype 1 takes measurements in the probe itself while prototype 2 takes measurements from the drive mechanism. In this way two independent measurements could be recorded on the same area of snow.

#### **3.2.1 Batteries**

In previous prototypes cheap cordless drills were used. These often had problems working at low temperatures. For this prototype it was vital that the drill battery have a consistent charge profile, even in cold temperatures. A high quality Makita 12V cordless drill (model 6270DWE) was purchased with a spare NiCd battery. Nickel Cadmium and Lithium ion batteries were found to have good properties in cold condition (down to -10). Lithium ion batteries are not normally used for cordless drills due to their high price though this is likely to change.

The downside to NiCd batteries is that they have a charge memory. For this application the batteries must be fully charged. During testing it was found that a NiCd battery only behaves as a constant voltage source when it is fully charged. A constant voltage source is essential when only the current is being read. At lower charge the voltage starts to vary, invalidating results. To extend the life of the battery it had therefore to be discharged each time before it is recharged. A simple resistive heater element was used to fully discharge the batteries after testing.

### 3.2.2 Electrical Configuration

Attached to the drill in a separate box was a pulse modulating power controller giving good control of the rotational speed. Figure 3.4 shows the electrical layout of prototype 2. A signal from the main drill circuit was obtained via a current transducer. The current signal was sent to a signal conditioning unit and amplified with a 9V battery. The signal conditioning unit converts the current level into a voltage proportional to the current. The signal is then converted back in to a current reading in the laptop.

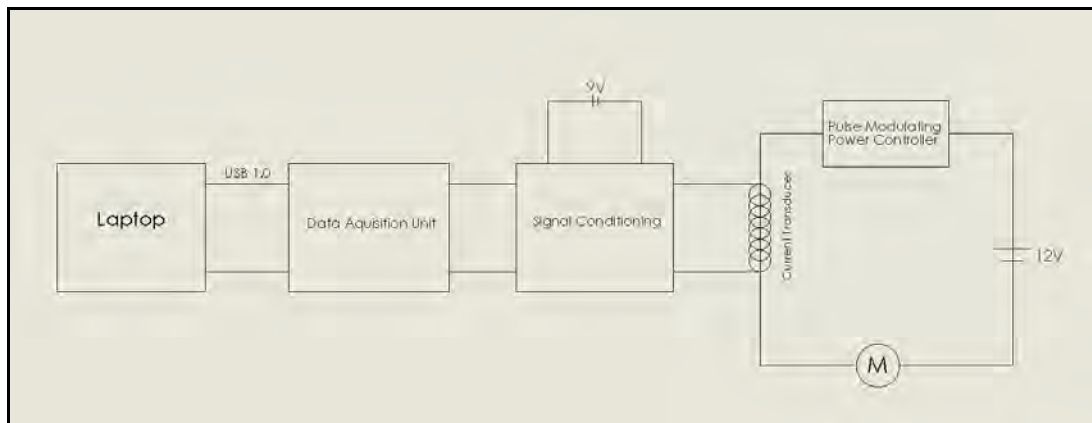


Figure 3.4 Electrical diagram of prototype 2.



**Figure 3.5 Prototype 2 (the drill), the ruggedised laptop and a 100cm<sup>2</sup> shear vane.**

## 4 Testing 2006

Tests were conducted in the Arthurs Pass region between the 29<sup>th</sup> of June 2006 and the 17<sup>th</sup> of September 2006. Testing procedures and equipment were continuously improved, completing the winter with a sound testing method to be implemented in following seasons.

### 4.1 Testing Sites

It was not necessary to conduct tests on a steep slope, considering that the aim of this project is to show that this embodiment of the rotational shear vane is able to measure shear strength to the same standard as a shear frame or better. Chosen test sites needed to:

- Be relatively uniform and at least 5m from any significant feature.
- Have a noticeably weaker layer in the snow pack to test.
- Have not been disturbed by any kind of previous activity.

Most tests were conducted next to the weather station by the Palmer lodge at Broken River (5 days) though tests were also done at locations at Porter Heights (1 day), Craigieburn ski area (3 days) and Temple Basin ski area (1 day) (See Figure 4.1 & Figure 4.2).

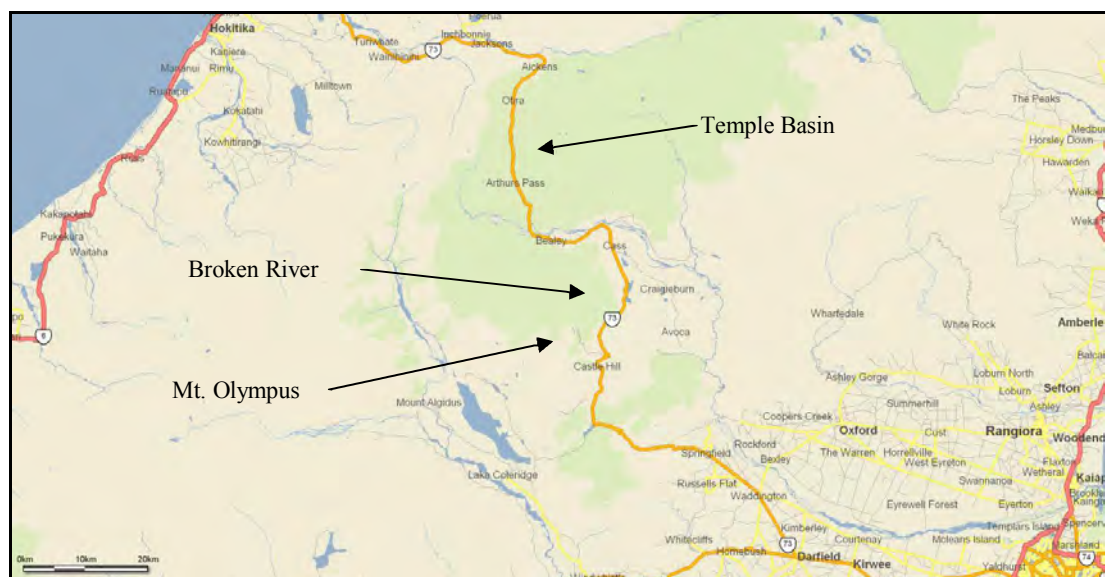


Figure 4.1 Map of Arthur's Pass indicating test sites used during the 2006 winter.



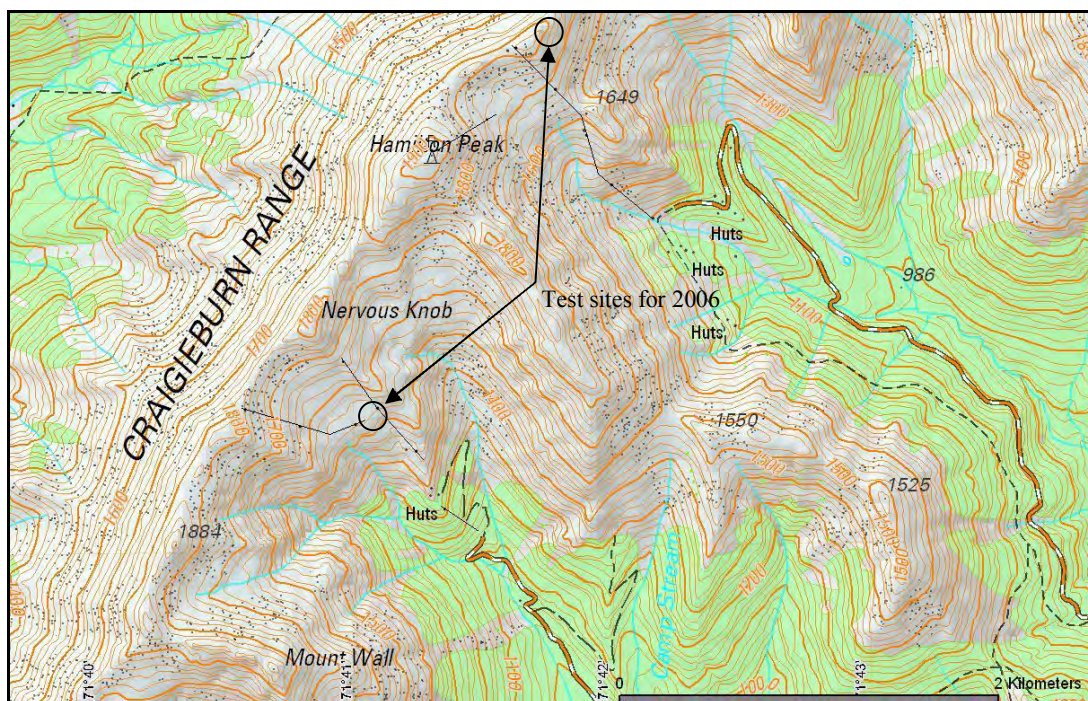


Figure 4.2 Testing site at Broken River Ski Area and Craigieburn Ski Area.

## 4.2 Preliminary Testing

Initial tests were used to understand how the new prototype worked and reacted in an alpine environment. Each test was started by digging a snow pit and doing a standard snow profile hand hardness test. The weakest layer was then found using a simple shovel test. Shear frame tests were done according to methods described by Jamieson and Johnston, 2001.

Shear vane tests were conducted next to the shear frame tests. Generally 3 different power levels were used. The power level refers to a qualitative power level indicated on the drill which regulates the speed (higher power level = higher speed).

Table 4.1 Approximate no load rotational speeds

Power Level	Approximate rotational speed (revs/s)
1.2	0.7
1.4	0.9
1.6	1.15

### 4.2.1 Prototype 2 Results

Initial results show quite good repeatability in general trends. Clearly a relationship exists between the hardness profile data and the shear vane data.

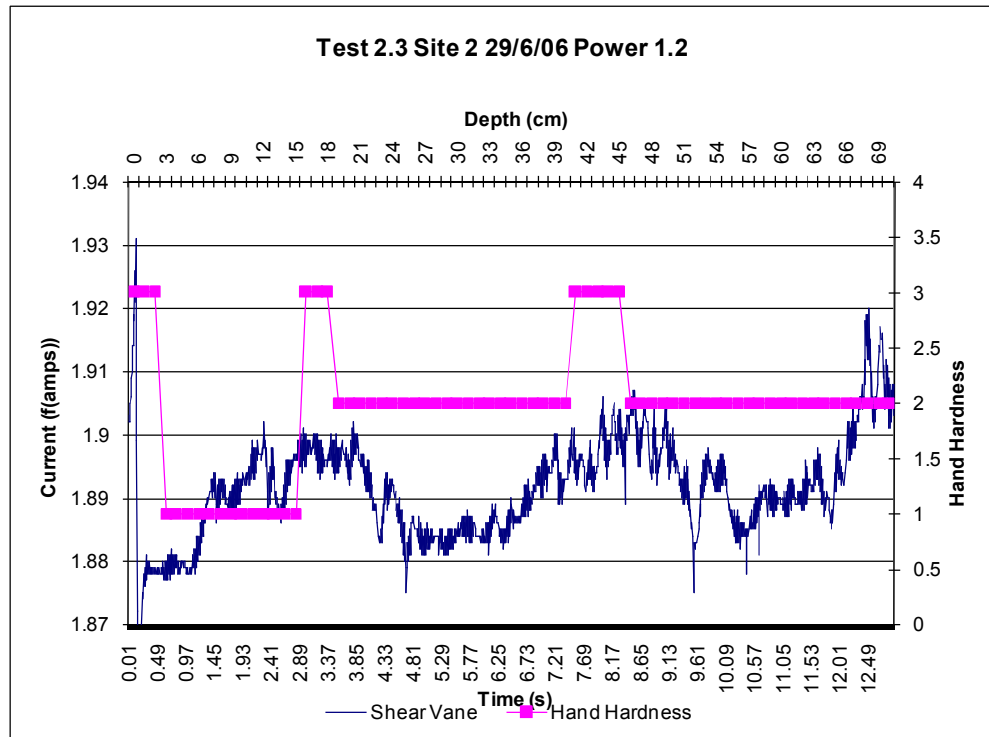


Figure 4.3 and Figure 4.4 show very similar trends in shear vane data results. These were done on the first day of testing.

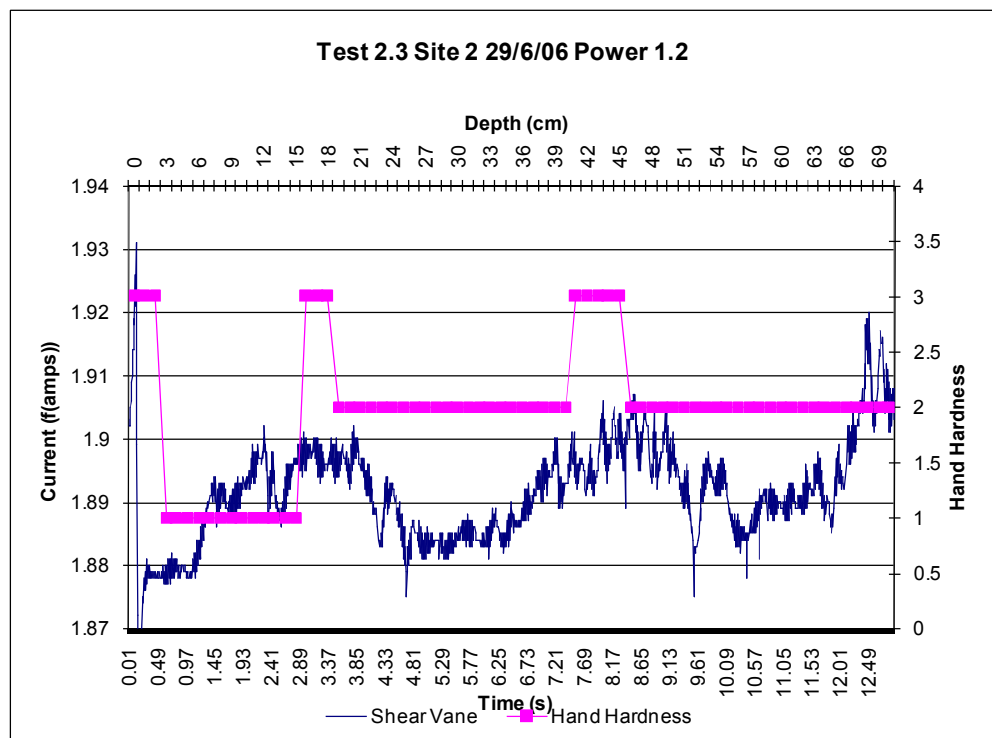
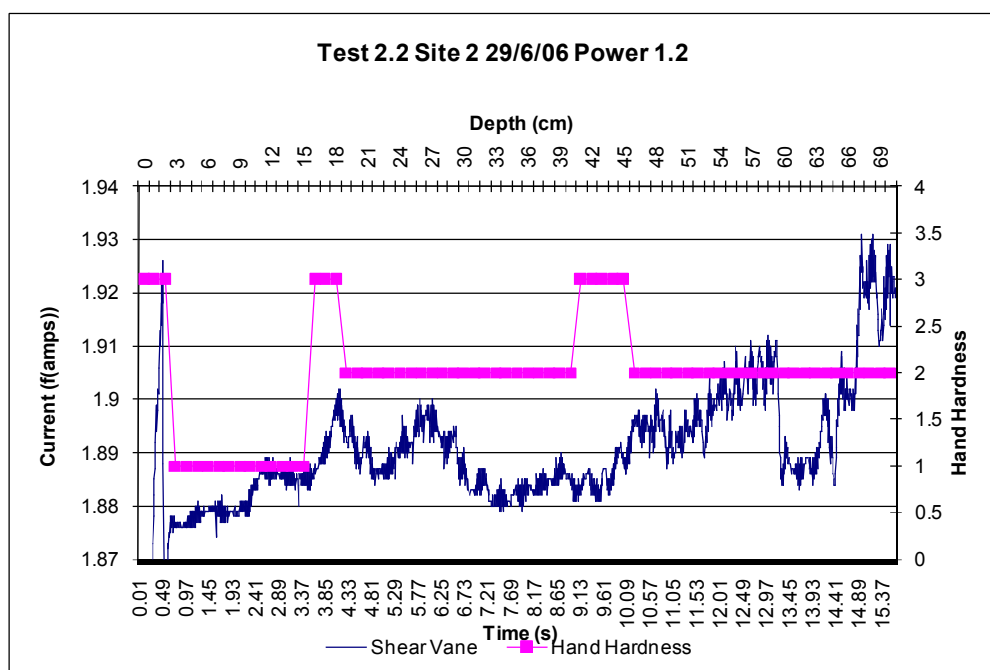


Figure 4.3 a test done at Porter Heights



**Figure 4.4 a test done at Porter Heights**

The first spike on these graphs does not represent the first layer of snow but rather the initial back current created when the drill is switched on. This spike is characteristic of all such tests. It is also important to note that all tests done in 2006 are based on a times scale rather than depth. Time does give some indication of the depth but it does not correlate absolutely with the depth measurements from the hardness profile. It should therefore be remembered that the depth scale comes from the hardness profile and not from the shear vane profile.

In these first two tests the top layer was not detected. Deeper within the snow pack two increases in the current seem to correlate well with the increased hardness shown on the hardness profile.

Figure 4.5 again shows a loose correlation to between the hardness and shear vane profiles. On this test it should be noted that the current scale is backwards. This is due to the connection between the drill and the signal conditioning box being plugged in backwards. This is irrelevant for comparing the form and clarity of the two plots. Several more tests were done on different days and indicated similar results.



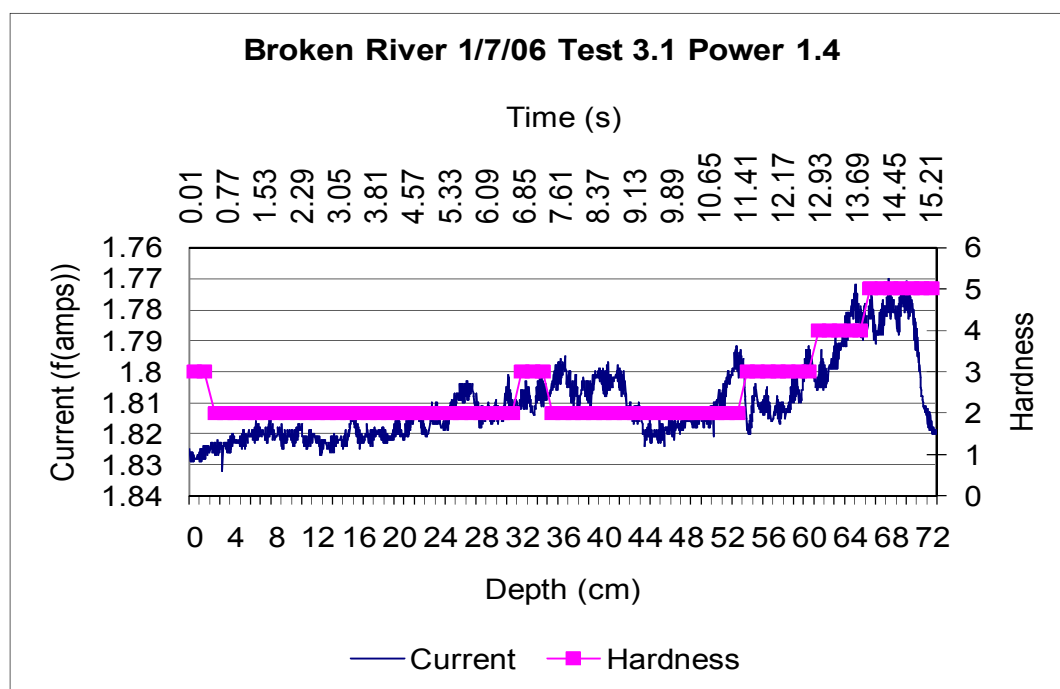
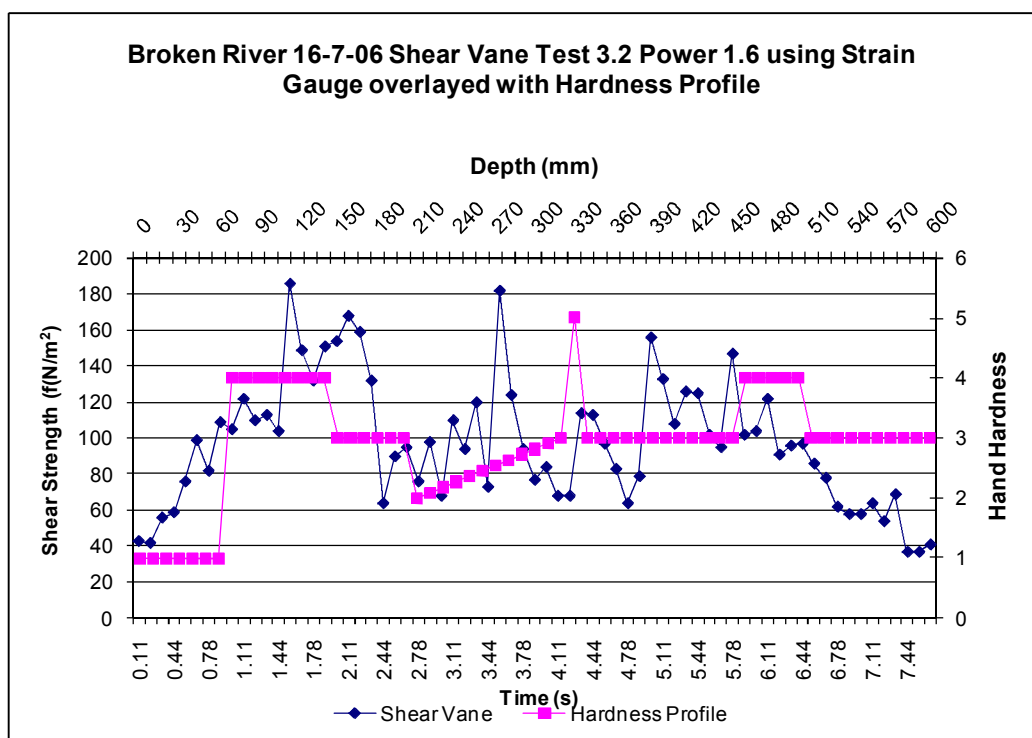


Figure 4.5 shows a function of current and hardness vs time and depth.

#### 4.2.2 Prototype 1 Results

This prototype was taken into the field for testing on several occasions but only one day of test results was obtained. These results (Figure 4.6) show some correlation to a hand hardness profile. It should be noted that the two plots do not overlay exactly because the Time and Depth scales do not necessarily correlate perfectly. Therefore some of the peaks in each plot are separated horizontally.



**Figure 4.6 Results from prototype 1. Shear strength data is indicated as a function of  $N/m^2$  because insufficient data was collected to properly calibrate the device.**

The rate of data collection on this plot is almost 9Hz. The low density of data points means that thin weak layers may be represented by only one data point which may not actually represent the weakest part of that layer. On average (depending on the speed of penetration) 1 data point is recorded for every 9mm of snow depth. The plot could be misleading. A data density of 1 data point per 1mm penetration would give sufficient accuracy to make the plot unambiguous.

## 4.2.3 Problems Encountered

### 4.2.3.1 Prototype 1

- When using the complete probe (including the blue tooth and strain gauge units) there is a significant bend on the probe. This means that the shear vane not only rotates about its central axis but the whole vane ploughs a circular path through the snow about the drills central axis. This means that some of the shear strength in the snow is overcome by other means than pure rotation making these results not a true measure of shear strength. This is probably due to threads not being tapped completely straight and the two threaded parts not seating properly. This is made more noticeable by the fact that there are 6 threaded connections in this prototype.

- Melted snow penetrated into the strain gauge amplifier circuit board, which corroded the circuitry. A new amplifier circuit was manufactured and embedded in candle wax to try and rectify this. This modification was never tried in the snow due to an as yet unidentified problem.

#### **4.2.3.2 Prototype 2**

##### ***Batteries***

At first it was decided that batteries were to be used until they no longer rotated the drill properly. This would extend the life of the battery. However it was then observed that the variation in current decreased once the battery had been used for 2-3 days of testing. Figure 4.7 shows how there is almost no variation in the shear vane results and only a slight correlation between the hardness profile and the shear vane profile. The reason for this appears to be that the drill battery operates as a constant voltage source only when it is fully charged. Once the battery becomes slightly run down the amount of current it can give reduces. When an increased torque is applied to the drill the battery can no longer increase the current supply so it stays constant. The drop in the initial current can be seen between Figure 4.3 and Figure 4.7 where the no load current at the start of each graph after the initial spike is 1.88 and 1.64 respectively. For the remainder of the 2006 and 2007 testing seasons batteries were always fully charged before each day.

As a further measure, the voltage was recorded in all tests done in the NZ 2007 winter. It was then easy to detect any tests where a drop in voltage occurred. These tests were then discarded.

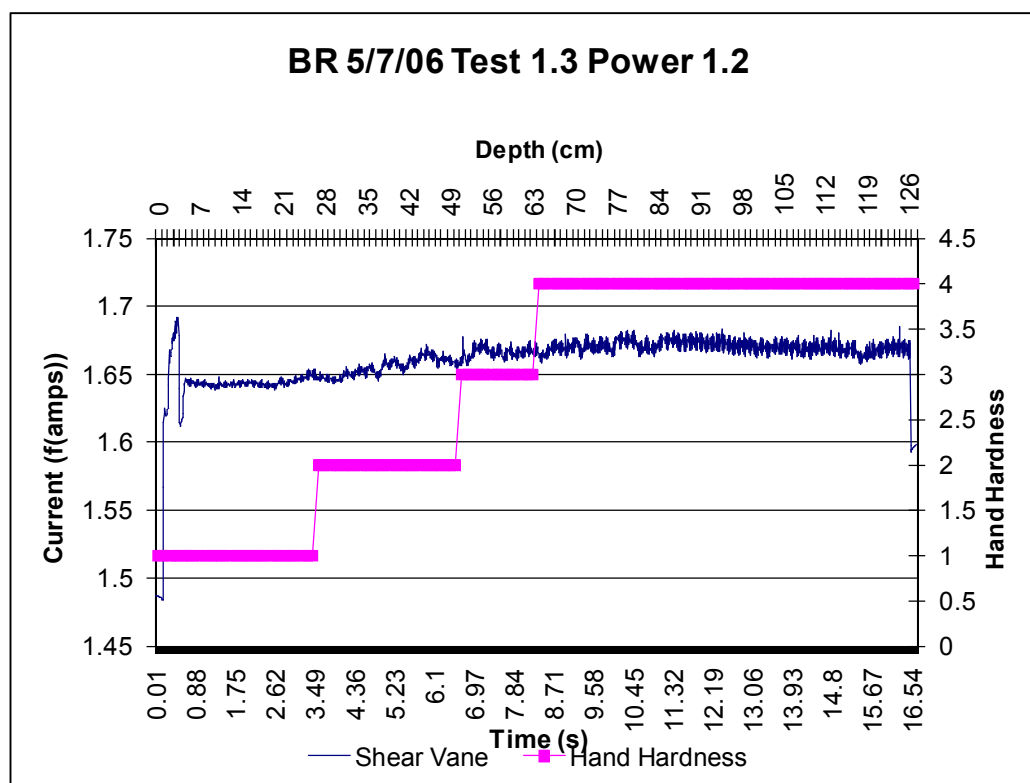


Figure 4.7 Shear vane profile when the drill battery is starting go flat.

### *Snow Types*

- Some tests were carried out on very soft snow bounded below by a much harder wind affected layer. Harder wind affected layers are often covered in ice protrusions making the surface bumpy. The shear vane gets caught on these protrusions, sending it sideways and making it hard to keep centred on the original course. This could be helped by adding a longer centre point on the end of the shear vane.

### *Laptop*

There were several inconveniences associated with using a laptop in the snow.

- In bright sunshine it was often very difficult to see details on the screen. This was helped by making all icons and script as large as possible and using highly contrasting colours. This was made even more difficult on windy days when wind blown snow would melt on the screen making it wet.
- The laptop was always in danger of getting wet, even though it was almost fully encased in plastic. During windy or snowy conditions the laptop would

get completely covered in snow which has the remarkable ability of finding even the smallest gaps.

- Because the laptop was sitting in the snow during tests it quickly became cold which reduced the battery life. Actual computer time was kept to a minimum during tests and a spare battery was always carried.
- The laptop was the largest and heaviest piece of equipment required for tests so any improvement here would greatly improve the devices usability.

### ***Accuracy***

- One of the biggest problems with the data was that the graphs did not show enough definition at the shear strength levels of interest. It was found that the difference in current output between applying no load and applying a load equivalent to a shear strength of 200N/m<sup>2</sup> using the 60mm diameter shear vane was insignificant. This was also seen in the plots obtained from tests in 2006 where a soft section of snow would give a current output almost the same as a no load current output. See the section on Calibration for more details.

## **5 Design Developments on Prototype 2 between November 2006 and June 2007**

The following sections cover testing completed in Austria during March 2007 and tests done in New Zealand between June and September 2007. The tests differ in that the New Zealand tests include a depth measure which was not present during tests done in Austria. The main difference in the results can be seen in the graphical presentation methods used in chapter 7.

Several improvements to prototype 2 were planned for the beginning of 2007. Some difficulties in the electrical modification meant that some of the modifications were not completed on time for testing in Austria, March 2007. Testing was done without the range finder meaning that output data would still have a time scale rather than a depth scale. It was also hoped that a rotation counter would be added during this development phase but time constraints made this unachievable.

### **5.1 *Electrical Modifications***

- A Palm pilot (Dell Axim X51v, see appendix C for more details) was programmed to record data transmitted by the Snow Probe using a Bluetooth connection. The Palm Top was encased in an Otter tough box and has an extra large battery to better withstand the cold wet environment.
- A more accurate power control unit was installed on the drill.
- The drill was fitted with a Bluetooth transmitter.
- A voltage meter was installed so that outputs could be given in terms of Power (W). This clearly showed when a battery is no longer behaving as a constant voltage source because the voltage started to drop during a test.
- An Ultra Sonic range finder was installed after testing in March 2007. This allows shear profiles to be displayed in terms of depth rather than time. It also allows variations in speed and their effects to be removed.

A diagram of the final electrical layout can be seen in Figure 5.1. The physical embodiment of the electrical components, are shown in Figure 5.2.

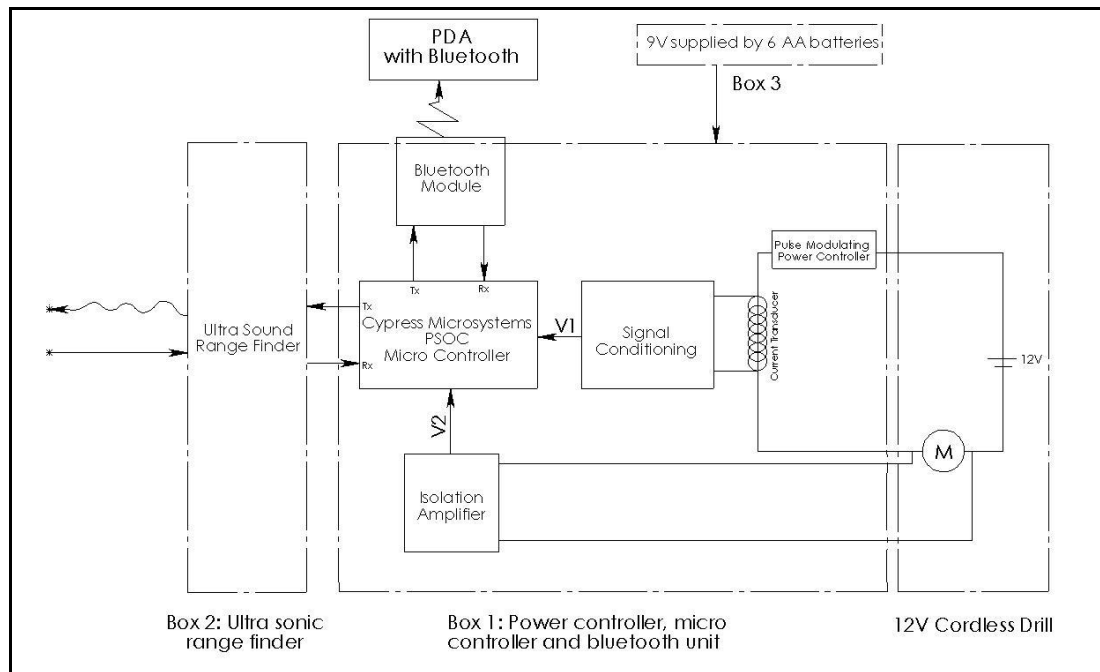


Figure 5.1 Electrical diagram of prototype 2 after modifications done in early 2007.

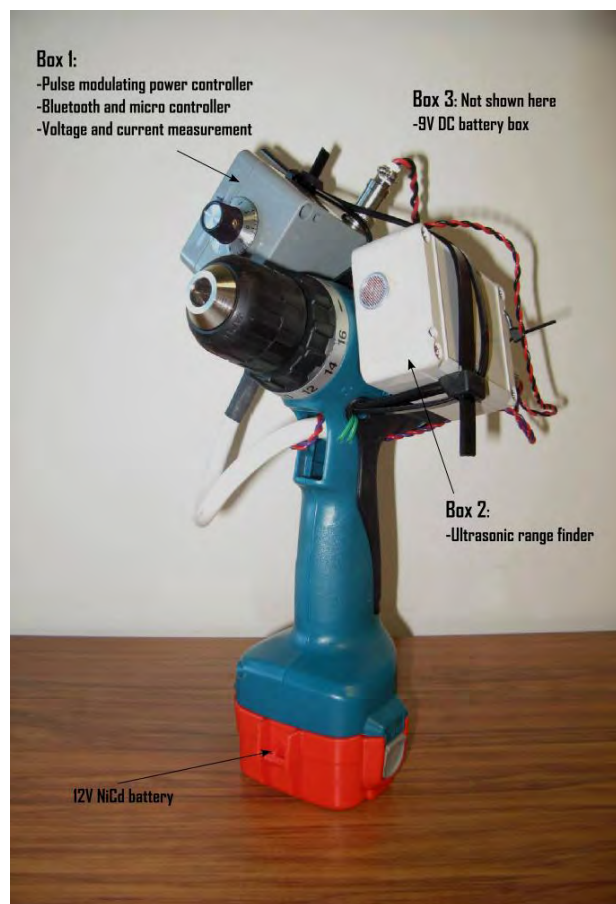


Figure 5.2 Prototype 2 being tested in Austria.

These modifications significantly increase the portability of the device and make it far more durable in wet cold climates.

## **5.2 Mechanical Modification**

Two extra shear vane sizes were manufactured to enable the snow probe to give more accurate readings in softer snow. One of the biggest problems apparent from testing in 2006 was that the current readings showed very low definition in soft snow.

The drill gave good definition when a larger torque was applied to the shear vane so larger shear vanes would apply greater forces to the drill giving greater definition. The torque at which drill power readings became obviously distinguishable from no load power readings was determined using a De Prony Brake test. The size of the new shear vanes was calculated assuming a minimum shear strength to be measured of  $200\text{N/m}^2$ . The size of an optimum shear vane was determined using equation 6.4 for a range created by using both single and double shear theory.

This gave a diameter range of 100mm for double shear to 180mm for single shear. To make sizes consistent with the shear frames used in testing, shear vane sizes of 113mm in diameter and 179mm in diameter were chosen. These sizes equate to  $100\text{ cm}^2$  and  $250\text{ cm}^2$  respectively.

The vane sizes used for tests in 2007 are shown below in Table 5.1 Shear vane sizesTable 5.1.

**Table 5.1 Shear vane sizes.**

Vane sizes	Diameter (mm)
V1	60
V2	113
V3	180



## 6 Calibration

Two calibrations were used to convert the microprocessor output into a recognisable unit. The first calibration converts the raw output data coming from the microprocessor on the drill into a current and voltage. From this a power input is calculated (equation 6.1).

$$P_{in} = VI \quad (6.1)$$

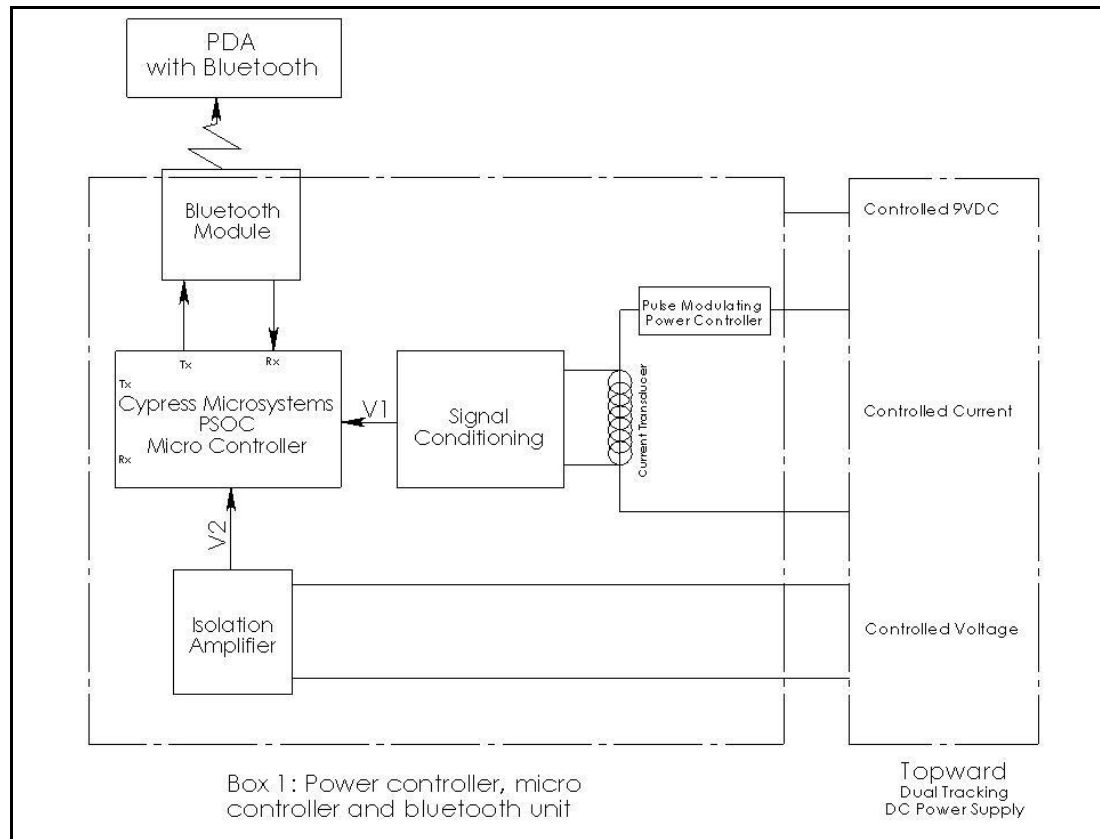
The second calibration converts the power input into a torque output (equation 6.2).

$$P_{out} = T\omega \quad (6.2)$$

Because the rotational speed is not recorded, and the efficiency of the motor is not known, a prony brake test is used to compare torque output and power input.

### 6.1 Voltage and Current Calibration

For this test the Bluetooth/microprocessor box was completely removed from the drill. All power sources were provided by a Topward DC power supply. An electrical diagram of the calibration setup is shown in Figure 6.1 below.

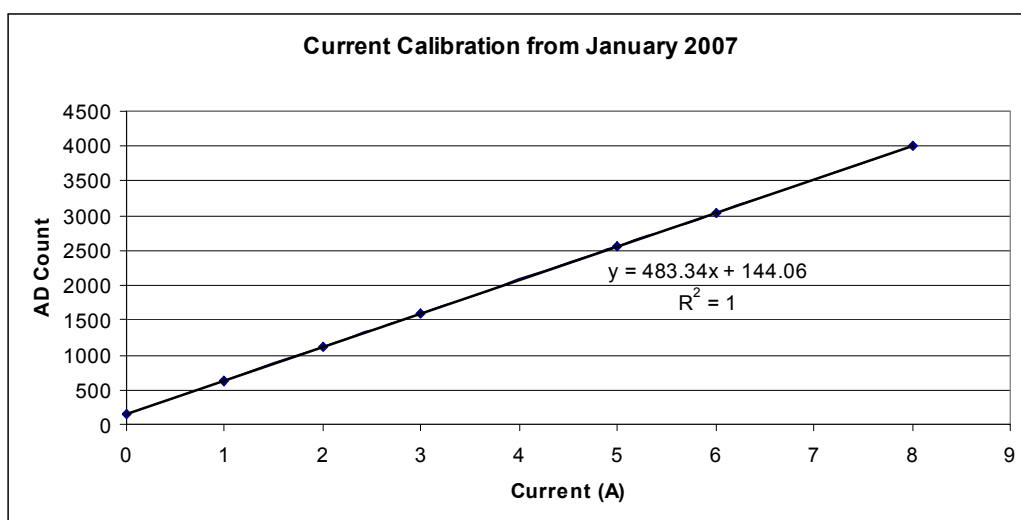


6.1 Voltage and current calibration electrical diagram.

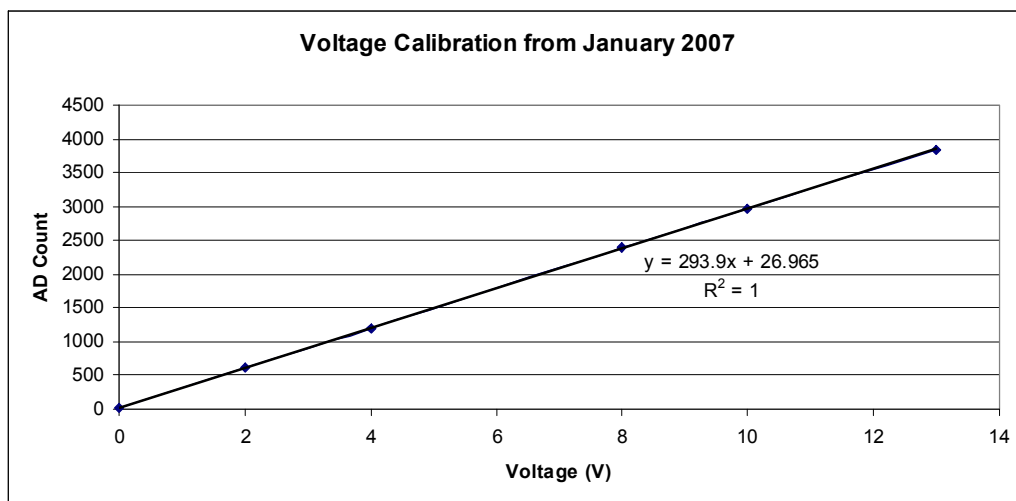
Current and voltage measurements were taken in two separate tests. For the current test the voltage sampling wires to the drill power controller were disconnected while keeping the voltage constant through the current sampling wires. For the voltage test the current sampling wires were disconnected and the current held constant through the voltage wires.

A known current (varying between 0 and 6 amps) or a known voltage (varying between 0 and 12 V) was supplied to the data acquisition unit. The data acquisition unit generated output (AD count) was then graphed against the input voltage. A series of these tests then generated a calibration curve which was applied to all output data received during field testing. It should be noted that 6 amps and 12 volts were never applied at the same time as either one was held constant at a low level while the other was varied.

This test was carried out after each electrical modification to the drill. Before the range finder was installed the calibration curves were perfectly linear and repeatable (See figure 6.2 and 6.3 below).

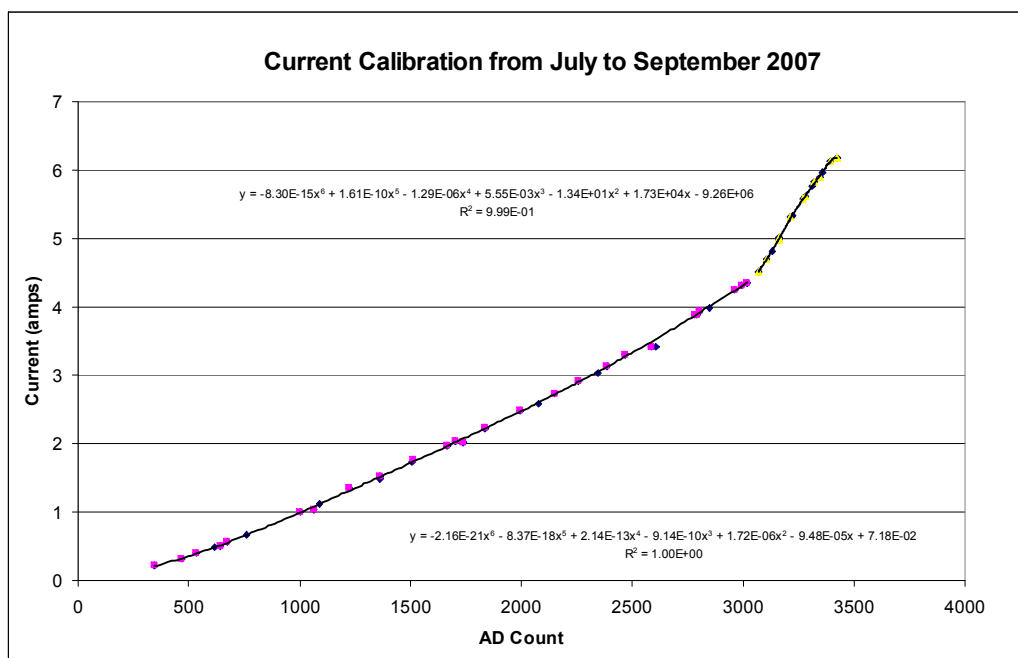


**6.2 Current calibration from January 2007**

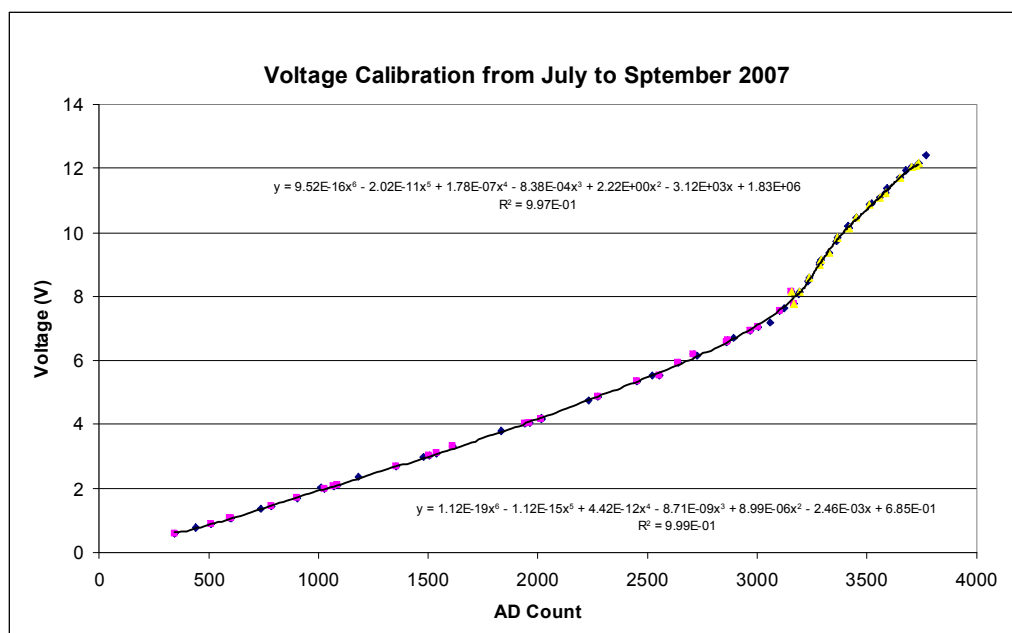


### 6.3 Voltage calibration from January 2007

These were used throughout testing done in Austria. The range finder was installed prior to the 2007 New Zealand ski season. The new calibration curves are significantly different to the earlier versions (See Figure 6.4 and 6.5 below).



### 6.4 Current calibration curve used in the NZ 2007 ski season.



### 6.5 Voltage calibration curve used in the NZ 2007 ski season.

The reasons for this change have not been determined. It was estimated that to try and find the cause of this change would take several weeks of technician time. This would have resulted in a significant part of the winter season being wasted. Instead the curve was modelled and continuously monitored to ensure no changes occurred over time. The best fit solution was found to be a piece-wise function containing two 6th order polynomials. 15 significant figures were used throughout these calibration calculations.

## 6.2 Power to Torque Calibration Method

A De Prony Brake test was used to calibrate the drill out puts. The test rig can be seen in Figure 6.6 below. A 112mm diameter V-belt pulley wheel was used as a friction drum. A Samson salter 1kg x 5g spring balance was used to measure the tension in the string above the pulley. Known weights were applied to a tray below the pulley. A 2mm spectra cord was used to connect the spring balance to the weight tray. The cord was wrapped around the pulley once.

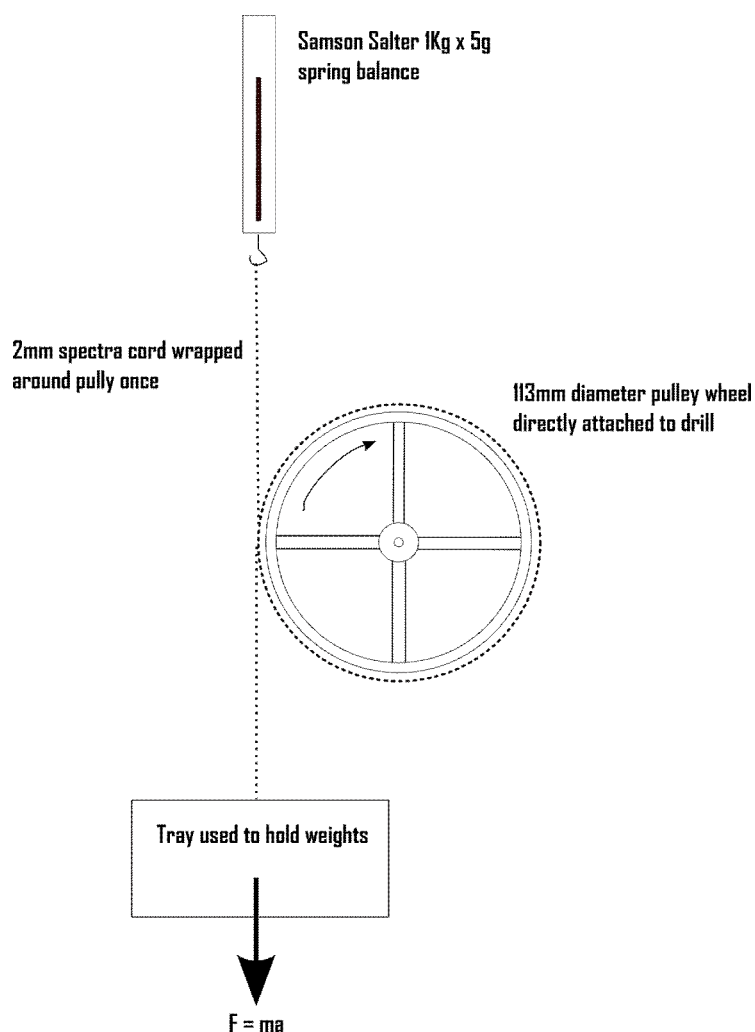


**Figure 6.6 the setup used for the prony brake tests.**

Tests were run for each of the drill settings used, over a torque range from 0-1.2 Nm. From this data a linear relationship was found between the applied torque and the power output from the drill.

A typical chart showing the relationship between the drill power input and the drill torque output is shown in Figure 6.7 below.

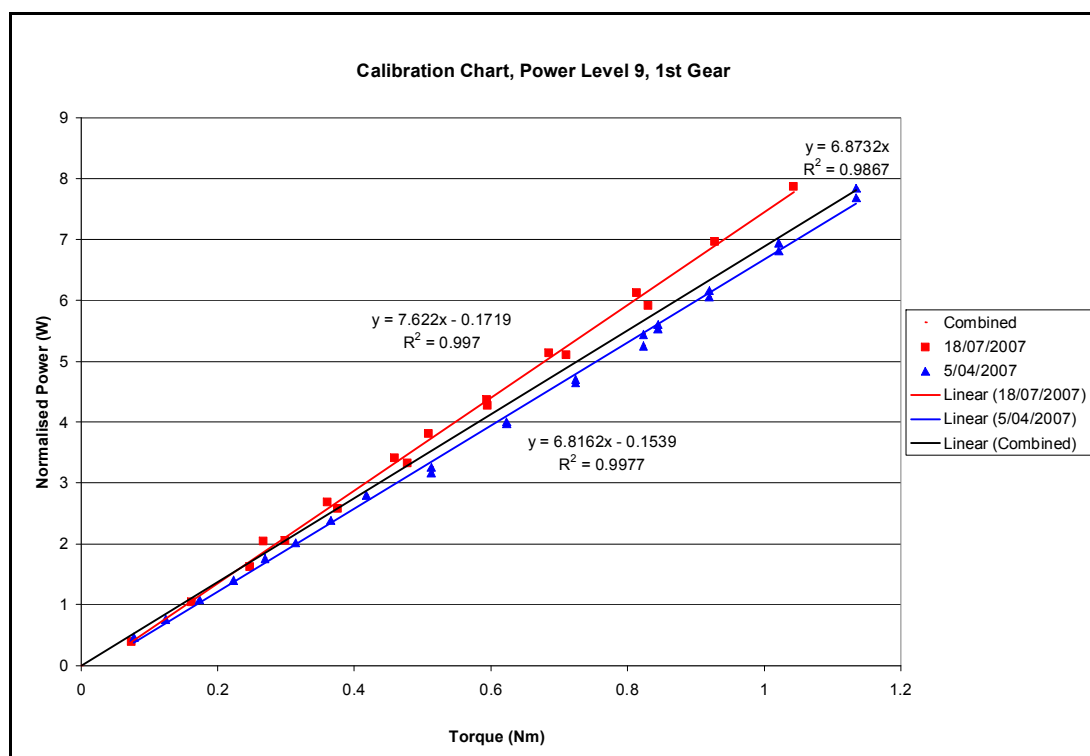


**Figure 6.7 A typical graph relating power input to torque output.**

Two series of tests were carried out. The first test was done in April and the second in July 2007. These tests differed with the later tests indicating a higher gradient. This may be due to gear box degradation which would lead to a higher current being drawn for the same applied torque.

The later series of tests was conducted with one of the original batteries and a new one. The battery made little difference to the outcome so it is unlikely that the change in gradient was due to battery degradation.

In all tests the voltage remained relatively constant while the current changed. To try and avoid some of the variations in current each test is started with a no load test which is then used as a datum. The no load power level is subtracted from all other test data in the same series. The torque is therefore proportional to the difference between the no load power input and the loaded power input, not the absolute power input of a loaded test.

A relationship was found for each power and gear combination used during testing (See Table 6.1).

**Table 6.1 Linear relationships relating input power and output torque.**

	Gradient	y intercept	Max Deviation (%)
<b>Power Level 8, Gear 1</b>	6.2	0	10.5

<b>Power Level 9, Gear 1</b>	6.9	0	22.8
<b>Power Level 10, Gear 1</b>	7.6	0	14.4
<b>Power Level 12, Gear 1</b>	10.2	0	18.0
<b>Power Level 2, Gear 2</b>	10.8	0	13.8
<b>Power Level 3, Gear 2</b>	12.5	0	24.1
<b>Power Level 4, Gear 2</b>	14.3	0	17.1

As seen in Figure 6.7, individual calibration curves had a small - y intercept. These were set to 0 to ensure no negative shear strengths were obtained. This had a negligible effect on numerical values calculated from these curves.

The maximum deviations between the actual data and the line of best fit, range between 10% and 24%. Generally the highest percentage deviations were experienced close to zero where very small changes in power or torque, proportionally have a greater impact. In practice the measured torques are from 0.1Nm to 0.8Nm.

### 6.2.1 Test Variable Combinations

The power levels selected for use during 2007 differ from those used in 2006. A range of power levels was selected to try and detect an optimum power level rate of rotation. Various combinations of drill gear, vane size and power level were combined to determine the effects and benefits of these variables. A summary of test variable combinations is given below in Table 6.2.

**Table 6.2 Test variables**

Power Level	Test Gear	Vane Diameter (mm)	No Load RPM	Power (W)
2	2nd	60	100+	0.8
3	2nd	60	100+	0.9
4	2nd	60	100+	1.1
8	1st	113 or 180	72	2.1
9	1st	114 or 180	80	2.3
10	1st	115 or 180	84	2.5
12	1st	116 or 180	96	3

These test variable combinations were selected to try and maximise the difference between no load and test drill power inputs. Less torque was required to rotate a small shear vane therefore the second gear was selected and a lower power level. Conversely a larger torque was required to rotate the largest shear vane so a higher power level and 1<sup>st</sup> gear were selected. Because it was unclear exactly which combination would work best a range of combinations was tested.

### 6.3 Torque to Shear Strength Calculation

The basis for this calculation comes from a geomechanics application for testing soil shear strength. Equation 6.1 (Calding and Odenstad 1950; Craig 1995; Barnes 2000; Evans 2002) relates the maximum torque applied to a shear vane, the shear strength and the vane size.

$$T_{\max} = \tau_{\text{shearvane}} \left[ (2\pi r_0 h) r_0 + 2(\pi r_0^2 - \pi r_i^2) \left( r_i + \frac{2}{3}(r_0 - r_i) \right) \right] \quad (6.3)$$

The vane size variables  $r_0$ ,  $r_i$  and  $h$  are illustrated in Figure 6.8.

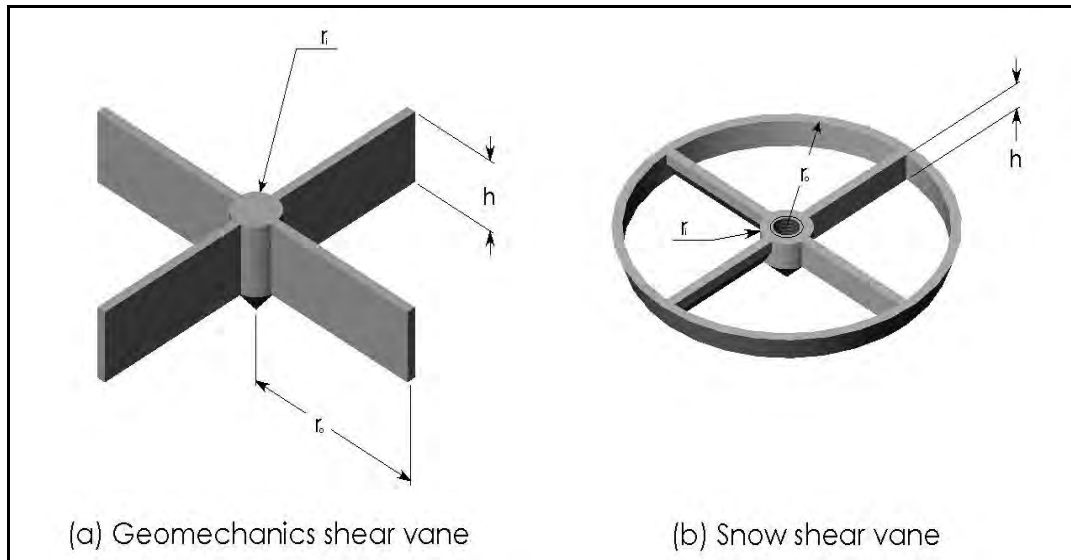


**Figure 6.8 (a) geomechanics shear vane and (b) snow shear vane.**

The main difference between the two vanes is the isolating ring. The first term in Equation 6.3 relates to the shear force created by the vertical height of the vane. Because of the isolating ring the shear force created can be assumed to be insignificant.

Equation 6.3 also assumes equal shear force is created above and below the vane. The geomechanics shear vane is used in a different way to snow shear vane. The geomechanics vane is inserted into the ground and rotated at a desired depth to get a measure of shear strength which would leave the surrounding dirt intact and justify the double shear theory. The snow shear vane on the other hand is continuously rotating while it is being inserted into the snow. This destroys most of the bonding between snow crystals so the snow above the shear vane is likely to have quite differing shear strength to the snow below the vane. Some of the snow above the vane may even rotate with the vane and crack some way up the affected cylinder. One can argue that the snow shear vane will have something between single and



double shear. The shear strength above the vane will not be as great as that below nor will it be nil.

A modified version of Equation 6.3 is presented in Equation 6.4. A ratio C has been introduced to account for deviations from the double shear theory as well as any other effects caused by the vanes helical descent through the snow. The ratio C can then be found through field tests of the snow probe. Equation 6.4 also assumes zero shear force between the isolating ring and the surrounding snow.

$$T_{\max} = \tau_{\text{shearvane}} C \left[ \left( \pi r_0^2 - \pi r_i^2 \right) \left( r_i + \frac{2}{3} (r_0 - r_i) \right) \right] \quad (6.4)$$

C values calculated from testing in 2007 are given in section 7.3.6 as part of the results. The value was calculated by finding the ratio of the average shear frame result to the average shear vane result at the same depth.

## **7 Testing 2007**

### **7.1 Testing Methods: 2007**

For the purpose of showing the accuracy of the snow probe, it was important that the chosen site was of a consistent gradient with consistent solar radiation over the whole area. A test always started with a standard hardness snow profile. This helped to identify the layers present and identified the layer of interest. Once a suitable layer had been identified, a row of 10 shear frame tests was carried out. This was then followed by several rows of shear vane tests (See Figure 7.1). Shear frame test results were also located on hardness profile graphs and shear strength or drill power graphs.

Shear frame results were compared to the corresponding layer on the shear strength profile graph. Hardness profile graphs and shear strength graphs were compared to show similarities in graph shape and form.

#### **7.1.1 Snow Profile**

##### **7.1.1.1 Equipment**

- Shovel
- Measuring stick or probe
- Electrical thermometer
- Light brush
- Inclinator
- Pencil
- Waterproof field book

##### **7.1.1.2 Method**

1. A suitable slope of medium to flat inclination was found.
2. The date, time, location, elevation, slope incline and weather (including air temperature) were recorded.
3. A snow pit was dug and a standard snow profile carried out, (The Avalanche Handbook, D. McClung, P. Schaerer, 2006) recording the temperature

gradient and hand hardness. Special attention was paid to locating the weakest layers using methods such as the shovel test.

### **7.1.2 Shear Frame Test**

The procedure used is based on standard test procedures published in various papers (Perla and Martinelli 1976; McClung and Schaerer 1993).

#### **7.1.2.1 Equipment**

- A 100cm<sup>2</sup> and a 250cm<sup>2</sup> shear frame.
- A Pesola spring balance (10kg and 2.5kg)
- Shovel

#### **7.1.2.2 Method**

1. The overlying snow was removed from the weakest layer or layer of interest to about 5cm above the layer in a strip approximately 2m x 0.3m across the slope.
2. The desired shear frame was placed in the snow 2-5mm above the layer of interest.
3. The shear frame was pulled using the spring balance (<1s).
4. Steps 2 and 3 were repeated 10 times, evenly spaced across the 2m cleared strip and starting on the left hand side (Figure 7.1).

### **7.1.3 Shear Vane Test**

#### **7.1.3.1 Equipment**

- Shear vanes of 28cm<sup>2</sup>, 100cm<sup>2</sup> and 250cm<sup>2</sup> size.
- Shear vane extension rods.
- Modified drill.
- PDA unit.
- Waterproof case.

#### **7.1.3.2 Method**

Snow probe tests were always carried out in conjunction with shear frame tests. An alternating pattern was created as shown in Figure 7.1. This allowed the test results

to determine significant variations in shear strength that may have existed over the test area. It also made comparisons between the shear vane and the shear frame results more apparent.

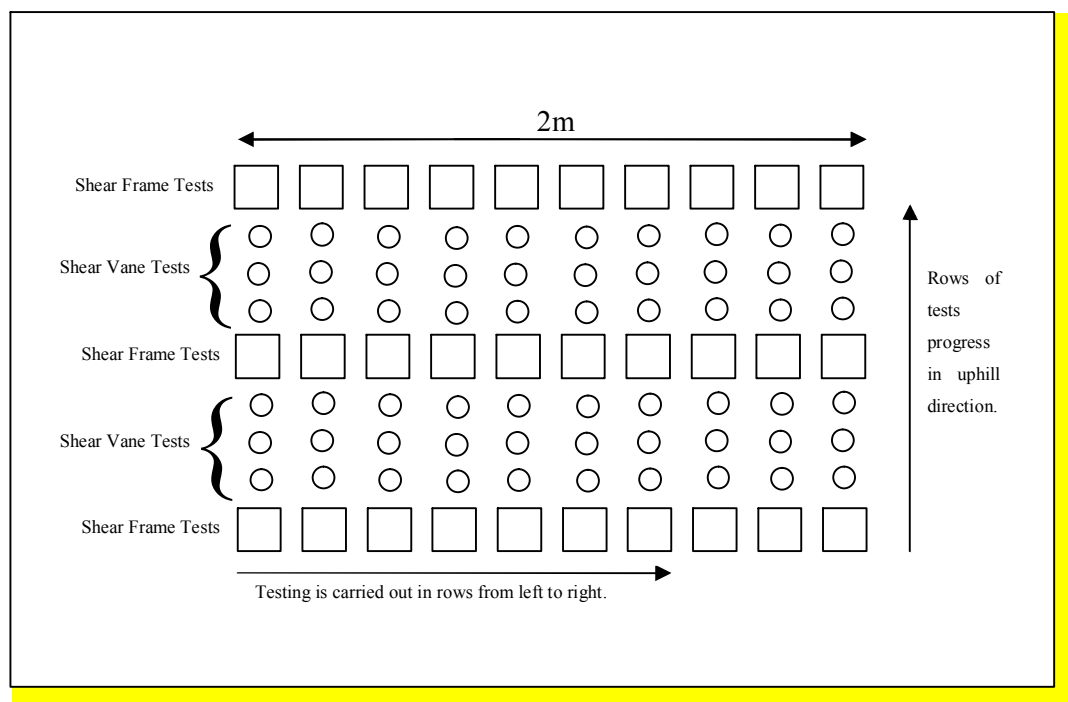


**Figure 7.1 Testing layout of snow probe and shear frame tests.**

Generally several rows of shear vane tests were carried out (a maximum of 4 rows, or around 400mm) before another shear frame test was done. This was done to speed up the testing process.

Tests were often done during periods of the day where temperatures could have changed significantly during the testing process. Therefore to minimize any errors due to temperature changes it was vital that the tests be finished as quickly as possible. A thermometer placed in the layer of interest was also continually monitored. A test was discarded if a change of more than 1 degree was observed.

Shear vane tests were carried out in sets of 5. This was done to limit the amount of data in one file. The same snow probe settings were used in all 10 of the tests included in one row. Subsequent rows of test were carried out with different drill properties, generally varying the power level. Typically the same shear vane was used for all rows of tests carried out between two shear frame tests.

During a set of 5 tests data was continually recorded by the palmtop. To make identification of individual tests easier, the drill was briefly stopped between each test. Before starting the next test the drill was switched on and held above the snow for between 1 and 5 second before entering the snow. This created a zeroing point

from which a relative drill power level could be determined (see Figure 7.2). Setting the no load power level to zero helped eliminate variations in battery charge levels and motor inefficiencies. All subsequent data in that test was then relative to the no load power level.

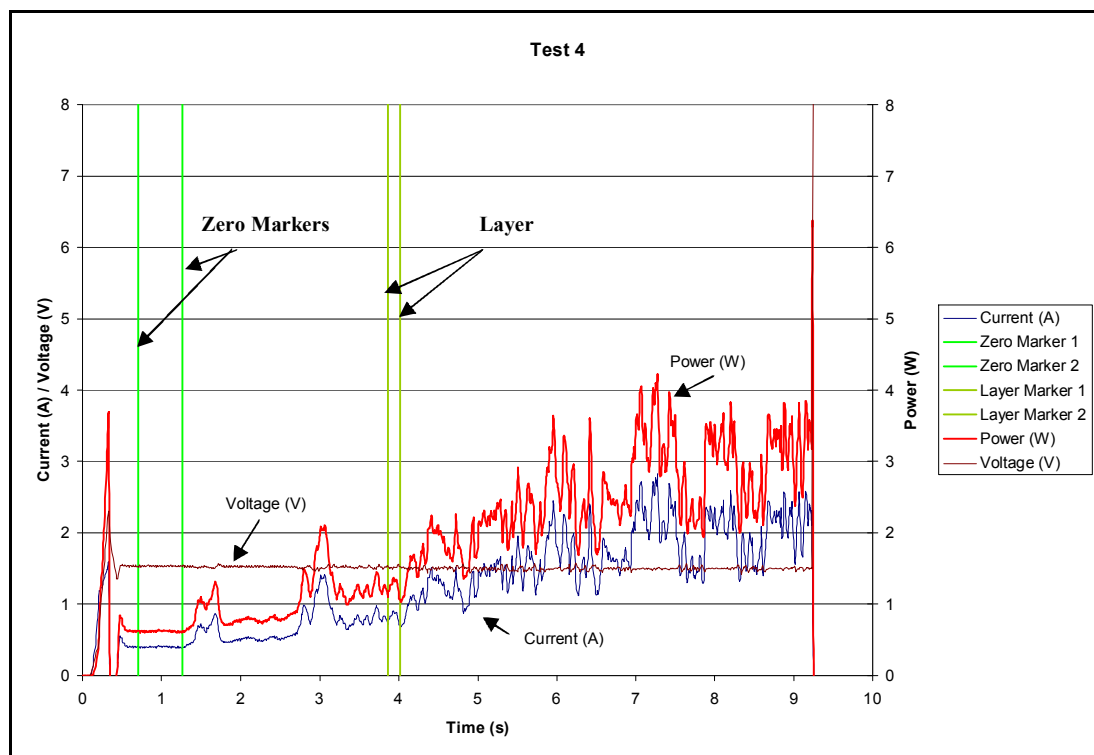


**Figure 7.2** Test number 4 of 5 in test set 20 on the 15<sup>th</sup> of March 2007. The test uses the 26cm<sup>2</sup> shear vane in 2<sup>nd</sup> gear on power level 2 (T20-P2-G2-V1).

The zero datum was defined as the average of a range of data at the start of a test (zero markers, Figure 7.2).

Figure 7.3 shows how data is processed in following tests. Austrian test results exclude the distance data. Power levels were converted into a torque level using the prony brake test described in section 6.2. The prony brake tests gave approximations for the rotational velocity and drill efficiency. The torque level could then be simply calculated using equation 6.3 or equation 6.4 if the ratio between single and double shear were known.

Austrian test results are displayed as above in Figure 7.2 with a time scale due to the absence of distance data while results from the 2007 New Zealand winter are shown on a distance scale. Bar graphs were used in all cases to compare individual layer strength results from shear frame and snow probe tests.

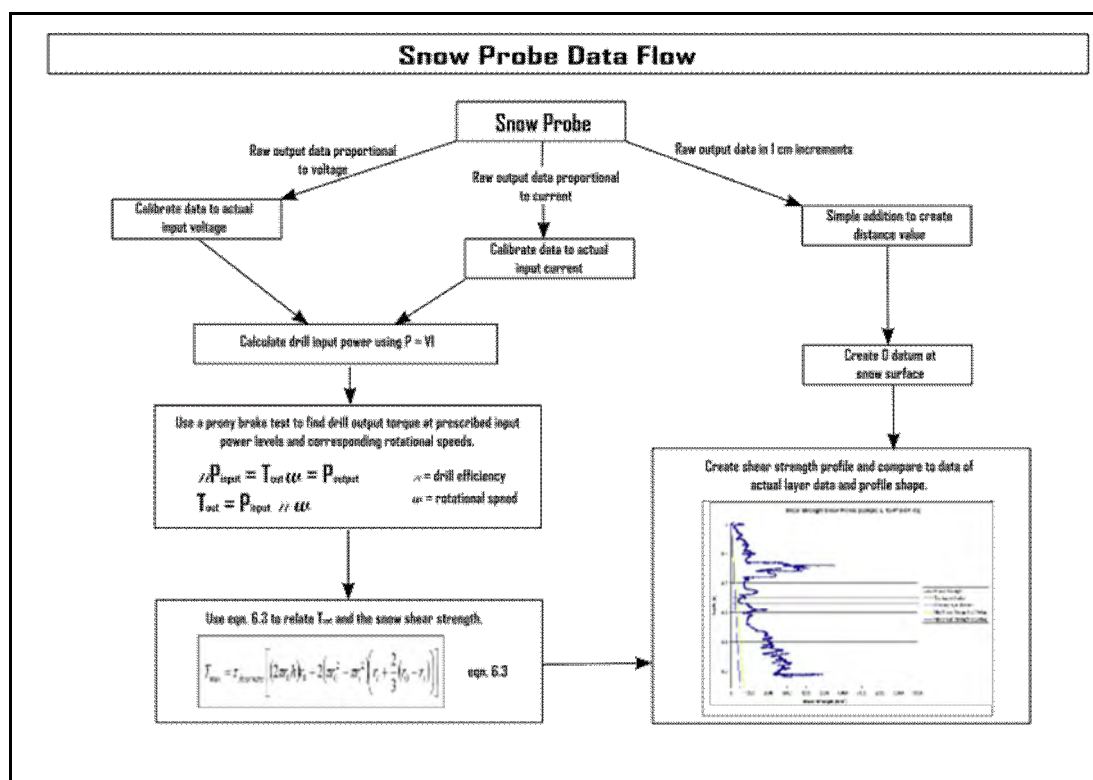


Figure 7.3 Snow probe data flow.

## 7.2 Austrian Test Results

Tests in Austria were carried out during mid March 2007 on the Boesenstein in Styria and Zell am See in Salzburg. During this period, snow levels were unusually low making access to snow slightly more difficult. Adequate layering was found above 1500m, all tests were done above 1800m.

Unfortunately an error was made during the manufacture of the two larger shear vanes. A press fit was used where a welded joint was designated. This caused the vanes to slip while rotating in the snow making the new vanes unusable. However, two vanes were manufactured in each size. One of the smaller vanes was found to have a stronger press fit than the others so a limited amount of data was obtained using the 100cm<sup>2</sup> vane. All other tests used the original 28cm<sup>2</sup> vane.

The first few days of testing used the 28cm<sup>2</sup> shear vane. The results showed a fairly good correlation to the shear frame results. The data in Figure 7.4 is depicted as closely as possible to the way it was collected. Each set of bars either represents a shear frame test or a snow probe test as indicated on the y-axis. Solid black bars and diagonally striped bars represent the average shear strength of the 10 test samples in that row. The grey speckled bars represent the standard deviation of those 10 tests,

giving an indication of the variability of the data. The layout of the tests is similar to that depicted in Figure 7.1, where “T1, P8, G1” represents the first row of snow probe tests after a shear frame test. The label “T1, P8, G1” denotes test 1 at power level 8 in 1<sup>st</sup> gear.

The two sets of snow probe tests in Figure 7.4 correlate reasonably well with the shear frame tests to either side. However, the two sets of tests (top half and bottom half) are significantly different from one another. This would suggest that the shear strength varied over the test area, with shear strength increasing further up the slope. Figure 7.5 shows all data averaged into top and bottom halves. Here it is clearly visible that the shear strength is either not consistent over the test area or that something changed during testing.

It should also be noted that the standard deviations for the snow probe and shear frame are of similar magnitude.

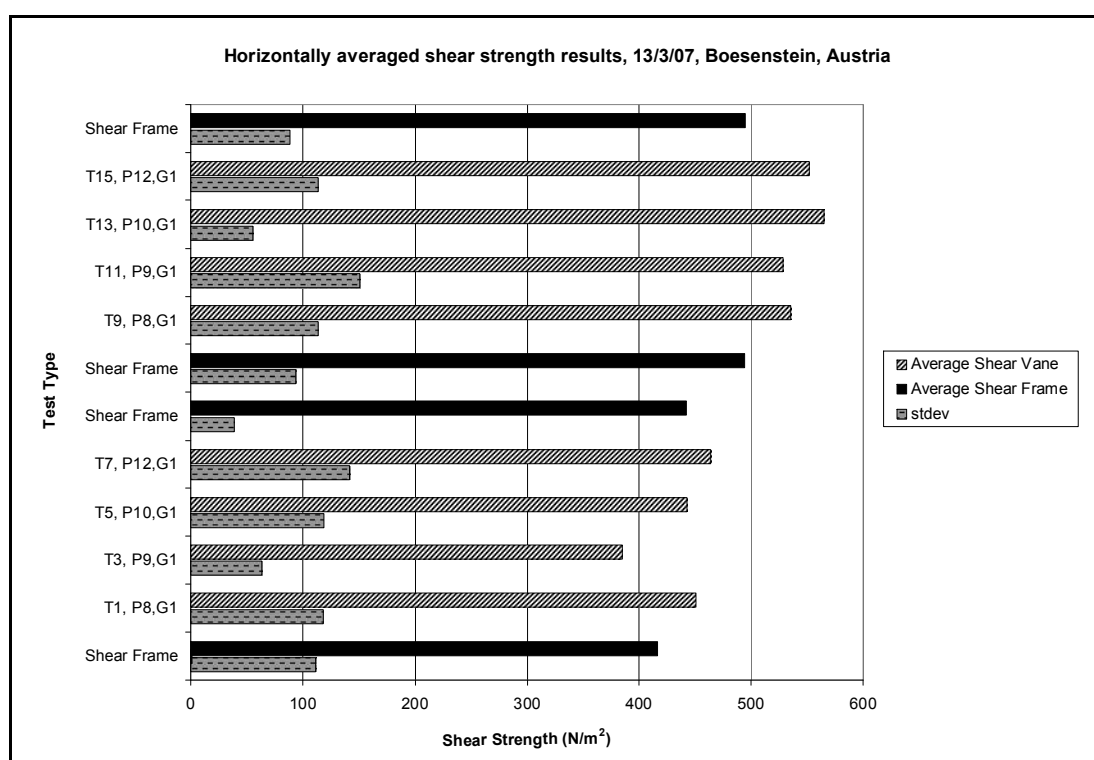


**Figure 7.4 10 point averaged shear strength values for shear frame and shear vane test results.**

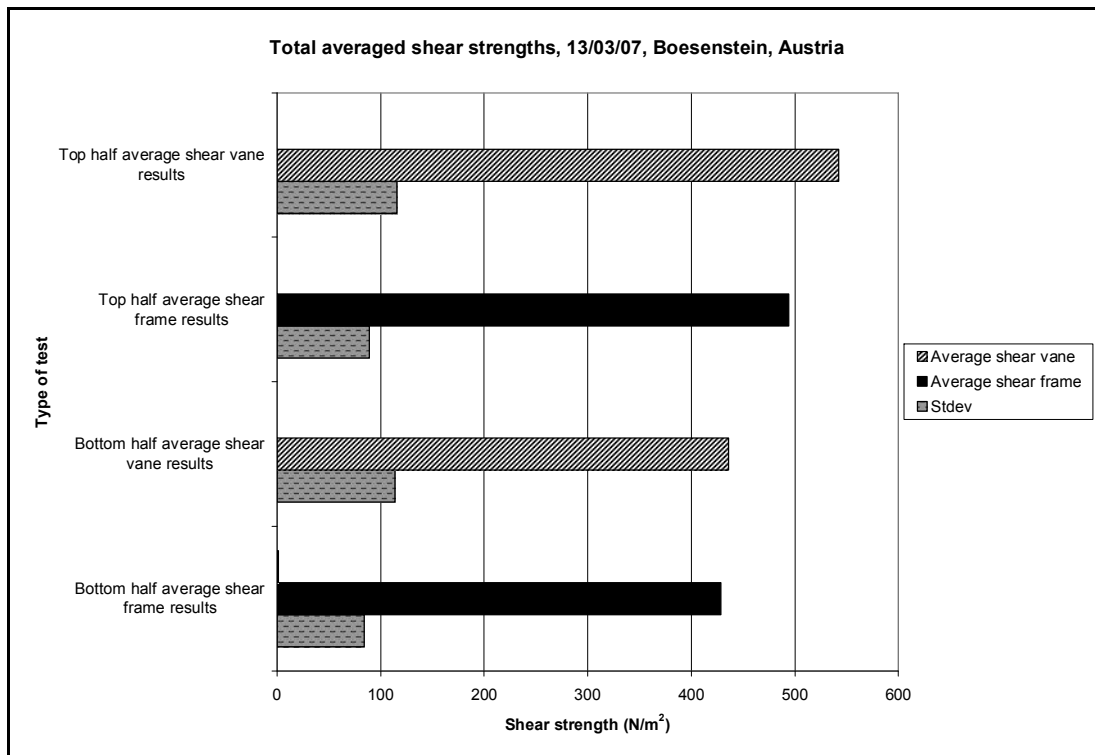


**Figure 7.5**

Figure 7.6 shows results using either a 100cm<sup>2</sup> shear vane or a low power level in 2<sup>nd</sup> gear.

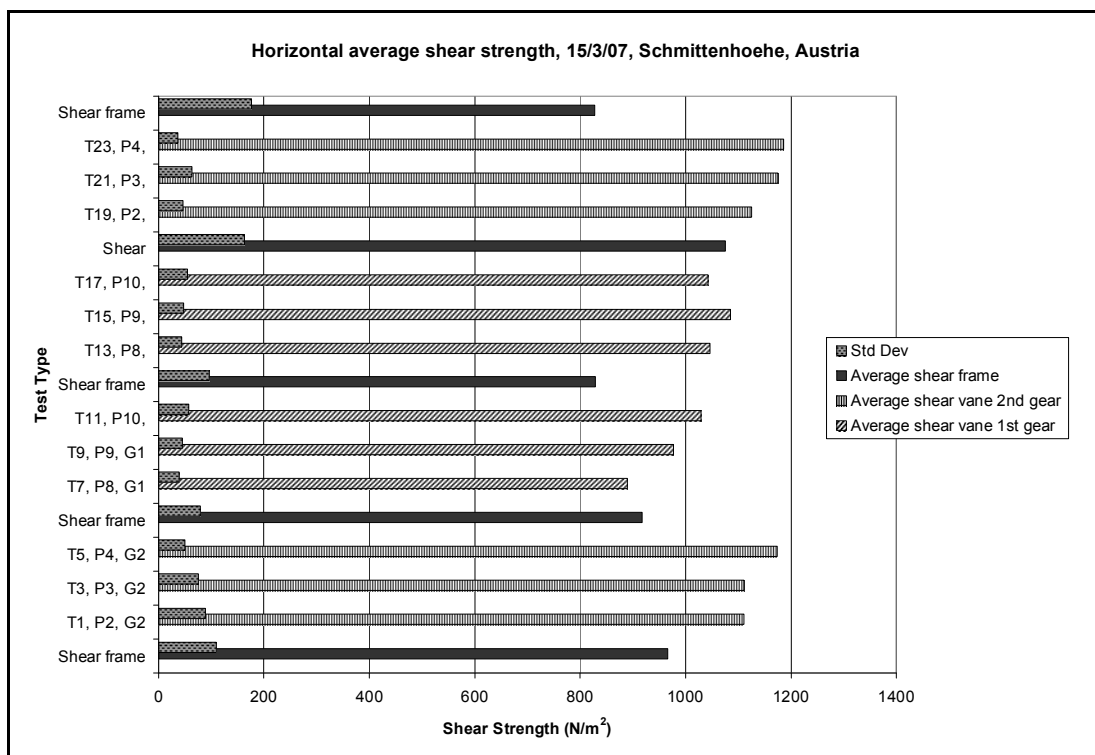


**Figure 7.6**

The data in Figure 7.6 is set up in a similar way to that in Figure 7.4. Vertically striped bars indicate tests carried out in 2<sup>nd</sup> gear using a 28cm<sup>2</sup> shear vane.



Diagonally bars indicate tests carried out in 1<sup>st</sup> gear with a 100cm<sup>2</sup> shear vane. In almost all cases the shear strength calculated by the shear vane is higher than that measured by the shear frame. This difference could be caused by:

- A characteristic of the snow probe.
- The way the snow probe was used.
- The way the shear vane was used.
- Variation in snow properties.
- Or due to the over burdening snow in the shear vane tests.

It is a well known fact that over burdening snow increases the friction component of the shear strength (McClung and Schaerer 2006). However, it is unlikely that this is the only contributing factor. Regardless of the cause differences could be accounted for in the constant  $C$ , given enough test data.

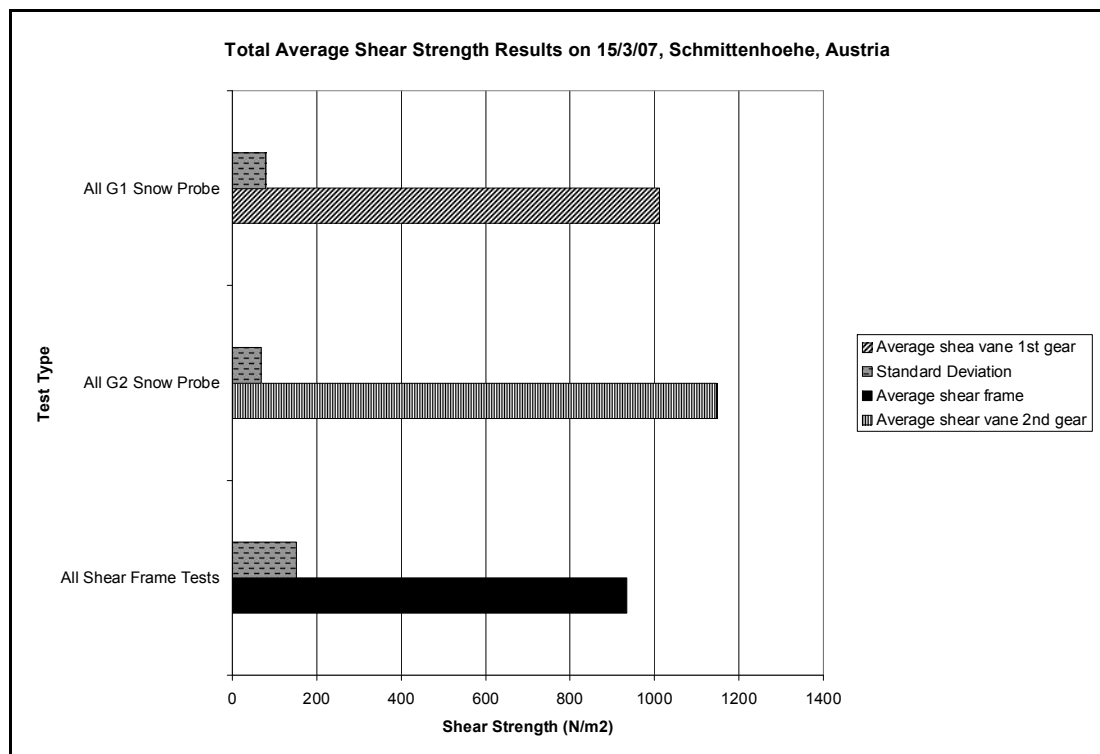


**Figure 7.7**

Even though there are differences between the tests types, values within a test type are consistent. Figure 7.7 shows the average values obtained from each test type. It is clearly visible that snow probe tests are higher than the shear frame tests. It can be argued that this is irrelevant if the results remain consistent. The standard deviations of snow probe tests are significantly lower than that of the shear frame values. This could mean that either:

- The shear frame is more susceptible to operator errors.
- The shear frame is more able to pick up variations in snow shear strength, assuming the shear strength was highly variable in the area tested.
- The snow probe is less susceptible to operator errors.
- The snow probe data is susceptible to interpretation errors.

The last two of these possibilities are likely to be the predominant factors affecting the results. Using a process of elimination, shear frame tests can easily be affected by:

- Placing the frame into the snow too deeply or not deeply enough.
- Disturbing the layer while the frame is placed into the snow.
- Variable strain rates applied by the operator.
- Non planar fracture.
- Changes in temperature.

It is unlikely that the area tested had highly variable shear strength since the area chosen was planar and had no significant features in the immediate surroundings. In conclusion the shear vane tests seem to be more consistent than the shear frame tests. Subsequent results will be shown to agree under certain conditions but in general a similar magnitude standard deviation was experienced in both shear vane and shear frame tests.

## **7.3 New Zealand Test Results**

### **7.3.1 Snow Pack Characteristics**

The winter of 2007 in New Zealand started off with a snowfall in early June followed by another in late June. July was dominated by a long clear cold periods. This cold period preserved what snow there was but also created an ideal temperature gradient for depth hoar and surface formation. These weak layers were still visible in mid August.

The winter snow pack was dominated by these deeply buried surface hoar and depth hoar layers. These layers were easily found when digging a snow pit and broke away very easily when the overlying snow crusts were cut (as in a rutschblock test or column compression test). Consequently the Snow Probe also indicated an unstable layer. However ski areas remained open due to gradual compaction of the weak layers. The untracked areas also seemed to remain relatively stable considering the

underlying snow conditions. Most of Allen's basin at Broken River did eventually avalanche on some of the deeper layers however this was spread over a several days following a major snowfall. The Remarkable Ski Area carried out extensive bombing on all of its steep easterly slopes after 50cm of new snow in early August. Nothing released for several days.

It appears the snow pack was being held together largely by the strength of the snow crusts developed in the clear cold period during July. This crust can easily be identified in both conventional snow profiles and profiles generated by the Snow Probe.

### 7.3.2 Test Sites

Because of the lack of snow in the Craigieburn range during July and August 2007, some testing was done further south at the Remarkables Ski area near Queenstown. Sites on the flat areas to the North and East of Lake Alta were picked as safe, consistent and easily accessible spots for testing (See Figure 7.8 below).

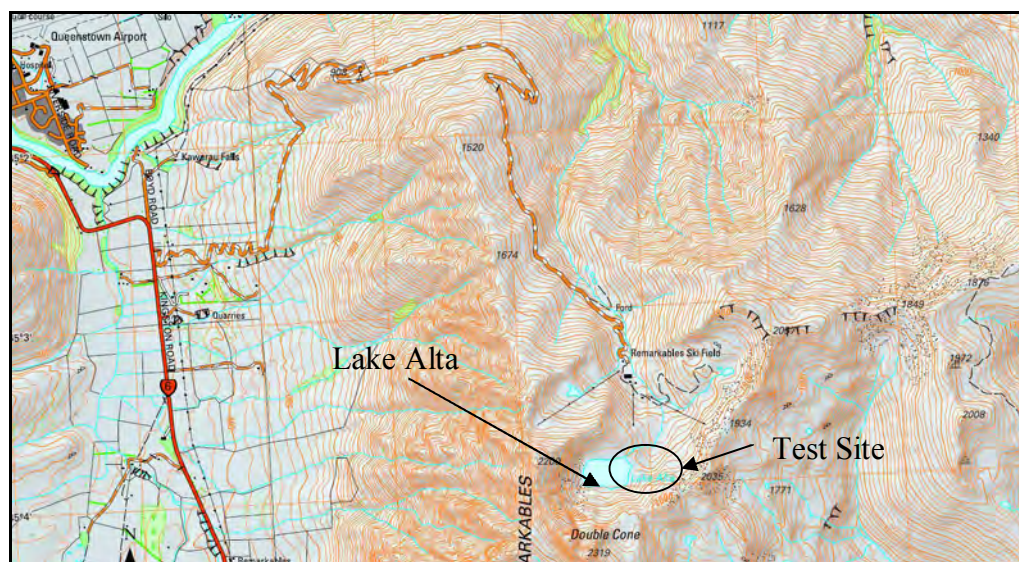


**Figure 7.8 A map of the Remarkables Ski Area near Queenstown showing Lake Alta (centre bottom) and the test sites to the North and East of Lake Alta.**

In the last few weeks of August a series of 4 tests were carried out at the Broken River Ski Area. The exact location is indicated in Figure 7.9.

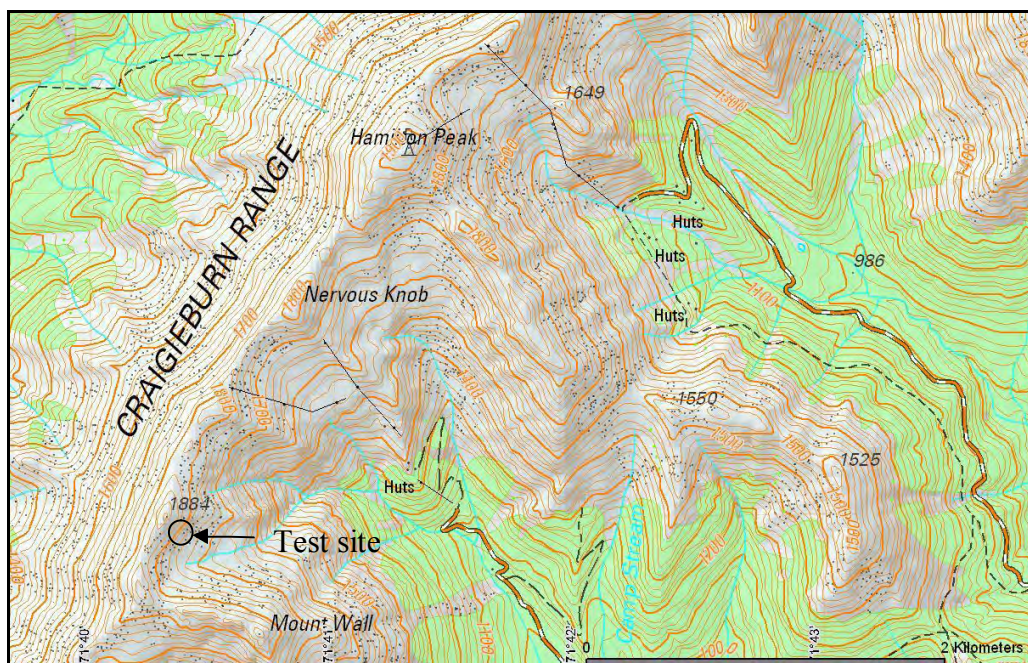
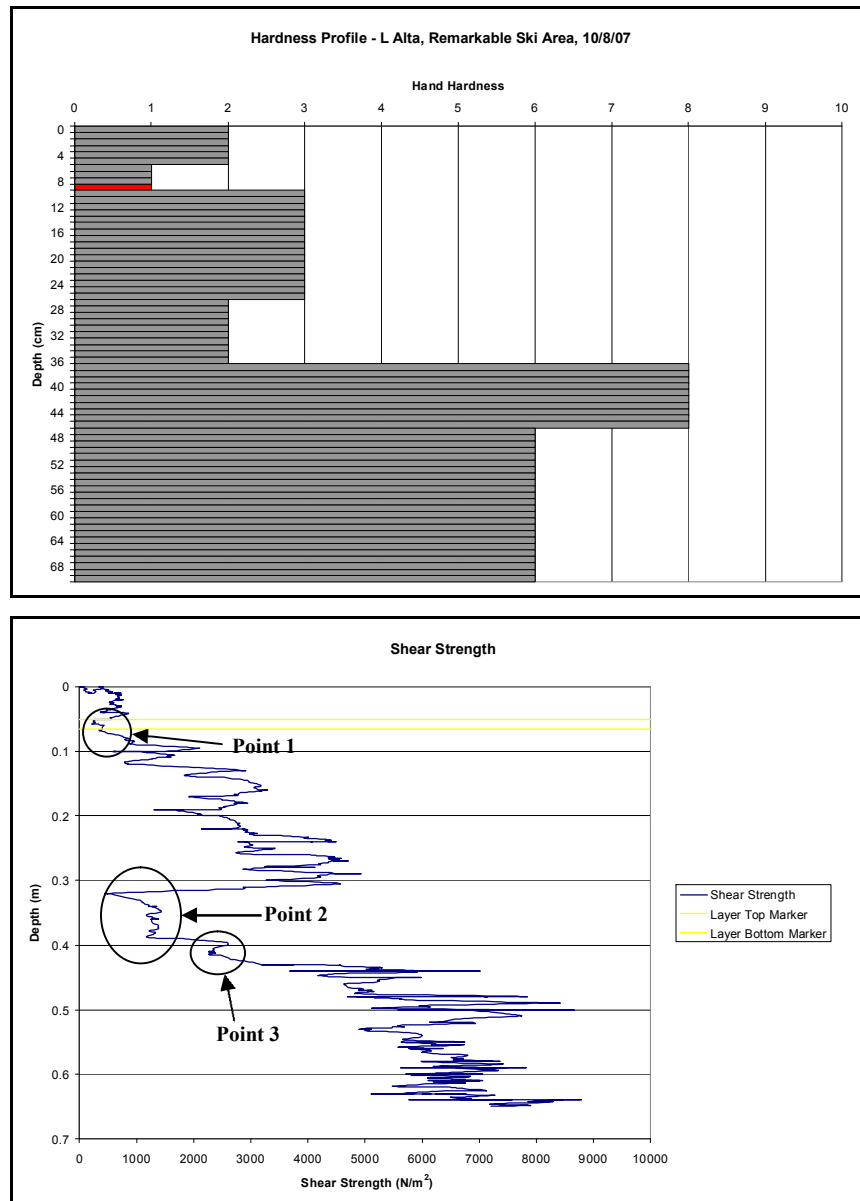


Figure 7.9 2007 test site at broken River Ski Area.

### 7.3.3 Layer Identification

Identifying layers on the graphs produced by the snow probe can be difficult at times and various methods and theories could be argued to work better. In order to assess whether repeatable results are being gathered by the snow probe, a system for identifying a layer on the results needed to be specified clearly and adhered to. Whether one chose to select data in a trough or around a peak would not have a huge impact on the final outcome as long as the selected feature is present in all graphs. The latest selection process used differs to the process used in Austria. With the addition of the range finder a graph could be produced which looked very similar to a standard snow profile as in Figure 7.10. Note that the orientation of the graphs changed to mimics standard snow profile methods.



**Figure 7.10 A hand hardness profile above and the equivalent snow probe result below.**

The general location of each layer is fairly clear. It is much more difficult to decide exactly where the shear frame measurement took place because the graph indicates a gradual increase in shear strength rather than a step change at layer interfaces, such as points 1 and 2 in Figure 7.10.

The gradual increase could be representative of the actual snow properties but it could also be caused by shear vane misalignment relative to the layer. If one assumes that the shear strength throughout a layer is relatively constant, the trough or weakest point in a layer would give the best indication of shear strength for that layer. This method becomes ambiguous when one considers the layer at point 2 in Figure 7.10. The weakest point in that layer is just below the top layer interface. Some of the reasons for this are:



- The snow at the top of the layer has the least amount of overburden loading so it is the least compacted.
- Ice layers act as vapour barriers so re crystallisation will often start just below an ice layer.
- The shear vane is driven into the snow manually so when a hard layer is reached, the rate of penetration will decrease. Once the hard layer has been broken or worn down by the shear vane the rate of penetration will increase again. The operator will try to keep the speed constant but some acceleration followed by some deceleration is inevitable. The deceleration phase may result in stand still which could in theory reduce the torque applied to the vane to near zero.

Considering this it would be logical to look at the rate of penetration and compare that to the snow profile. Figure 7.11 shows the power level and depth of penetration over time. When a hard layer reached it is possible to see a flattening of the depth line because the rate of penetration is likely to decrease when a harder layer is reached. This can be used as a visual aid in placing the lower marker line for the layer range.

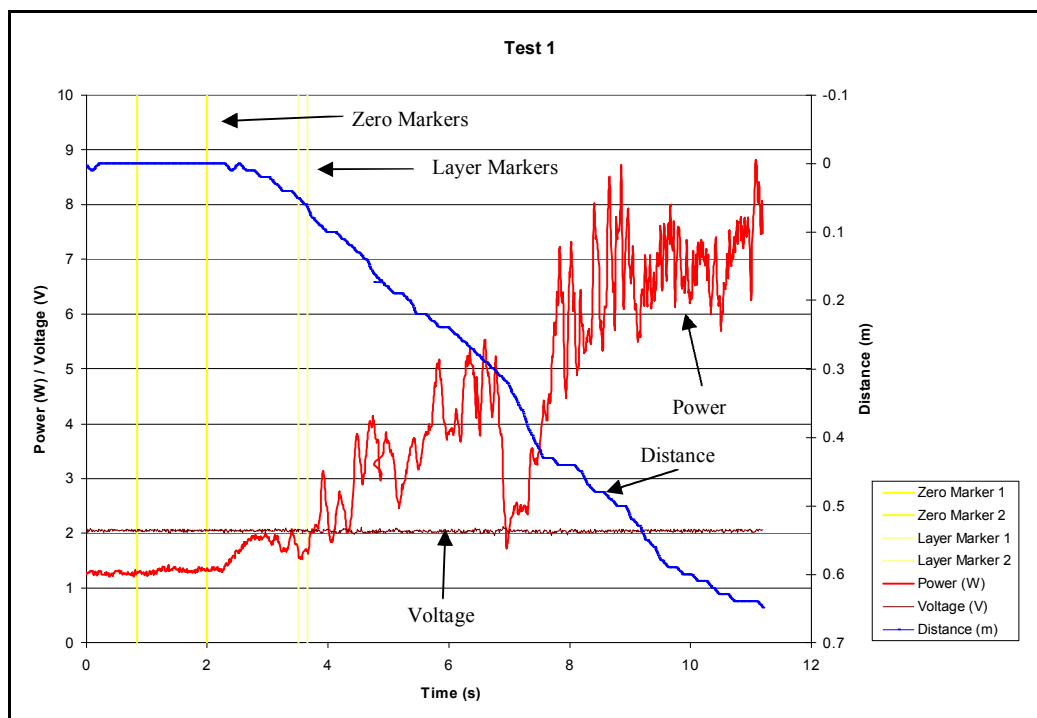


**Figure 7.11 The corresponding power profile to Figure 7.10**

If it is unclear where the layer of interest is located on the graphed data then the nearest trough is selected in all graphs.

### 7.3.4 Range Finder

Initial results from the range finder included a huge amount of scatter. It appears that the range finder was able to penetrate the snow. At times the sound waves reflected off the snow surface and at other times they reflected off a surface much further away, probably the ground. This is clearly shown in Figure 7.12. This test was done without using a reflector. Ultrasonic range finders have been used previously for measuring snow accumulation (Earl, Grey et al. 1985) but these were always as a stationary measuring device. Figure 7.12 validates this use of ultrasonic range finders since the period at the start of the test where the range finder was held stationary produce consistent results. However it appears that once the rangefinder is moving, a better reflective surface is required for it to provide accurate distance measurements.

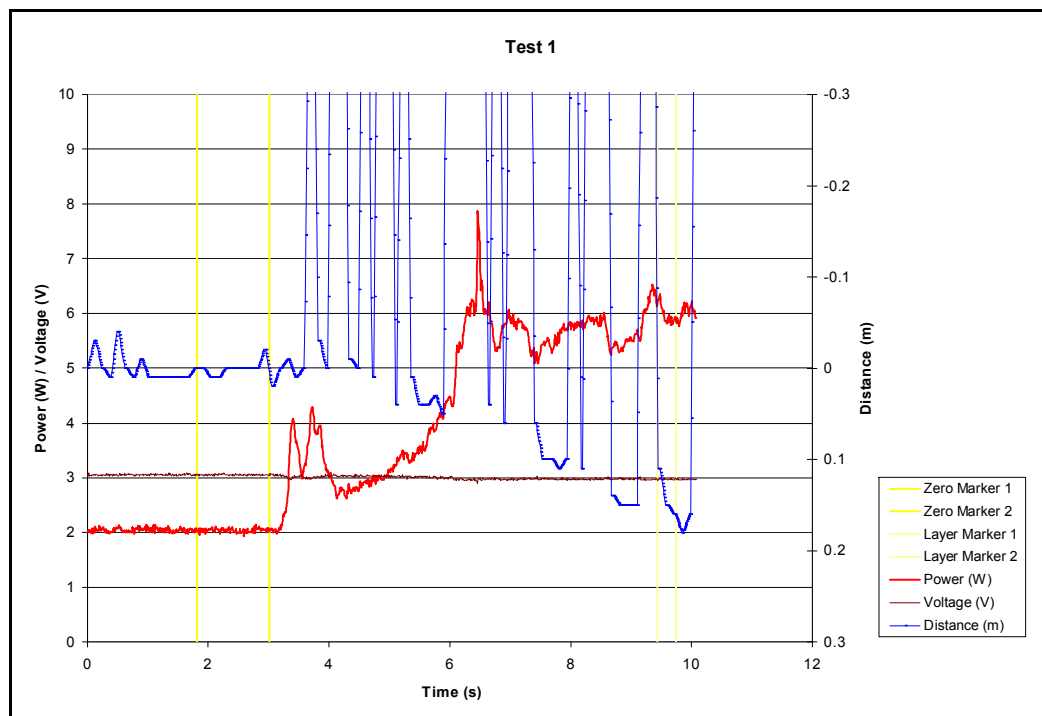


**Figure 7.12 An initial test without using a reflector.**

This problem was solved by using a 1.5mm thick aluminium plate as a reflector. The plate was 330mm x 230mm with a 30mm diameter hole in the centre (Appendix A: Prototype 1 Modification Drawings). The plate could then rest on top of the snow while the probe was being pushed through the snow (Figure 7.13).



**Figure 7.13 The snow probe with the Al reflector.**

This method was quick and easy to produce and therefore did not delay testing significantly. The design of this reflector could be modified to be far more user friendly. In this form, the user was required to hold the plate above the snow while the probe was being calibrated before each test. This introduced errors to the depth measurement:

- Because the plate was held 2-4cm above the snow during calibration, a displacement of 2-4 cm occurred on the snow profile.
- Because the plate was being held by the user its height varied slightly introducing more variability.

These two factors could largely be eliminated by manipulating the data after a test. This manipulation did not affect the actual test data although a small vertical shift of the whole profile was possible. This was only a problem when one tried to overlay several profiles.

The plate did not eliminate all scatter from the profile data. Spikes in the depth measurement did occur. This was likely due to the probe, range finder and and/or reflector not being aligned properly. This type of error has been corrected by replacing the spike with an assumed constant rate of penetration equivalent to a straight line bridging the gap where the spike once was.



Another significant issue with the range finder was that it had a 1cm resolution and a sample rate of about 10Hz, while the remaining probe devices sampled at 100Hz. It was logical to assume that the probe moved at a relatively constant rate so a 10 point moving average was used to smooth the data. This gave the snow profiles far greater definition.

### **7.3.5 Minimum Shear Strength Lines**

The minimum shear strength line refers to lines drawn on shear strength profiles in the following sections. If the shear strength is measured at a given layer and an approximate weight is known for the overburdening snow one could calculate the shear strength required to hold an isolated block of snow on a given slope of a given angle. A continuation of this would be to draw a line of minimum shear strength on a shear strength profile. Any shear strength dropping below this line would be potentially unstable. These lines give the minimum requirement for failure but do not mean there will be a snow failure. There are other forces which help to keep the snow on the slope such as compression below and tension above.

To estimate these lines, a constant density of  $250\text{kg/m}^3$  was estimated for the overburdening snow and angles at  $10^\circ$ ,  $20^\circ$ ,  $30^\circ$  or  $40^\circ$  were selected.

These are estimates only and do not provide accurate conclusions in the present form but demonstrate a good method for data display in future work.

### **7.3.6 Results**

An explanation of some of the more noteworthy days will be given in the following section. Several more days of testing were completed which are not included here but also reinforce the results shown in these following sections. All tests can be viewed in Excel format located on the attached CD. The folders are labelled according to date and testing location. The files are labelled T1-P4-G2-V1.xls which corresponds to test 1, power level 4, gear 2 and a 60mm diameter shear vane. The shear vanes were named V1, V2 and V3 corresponding to the 60, 113 and 180mm diameter shear vanes respectively. Each data file contains 5 tests which feed results to a summary workbook.

The results in the coming section show that the shape of the hardness profile and the shape of the shear vane strength profile compare well and that the results are very repeatable. However the results also show that there is an inconsistent difference

between shear frame and shear vane strength results. An attempt has been made to explain this difference by looking at the rate of penetration into the snow and the rate of rotation in more detail. These two velocities combine to give a vane approach angle (Figure 7.38).

To give an indication of the rate of descent and the rate of rotation, average values have been calculated. These assume constant rates throughout the test which is clearly not very accurate. The probe descent and rotation will slow down if a hard layer is encountered. The values have been calculated to illustrate the effect of the rate of descent and rotation on the accuracy and clarity of the profile. These values are not used in any further calculations. Rotational rates were taken to be constant at about 10% below the no load speed which is also in accurate. Rotational rates also varied depending on layer hardness so this assumption of constant rotation was used illustratively only.

A minimum approach angle was defined as the smallest angle for which the shear vane still rotated through undisturbed snow (Table 7.1). This gave a base line for which to compare other approach angles to. See Figure 7.38 for more details on approach angles.

**Table 7.1 The minimum approach angle required to ensure that the shear vane is always rotating through new snow.**

Vane Radius m	Vane Circumference m	Vane Height m	Approach Angle Degrees
0.0300	0.188	0.005	6.1
0.0565	0.355	0.005	3.2
0.0900	0.565	0.006	2.4

The helix pitch has also been estimated to get an indication of the required space between blade passes. The helix pitch is the vertical distance between blade passes. The amount of undisturbed snow remaining between passes is the helix pitch minus the vane height (5mm or 6mm depending on the vane)(See Figure 7.38).

### **7.3.6.1 Remarkables Ski Area, lake Alta, 7/8/2007**

The snow pack on the 7<sup>th</sup> was relatively simple. Layers were widely spaced (See Figure 7.14) making testing much easier. Shear frame tests were done above a layer at about 21cm from the top. The test area faced SW. The snow profile generated by the snow probe in Figure 7.15 below follows a similar trend as the manual snow

profile. The layer at 21cm is clearly visible though slightly closer to the top than in Figure 7.14. The next layer interface shown in Figure 7.14 at 31cm is also clearly visible in Figure 7.15 at 30cm. The layer at 21cm is harder to see in Figure 7.16 even though it had the same test parameters. It is also evident that the scatter at higher shear strengths is much greater.

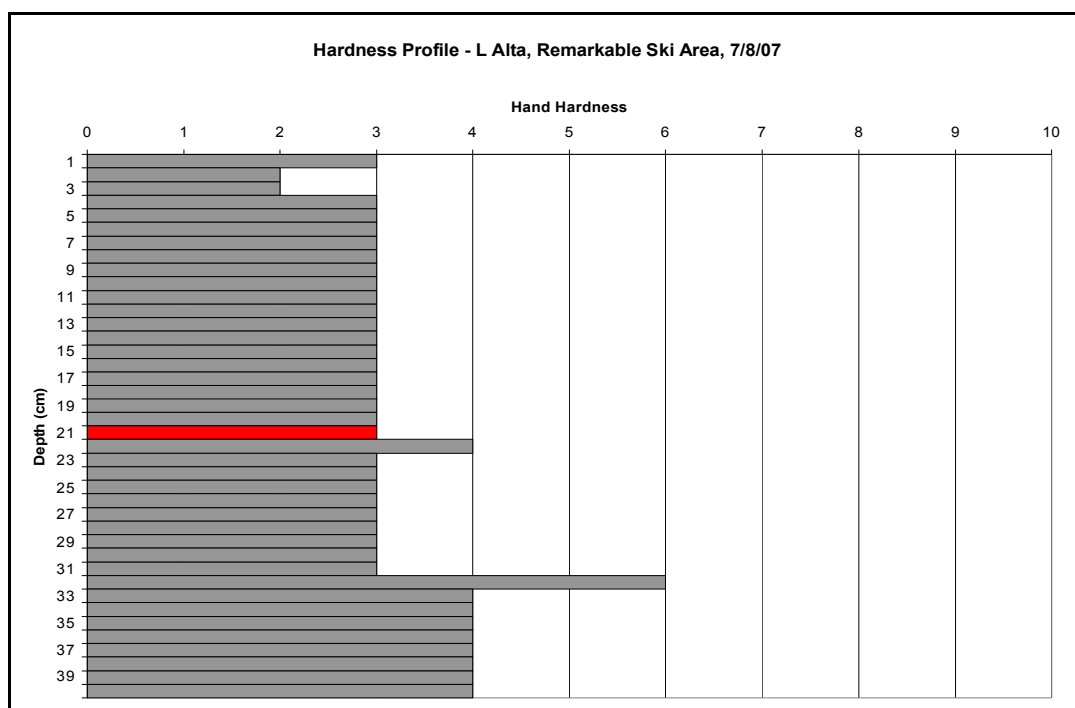


**Figure 7.14 A standard hand hardness snow profile indicating the layer tested with a shear frame in red.**

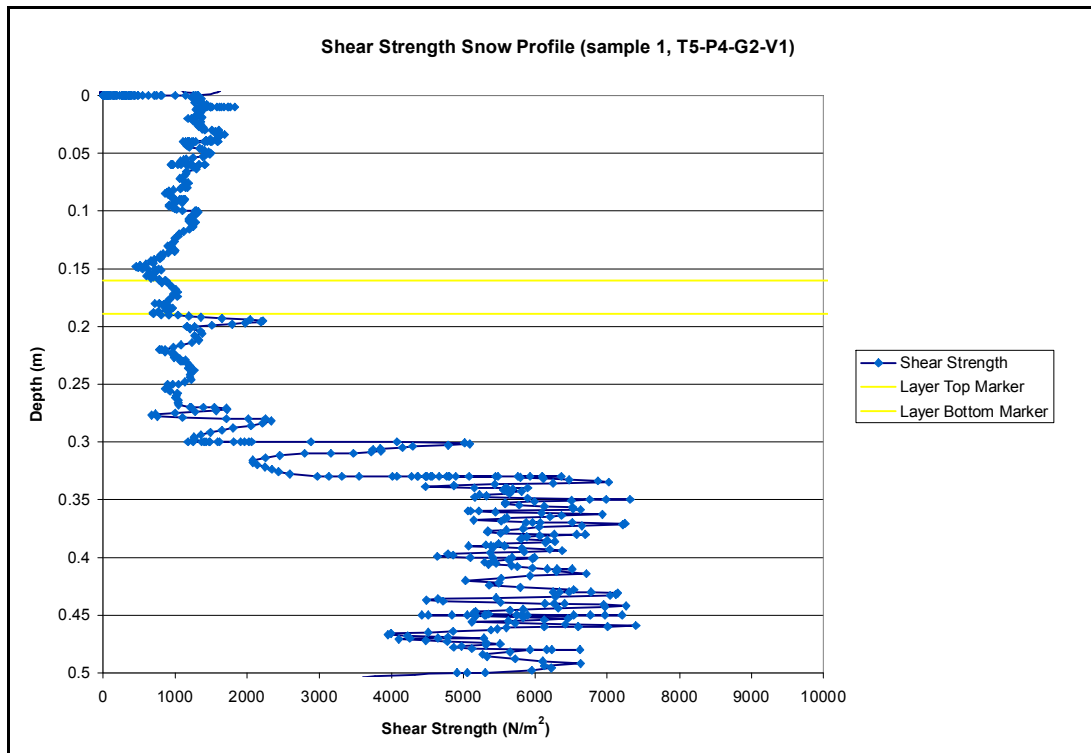


**Figure 7.15** A typical profile generated by the probe using, power level 4, gear 2 and a 60mm diameter shear vane size. The rate of penetration was estimated as 0.079m/s.

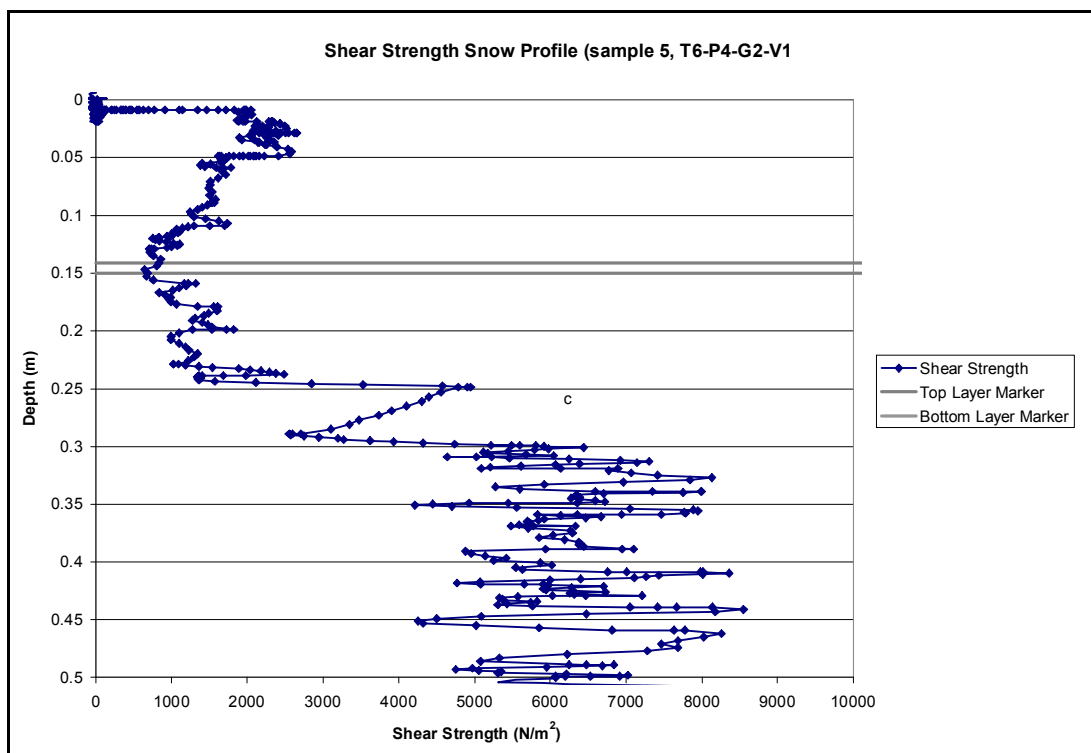


**Figure 7.16** A typical profile generated by the probe using, power level 4, gear 2 and a 60mm diameter shear vane size. The rate of penetration was estimated as 0.118m/s.

The repeatability of the graphs is illustrated to some degree in Figure 7.17 (right side) where 5 test profiles are shown on one graph. All features are still visible

though the tested layer has moved from 21cm in the hardness profile to about 17cm. This graph was also compared to the hardness profile (Figure 7.17 left side) which shows good correlation between the two graphs.

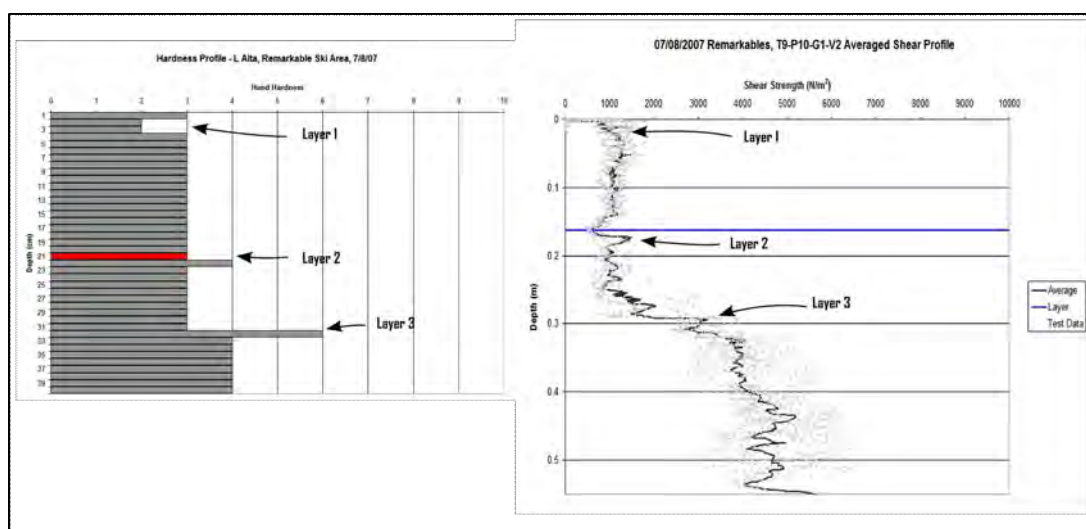


**Figure 7.17 an average of the 5 profiles done in test 9 (right) compared with the standard hardness profile (left).**

Table 7.2 gives overall estimates of the rate of descent and the approach angle. Approach angles for tests 5-8 were the highest found in any tests done during the 2007 season. This corresponds to a C value very close to 1 which is evident in Figure 7.18.

**Table 7.2 An estimate of the approach angle assuming a rotational velocity and constant penetration rate.**

07/08/2007 Remarkables						
Test Name	Estimated Average Rate of Penetration	Vane Radius	Estimated RPM	Approach Angle	Helix Pitch	C
	m/s	m	rpm	Degrees	mm	
T3 & T4, P9, G1, V2	0.07	0.0565	70	9	14	0.8
T5 & T6, P4, G2, V1	0.10	0.03	90	19	16	0.9
T7 & T8, P4, G2, V1	0.10	0.03	90	19	16	1.0
T9 & T10, P10, G1, V2	0.09	0.0565	75	11	17	0.9

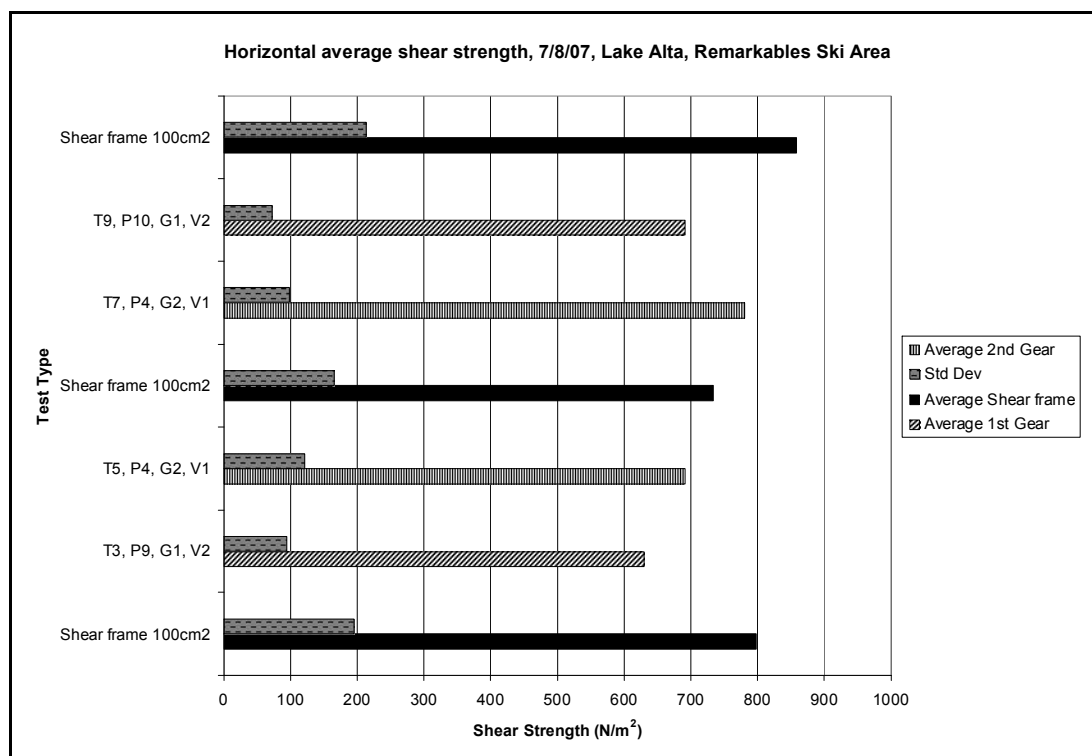


**Figure 7.18 averaged shear strength over 10 sample probes.**

Figure 7.18 shows the average of each horizontal row of 10 test profiles and standard deviation in speckled grey as a measure of variability. This graph is significant because it shows a test result with a C value very close to 1 ( $C=0.90$ ). Standard deviations were also lower than those recorded in shear frame tests. This indicates shear vane tests had lower variability and reasonable correlation with shear frame tests with the conditions outlined above.

### 7.3.6.2 Remarkables Ski Area, lake Alta, 10/8/2007

This test was done in close proximity to the previous test on the 7<sup>th</sup> however this test was done on a NE face. The hand hardness snow profile (Figure 7.19) is significantly different and illustrates how dependant snow characteristics are on orientation and proximity. The profile is still relatively simple, layers are widely spaced and easily recognisable. It was found that the weakest layer in the snow pack was the interface about 26cm below the surface. Unfortunately it was not possible to test this interface using a shear frame. Shear frames require the weak layer interface to have the harder surface below so as not to destroy the interface when inserting the frame.

Several different vane sizes and power levels were tested with the snow probe so as to get an understanding of how this affected results and potentially find an optimum

combination of variables. The following 3 graphs (Figure 7.20, Figure 7.21 and Figure 7.22) all show similar form to the manual snow profile in Figure 7.19.

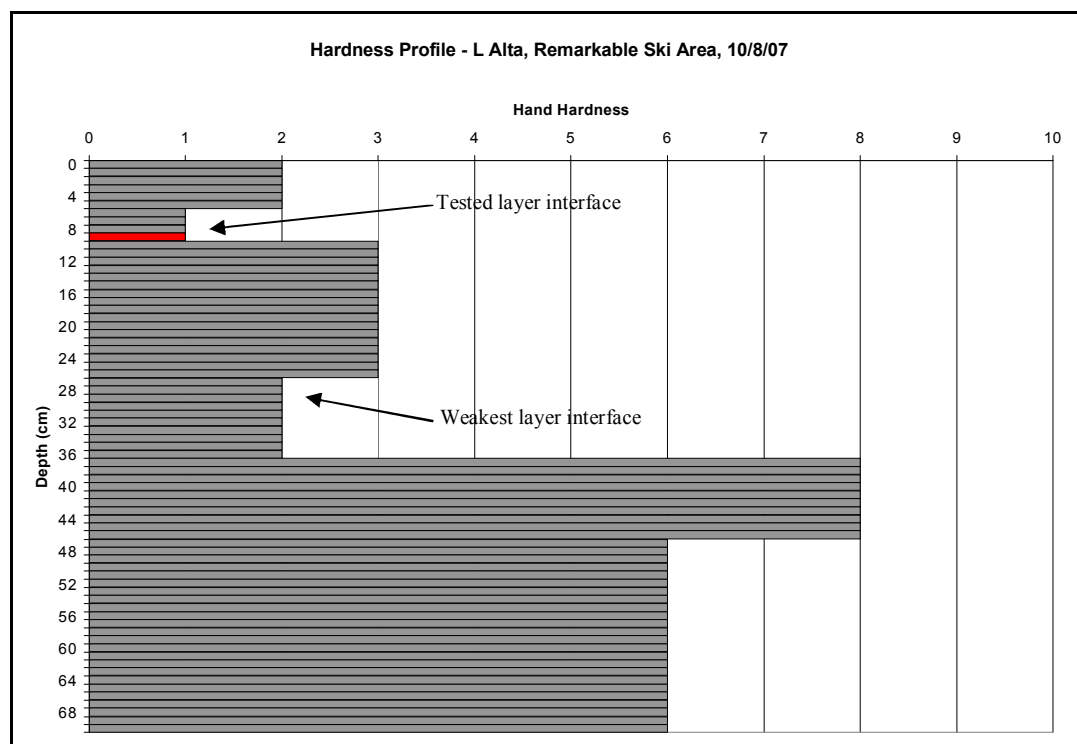


**Figure 7.19** a standard hand hardness profile with the layer tested with a shear frame indicated in red.

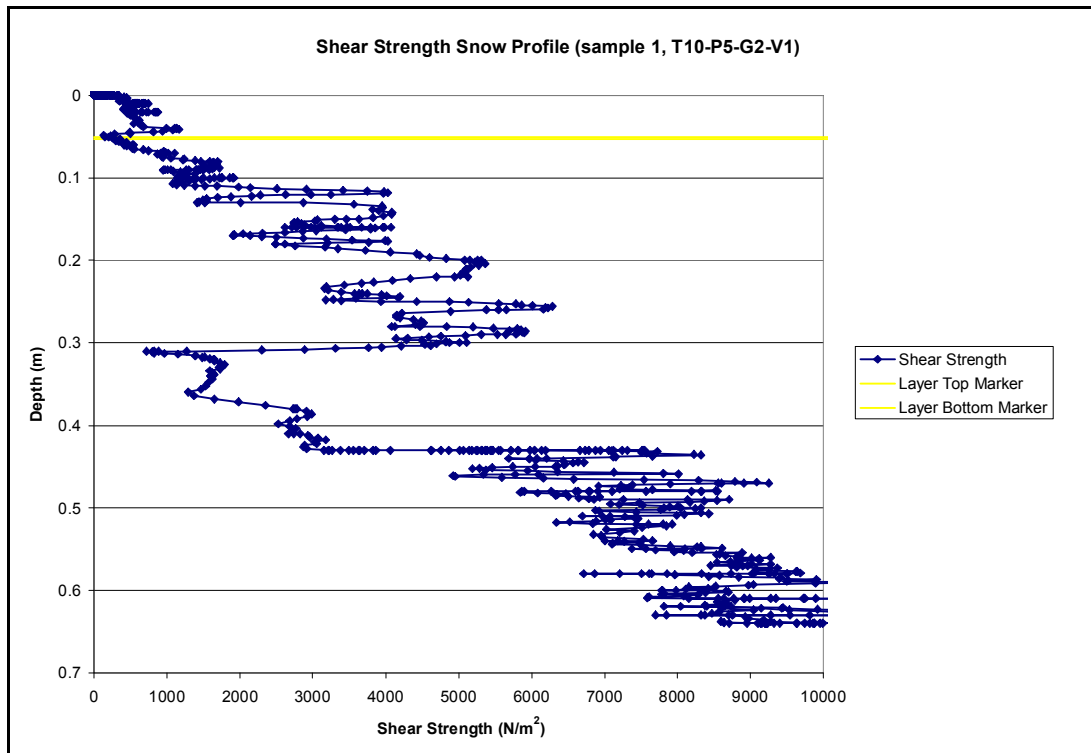


Figure 7.20 a shear strength profile generated using power level 5, gear 2 and a 60mm diameter shear vane.

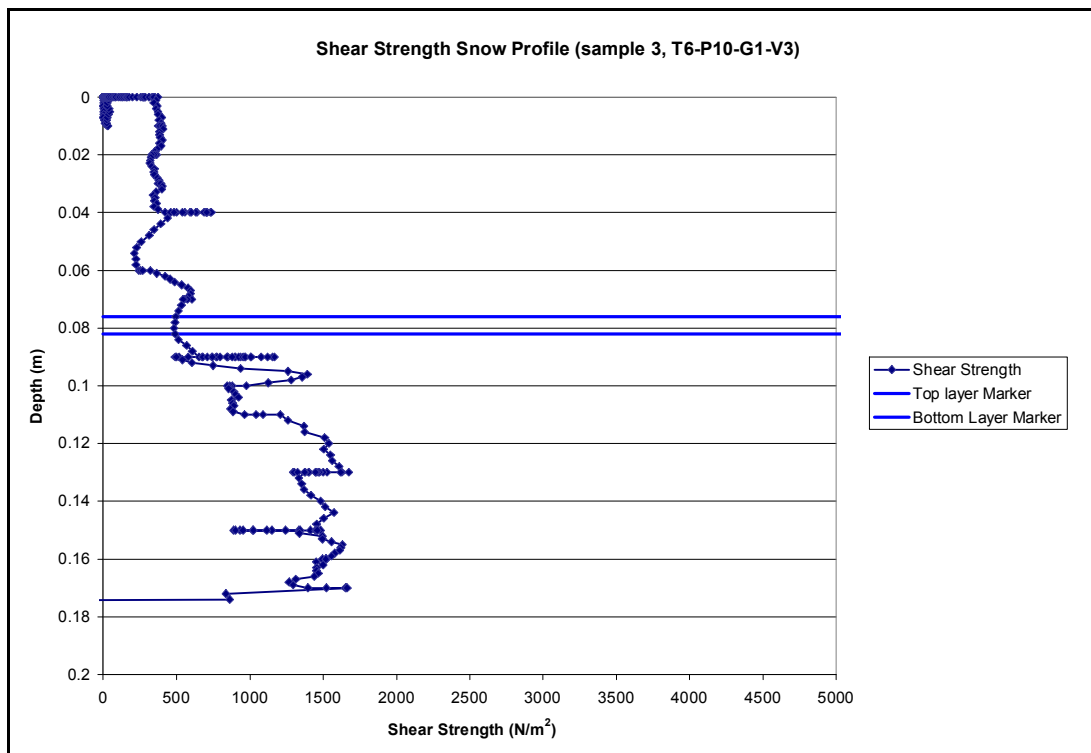
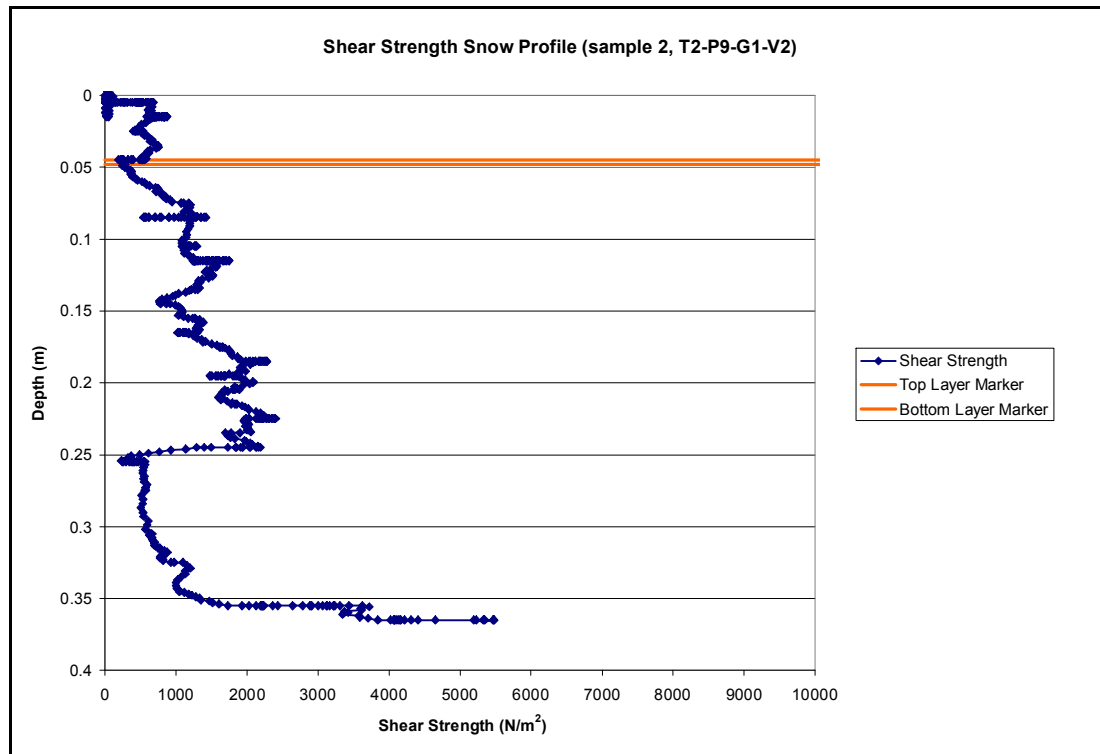


Figure 7.21 a representative shear strength snow profile using power level 10, gear 1 and a 180mm diameter shear vane.





**Figure 7.22 a representative snow profile using power level 9, gear 1 and a 113mm diameter shear vane.**

Figure 7.20 depicts a full length profile using a small shear vane (60mm). The profile is a very good approximation of Figure 7.19. The weakest interface at 26cm is clearly visible as is the tested layer. Selection of the tested layer was somewhat tricky. The shear strength within the layer seems to increase semi linearly making it difficult to decide where to select a representative range. The weakest point in the layer was chosen, as described in section 7.3.3. This method under estimates the shear strength since the selection is at the top of the tested layer rather than at the bottom. This also applies to Figure 7.22 where the top of the weak layer was selected rather than the bottom.

Figure 7.21 depicts a profile where a 180mm diameter shear vane was used. The larger vane size meant the probe was only able to test the softer upper layers of snow. The layer at 9cm is clearly visible and a section between 7 and 9cm has been selected as the range tested by the shear frame. The selection is located at the weakest point in that layer rather than directly on the interface as described in the layer identification section (Section 7.3.3).

This explains why in Figure 7.23 the average shear strength for tests 5 and 6 is significantly higher than for the other tests. The average shear strength obtained from the shear frame tests is between 0.5 and 0.6 times the size of those generated by the

snow probe, excluding test 5. The ratio for test 5 is 0.8. This ratio could in theory be substituted in to Equation 5.4 if a consistent ratio were found. The standard deviation for the snow probe tends to be slightly larger than that of the shear frame tests.

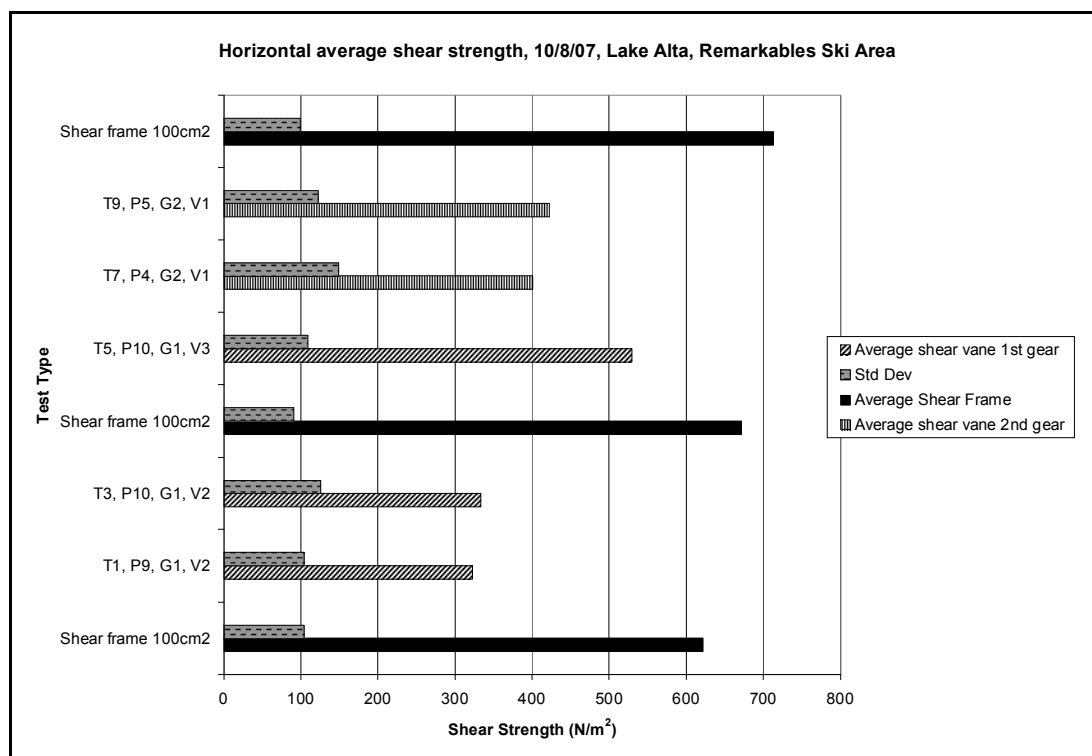


Figure 7.23 averaged shear strength over 10 sample probes.

Test 5 has a higher average shear strength because it was relatively easy to locate exactly where the layer interface was with little scatter. The difference in this test is that a larger shear vane is used.

Table 7.3 shows the approach angles estimated for this series of tests. Although the approach angle is far lower for tests 5 and 6, the helix pitch is similar to other tests.

Table 7.3 An estimate of the approach angle assuming a rotational velocity and constant penetration rate.

10/08/2007 Remarkables						
Test Name	Estimated Average Rate of Penetration	Vane Radius	Estimated RPM	Angle of attack	Helix Pitch	C
	m/s	m	rpm	Degrees	(mm)	
T1 & T2, P9, G1, V2	0.08	0.0565	70	11	17	0.5
T2 & T4, P10, G1, V2	0.09	0.0565	75	11	18	0.5
T5 & T6, P10, G1, V3	0.07	0.09	75	6	15	0.8
T7 & T8, P4, G2, V1	0.07	0.03	90	13	11	0.6
T9 & T10, P5, G2, V1	0.08	0.03	100	14	12	0.6

### 7.3.6.3 Broken River Ski Area, Yukon Basin, 30/8/2007

Several short fronts over the preceding weeks made the snow profile far more complex with several very thin layers present (Figure 7.24). There were several weak

layers buried below a 40cm depth. Selection of a layer thick enough to test with a shear frame was difficult. A layer at about 13cm from the surface was chosen. This layer proved to be very consistent and sheared cleanly with the shear frame. Consequently the shear frame strength was very consistent. The general shape of the hardness profile is clearly visible in the shear strength profile, Figure 7.25 where us a 60mm diameter shear vane was used, however when a 113mm diameter shear vane was used in Figure 7.26, much of the finer detail was lost. Figure 7.27 gives an indication of the rate of penetration. Clearly this rate was not very constant which may be why some of the finer detail was lost.

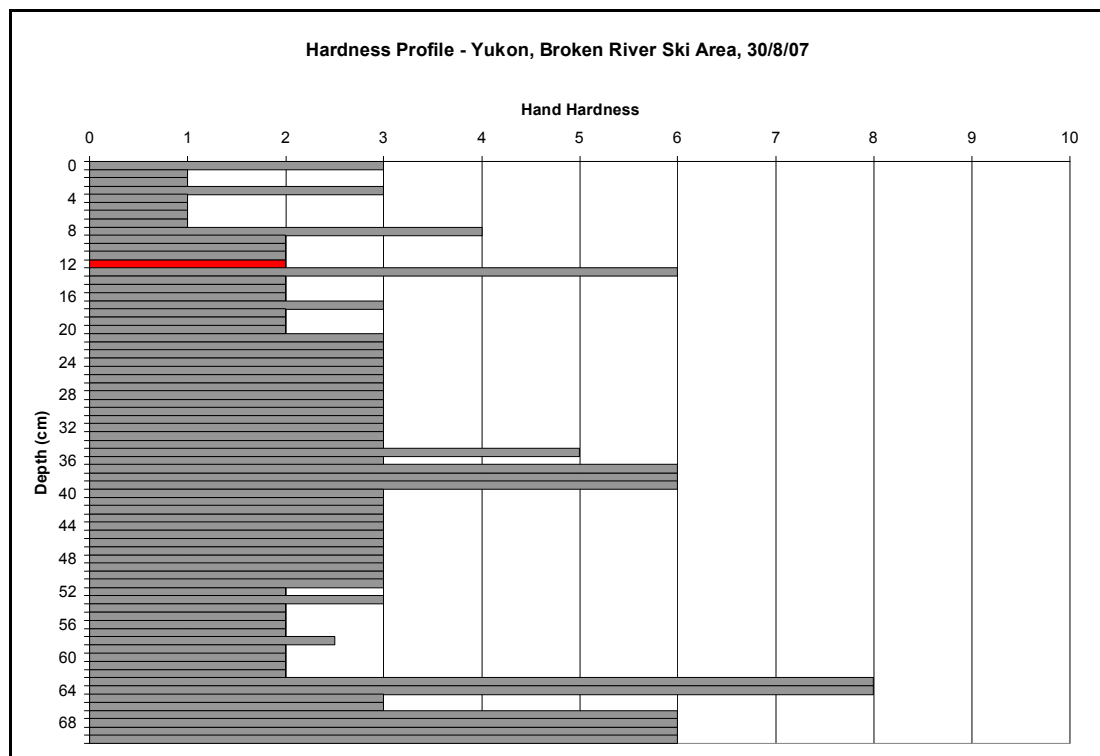


**Figure 7.24 a standard hand hardness profile with the layer tested with a shear frame indicated in red.**

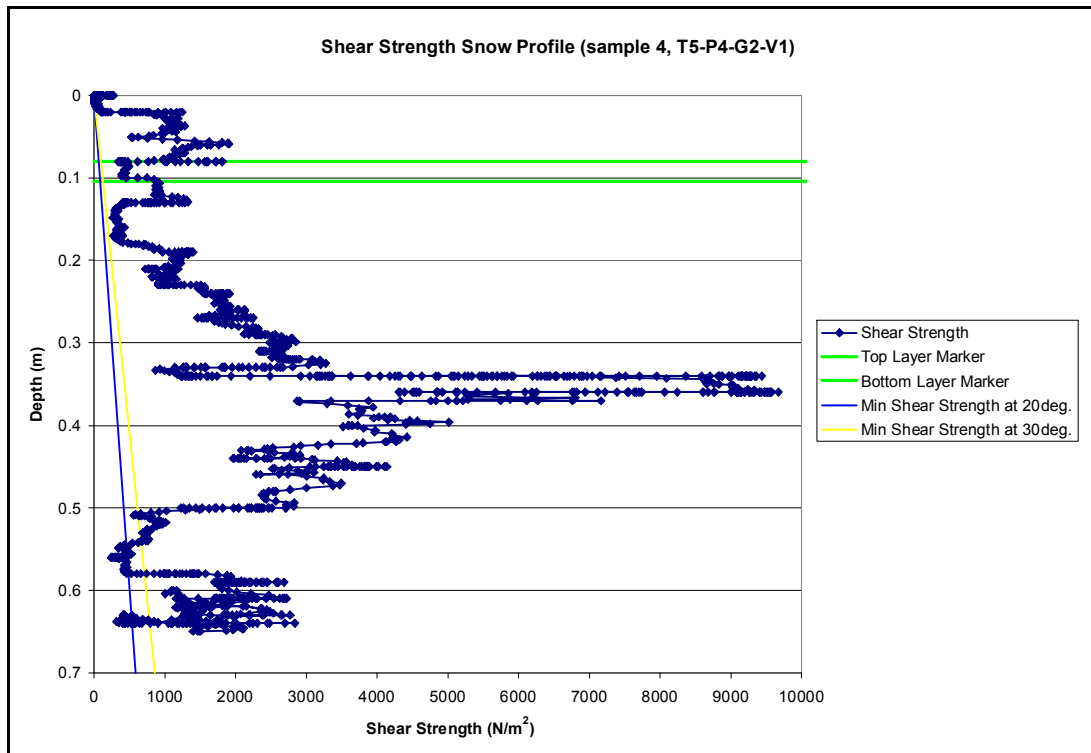


Figure 7.25 a representative snow probe profile using power level 4, gear2 and a 60mm diameter shear vane.

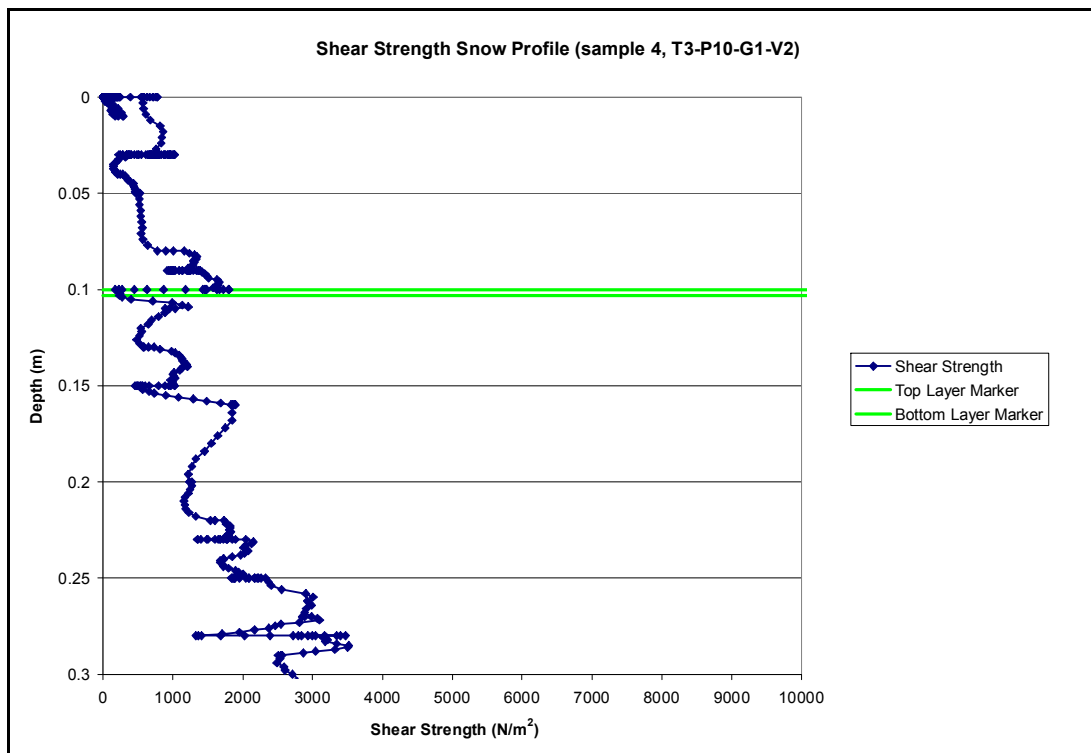
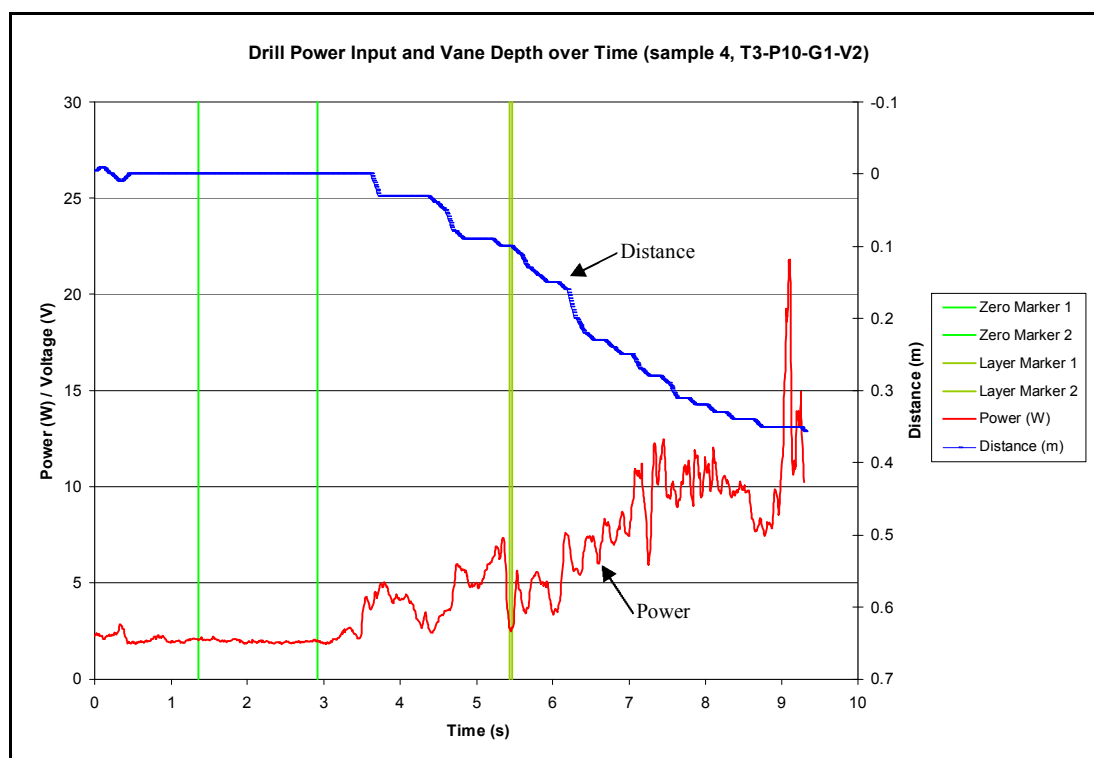
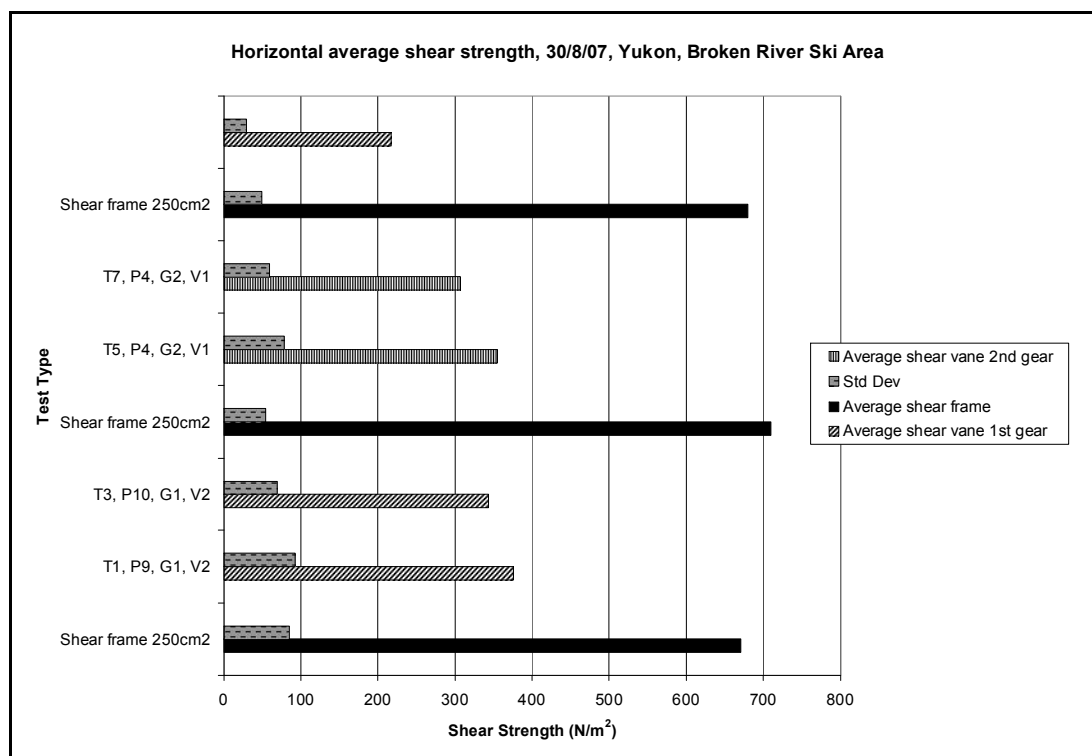


Figure 7.26 a typical profile generated by the snow probe using a power level of 10, gear 1 and a 113mm diameter shear vane.



**Figure 7.27 The graph used to generate Figure 7.26 showing the penetration depth and the drill power input.**

Figure 7.25 is typical of the full depth tests done with the 60mm diameter shear vane on this day. Some of the thinner layers cannot be identified but the general trend is easy to see. The weak layers below 50cm depth are most interesting. The two blue and yellow diagonal lines indicate the minimum shear strength required to hold the snow on the slope assuming a slope of 20 or 30 degrees respectively. A constant density of  $250\text{kg/m}^3$  was assumed for these guide lines. If the shear strength depicted on this graph is assumed to be correct, then weak layers below 50cm depth have lower shear strength than would be required to hold the snow on the slope. However the shear strength was likely to have been somewhat higher as can be seen in Figure 7.28 and Table 7.4, snow probe results are between 0.3 and 0.5 times the size of shear frame results. This means that shear strength profiles are likely to show strengths lower than actual strengths.



**Figure 7.28 averaged shear strength over 10 sample probes.**

Figure 7.26 shows a typical profile generated using a 113mm diameter shear vane on the 30<sup>th</sup>. It is difficult to see the resemblance between this graph and the hand hardness profile (Figure 7.24). This could be due to the size of the shear vane. The larger the shear vane the more precisely the probe needs to be perpendicularly aligned to the snow surface. Any deviations and the shear vane could span two layers at once blurring the layer boundaries. However as mentioned previously and shown in Figure 7.27 the penetration rate was slightly erratic which would also lead to loss of definition.

Figure 7.28 indicates good constancy between the various tests and a standard deviation of similar magnitude to the shear frame tests. As mentioned previously a C ratio of between 0.3 and 0.5 exists between snow probe and shear frame results. This ratio is quite low and will partially be due to the way the layer was found on the graph, as discussed earlier.

**Table 7.4 An estimate of the approach angle assuming a rotational velocity and constant penetration rate.**

30/08/2007 Broken River						
Test Name	Estimated Average Rate of Penetration	Vane Radius	Estimated RPM	Angle of attack	Helix Pitch	C
	m/s	m	rpm	Degrees	(mm)	
T1 & T2, P9, G1, V2	0.07	0.0565	70	10	15	0.5
T3 & T4, P10, G1, V2	0.08	0.0565	75	10	16	0.5
T5 & T6, P4, G2, V1	0.05	0.03	90	11	9	0.5
T7 & T8, P4, G2, V1	0.06	0.03	90	11	9	0.4
T9 & T10, P9, G1, V2	0.03	0.0565	70	4	7	0.3

It is also worth noting that tests where the helix pitch was low (e.g. close to the vane height of 5mm), the C ratio was also low. This would tend to indicate a requirement for more space between blade passes.

#### **7.3.6.4 Broken River Ski Area, Yukon Basin, 31/8/2007**

Tests for this day were done on the same slope, aspect and within 5m of the previous days testing. The hardness profile (Figure 7.29) on this day was done by Henriette Beikirch, a ski patroller working at the Broken River ski area. The profile was similar to the previous days. It is possible that some of the differences between the two days come from differences in interpretation but it is certain that some of the differences come from snow degradation. Both days were very warm and virtually cloudless. The temperature at the top of the snow pack had increased by almost 1 degree while 10cm deeper it remained the same.

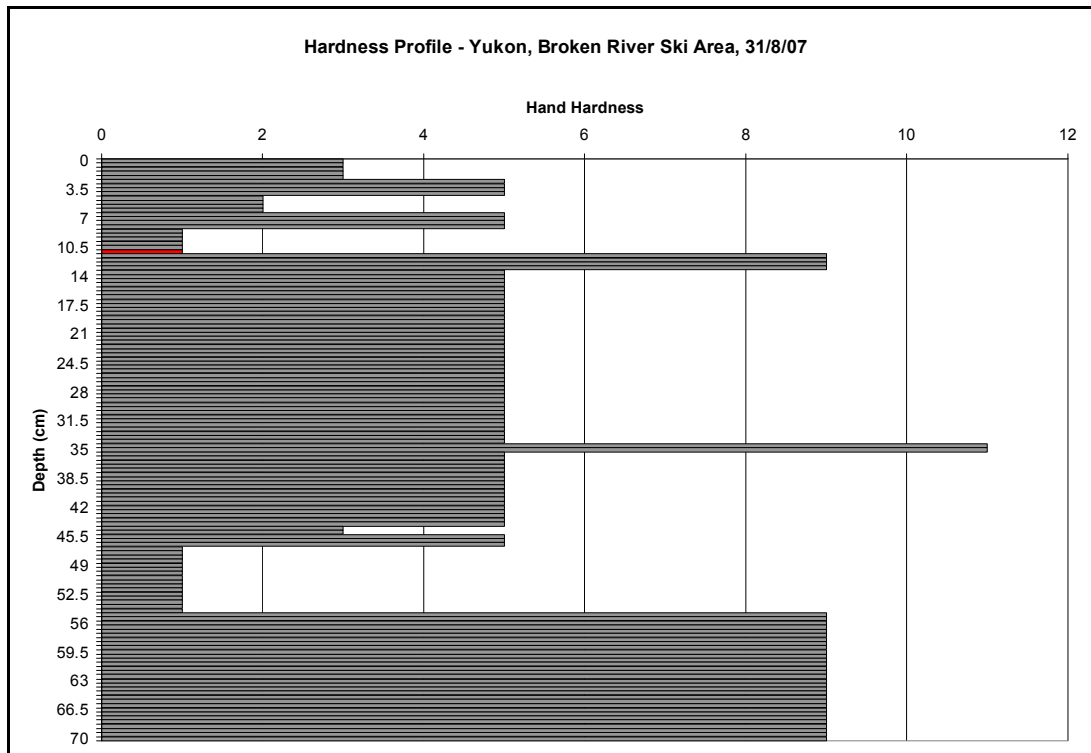


**Figure 7.29 a standard hand hardness profile with the layer tested with a shear frame indicated in red.**

The general trend remains the same though the individual layers are more defined. This is backed up with the results from the snow probe. Figure 7.30 and Figure 7.32 show very defined layers. This is note worthy because the testing in Figure 7.26 and Figure 7.30 have been done in exactly the same manner and in a snow pack that is also very similar. The main difference is illustrated in Figure 7.27 and Figure 7.31 where the depth of penetration over time can be seen. The average penetration speeds are about 0.064m/s for the earlier and 0.030m/s for the later of these graphs. The individual estimated approach angles were calculated to be  $8.3^{\circ}$  for the earlier and  $4.0^{\circ}$  for the later at the vane perimeter.

The stepped nature of the distance line on Figure 7.31 is due to low range finder resolution. Some smoothing has been applied to the distance line but in future prototypes a higher resolution would be beneficial.



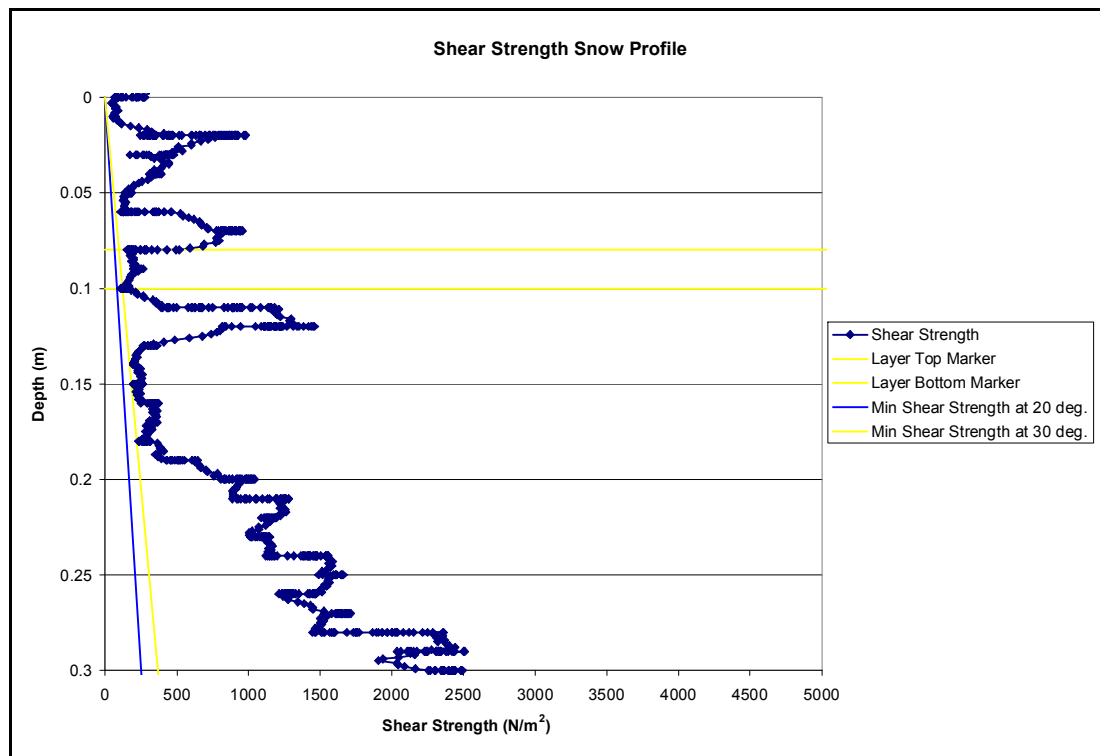


**Figure 7.30 a representative snow probe profile generated using power level 10, gear 1 and a 113mm diameter shear vane.**

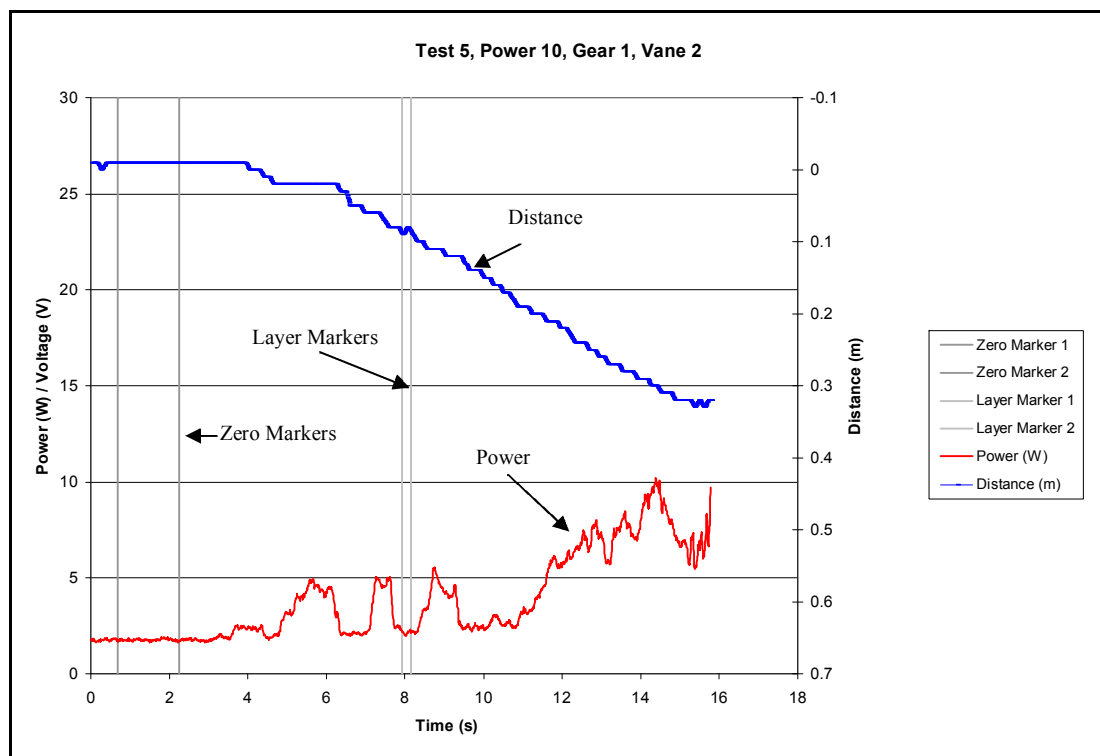


**Figure 7.31 the graph used to generate Figure 7.30 showing the penetration depth and the drill power input.**

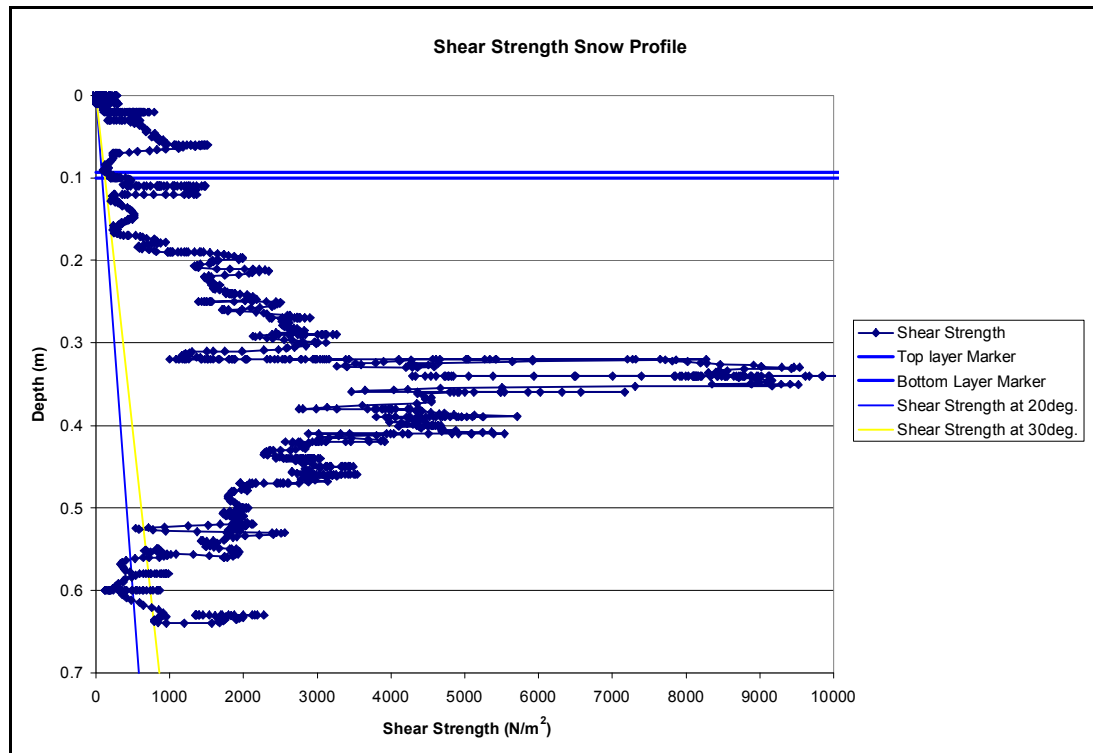


**Figure 7.32 a representative snow probe profile generated using power level 4, gear 2 and a 60mm diameter shear vane.**

Figure 7.32 has not changed significantly from the equivalent test Figure 7.25 on the 30<sup>th</sup>. The average rate of penetration was calculated to be 0.046m/s and 0.054m/s respectively. The no load rotational rate was far greater in these tests as the 2<sup>nd</sup> gear was used however the change in speed due to an applied torque was also much greater so it was difficult to estimate the approach angle in this case. The two rates are of comparable magnitude so no significant differences are present in the snow probe profiles for these tests.

A ratio of 0.4 exists between shear frame and snow probe results as shown in Figure 7.33 and Table 7.5. Standard deviations are of similar magnitude though the percentage variation is much greater for the snow probe results. This ratio is very low but also relatively constant.

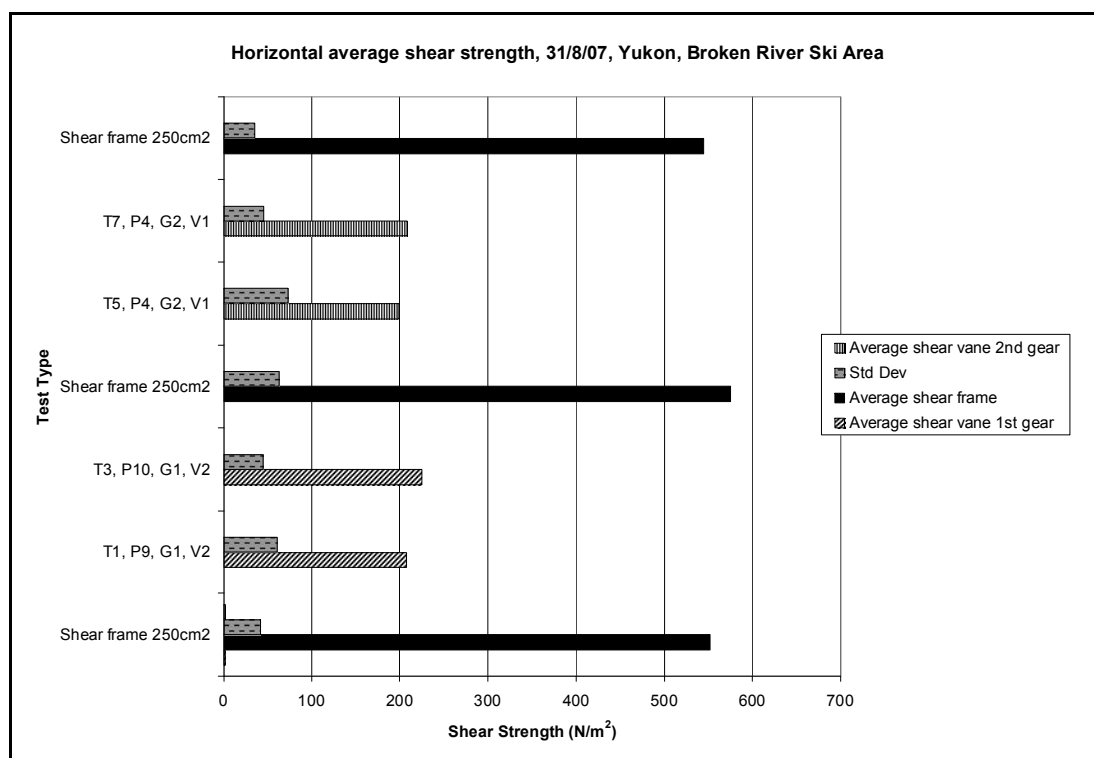


**Figure 7.33 averaged shear strength over 10 sample probes.**

The average rate of descent on this day of testing was lower than on any other day (Table 7.5). This seems to correspond to the clarity of the profiles done on this day. The minimum approach angle ratio was also lower than on any other day and the helix pitch was also only marginally above the vane height of 5mm. This suggests that the clarity of the results is more dependant on the rate of penetration while the C ratio is more dependant on the helix pitch and approach angle.

**Table 7.5 An estimate of the approach angle assuming a rotational velocity and constant penetration rate.**

31/08/2007 Broken River						
Test Name	Estimated Average Rate of Penetration	Vane Radius	Estimated RPM	Approach Angle	Helix Pitch	C
	m/s	m	rpm	Degrees	mm	
T1 & T2, P9, G1, V2	0.04	0.0565	70	6	9	0.4
T3 & T4, P10, G1, V2	0.05	0.0565	75	6	9	0.4
T5 & T6, P4, G2, V1	0.04	0.03	90	8	7	0.4
T7 & T8, P4, G2, V1	0.05	0.03	90	10	8	0.4

### 7.3.6.5 Broken River Ski Area, Yukon Basin, 2/9/2007

10-15cm of new snow settled on the test site in Yukon Basin. The test site was on a leeward slope so more snow accumulated here than in other locations. Once again testing was done within 5m of the previous tests. The hardness profile changed slightly to include the new snow (Figure 7.34). The profile does not go all the way to

ground and therefore does not include some of the deeply buried weak layers evident in previous days.

Layer distribution between the hand hardness profile in Figure 7.34 and the two snow probe profiles, Figure 7.35 and Figure 7.36 is slightly different. The distance between layers 2 and 3 is notably thinner in the snow probe profiles. This could be due to changes in snow depth created by differing wind directions. It could also be put down to errors in interpretation while recording the hand hardness profile.

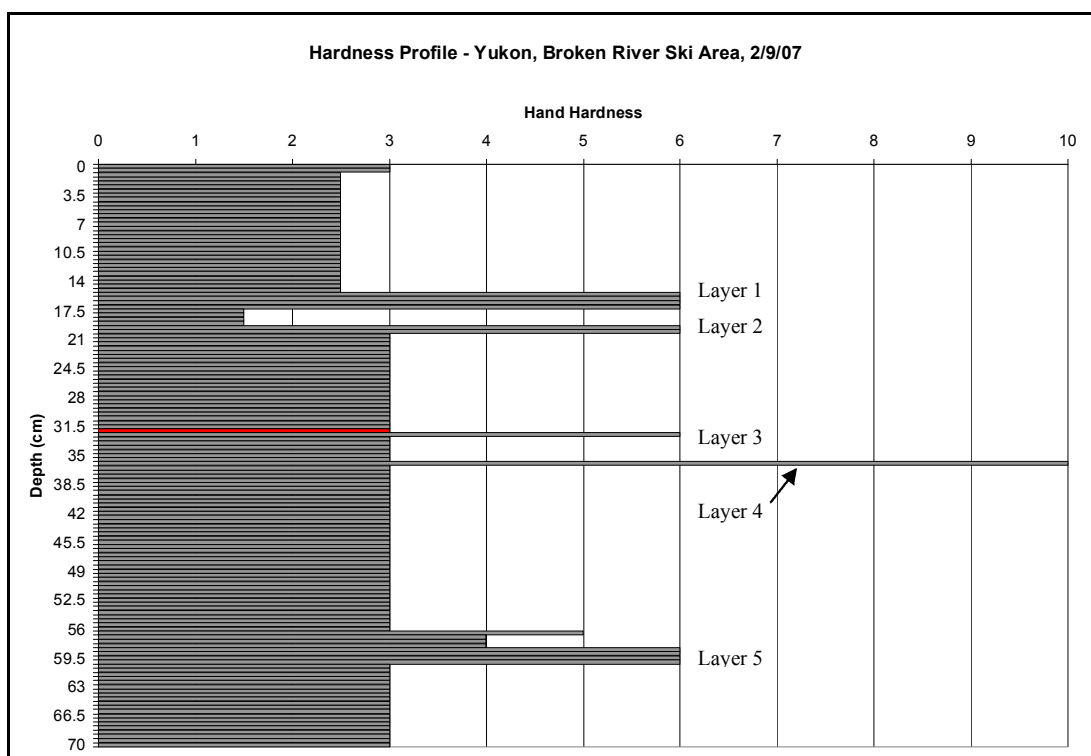


**Figure 7.34 a standard hand hardness profile with the layer tested with a shear frame indicated in red. Prominent layers have been named layer 1-5.**

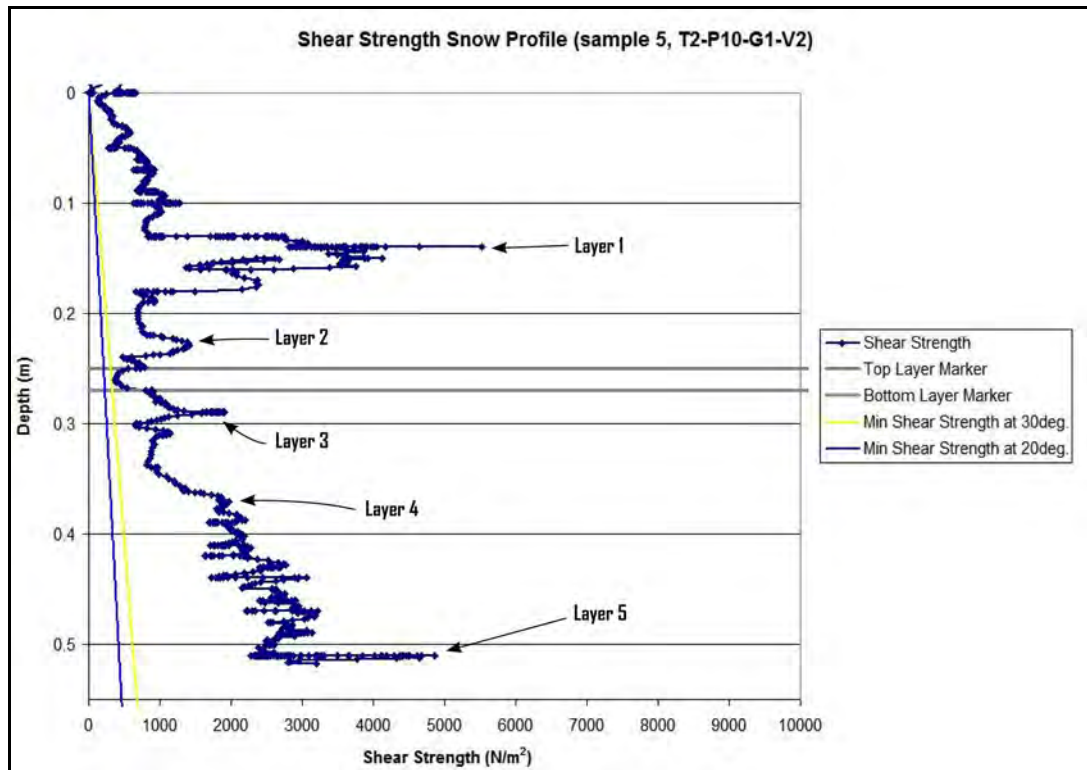


Figure 7.35 a representative snow probe profile generated using power level 10, gear 1 and a 113mm diameter shear vane.

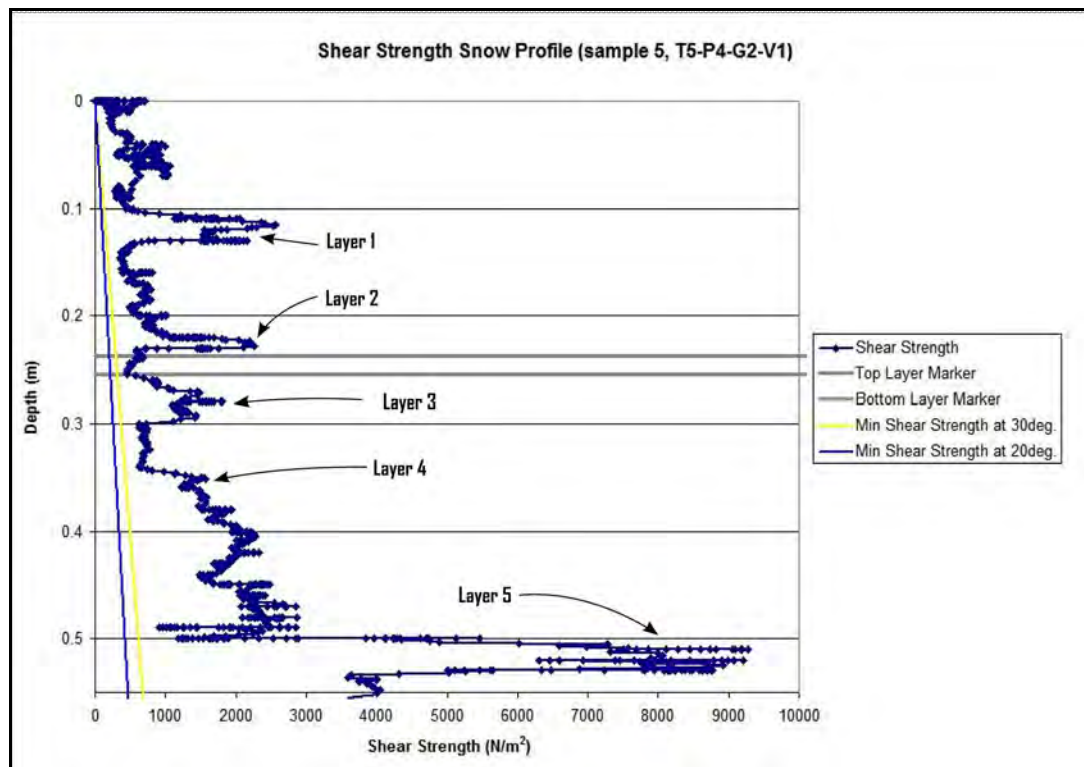
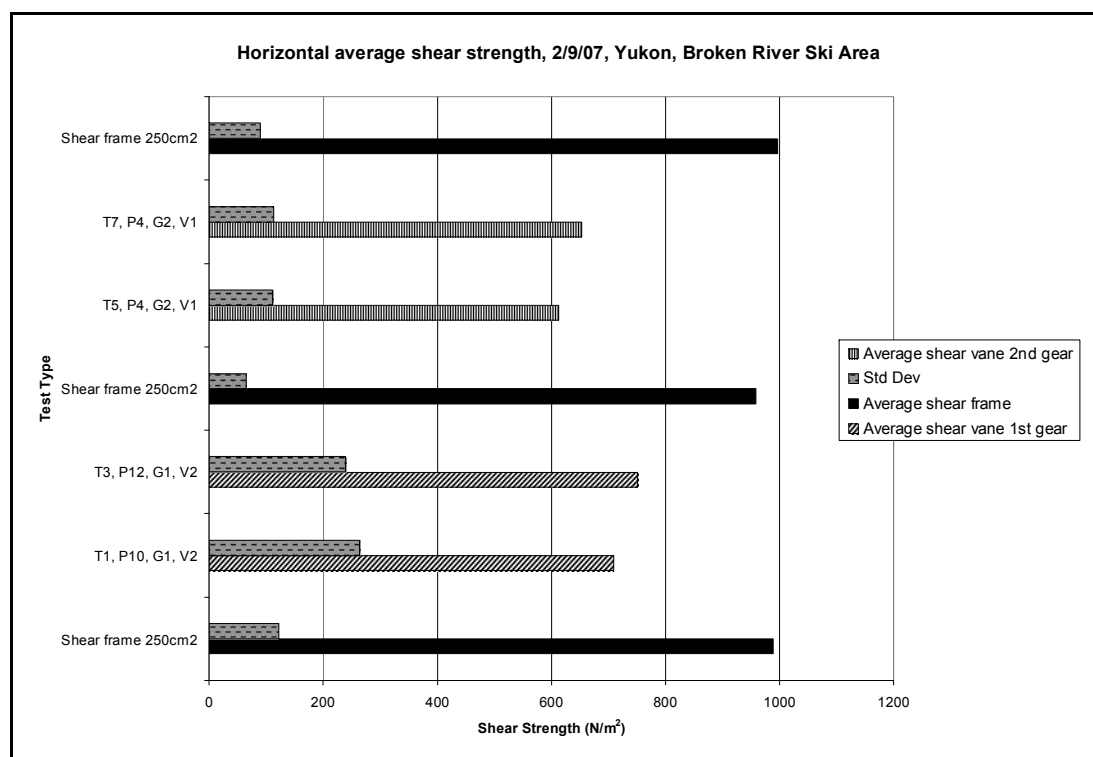


Figure 7.36 a representative snow probe profile generated using power level 4, gear 2 and a 60mm diameter vane size.

Both snow probe profiles fail to recognise a significant increase in shear strength at layer 4. This may be because the layer shown in the hand hardness profile as layer 4

was very thin. The snow probe profile also indicates an increase in shear strength below layer 4 which is not depicted in the hardness profile. This could be attributed to differing snow crystal structure between the layers. Although the layers have a similar hardness they may have quite differing shear strengths.

The ratio of the snow probe shear strengths to the shear frame shear strengths is on average 0.7 (Figure 7.37 and Table 7.6). This is higher than some of the previous ratios. Part of this is likely to be due to the fact that some of the test profiles had penetration rates of up to 0.083m/s. Some of the layers are not properly defined which means that weak areas may be missed. Although the layer of interest here was generally easily found, the shear strength was often higher with fewer data points in the weak section. This means that the average shear strength will be higher and the data scatter will also increase. This explains the significantly higher standard deviations in the snow probe results.



**Figure 7.37 averaged shear strength over 10 sample probes.**

Table 7.6 shows snow's penetration rates slightly higher than the previous test day. This corresponds to a slight reduction in clarity. The C ratio is also higher in those tests with a greater helix pitch.

**Table 7.6 An estimate of the approach angle assuming a rotational velocity and constant penetration rate.**

02/09/2007 Broken River						
Test Name	Estimated Average Rate of Penetration	Vane Radius	Estimated RPM	Approach Angle	Helix Pitch	C
	m/s	m	rpm	Degrees	mm	
T1 & T2, P10, G1, V2	0.06	0.0565	75	7	11	0.7
T3 & T4, P12, G1, V2	0.07	0.0565	80	8	13	0.8
T5 & T6, P4, G2, V1	0.06	0.03	90	11	9	0.6
T7 & T8, P4, G2, V1	0.05	0.03	90	11	9	0.7

### 7.3.7 Discussion

The results showed that although the shear strength profile shape was similar to the hardness profile shape, the actual shear strength values did not compare well with the shear frame results. Further more the ratio between the shear frame and snow probe results did not remain constant.

In an attempt to explain these inconsistencies, estimates of the approach angle, helical pitch, and average rate of penetration were calculated. It was only possible to calculate these in an approximate manner since rotational data was not recorded.

#### 7.3.7.1 Approach Angles and Related Variables

It is clear from the results in the preceding section that the rate of penetration, the helical pitch and the approach angle have a large impact on the results. The approach angle is defined as the angle of travel through the snow at the outer radius of the shear vane. In other words, the angle to the horizontal, of a helix scribed by a vane blade tip through the snow (See Figure 7.38). If this angle becomes very small (e.g. as the helix pitch tends to 0) the vane shears only a small amount of snow per rotation and the torque on the vane will get very low. In the extreme case of the approach angle being zero, the snow probe would record a very low shear strength created by the disturbed snow within the vane.

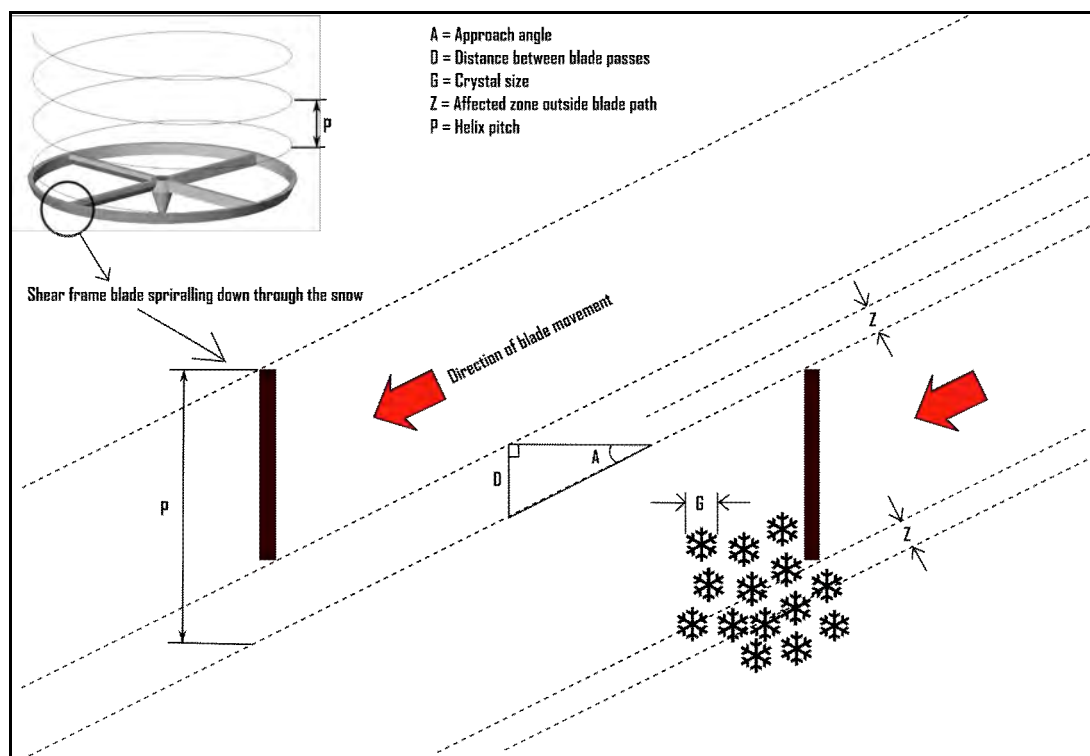


**Figure 7.38 Approach angle, affected zone and helix pitch.**

At the other end of the spectrum, if the approach angle becomes very large, the snow probe is likely to miss thin layers of interest. This in effect means fewer data points will be spread over a larger area leading to lower resolution.

As mentioned earlier, the minimum approach angle for which the vane always rotates through new snow can easily be calculated and is tabulated in Table 7.1. If the approach angle gets lower than this the snow being sheared by the vane would partially have been disturbed.

Although the results show that the approach angle is not directly related to the C ratio, it seems that the helical pitch is roughly related to the C ratio. Higher C ratios were experienced where the helical pitch was above 15mm (Figure 7.15, Figure 7.16, Figure 7.17, Figure 7.22 and Figure 7.26). Conversely, lower C ratios were calculated for tests with a helical pitch below 9mm (Figure 7.30, Figure 7.32 and Figure 7.36).

It should also be noted that the helical pitch is calculated from the average values of a set of 10 profiles and not individual profiles. The approach angle for each profile has been averaged over the whole profile but it would be more pertinent to calculate the angle continuously. However this can only be done if the rotation is also known continuously.



The clarity of a graph seemed to be more dependant on the rate of penetration than the helical pitch or approach angle. For example, tests done on the 31/8/2007 have a relatively low rate of penetration, C ratio and approach angle but all graphs had good clarity.

Profiles where a low C ratio was calculated are generally tests where great care was taken to move through the snow slowly and carefully. These profiles show a significant difference between peaks and troughs as well as large ratios between shear frame tests and snow probe tests. These large differences can be explained once again by thinking of the approach angle. In soft layers the shear vane experiences low levels of torque and consequently spins faster or closer to its no load speed. This has the effect of decreasing the approach angle, assuming that the rate of descent remains largely constant. Low approach angles are likely to create lower shear stresses as less snow is being disturbed. This explains the extra low troughs.

When the shear vane descends through an extra hard layer torque will increase and the rotational velocity will decrease. Again if we assume that the rate of descent remains relatively constant the approach angle will increase. This is likely to give higher torque readings as more snow is being disturbed during one rotation. One could argue that whether the vane rotates through new snow directly below the previous blade pass or at some distance below the previous blade pass makes little difference because it is all un-disturbed snow. However snow crystal can have quite strong inter-crystalline bonds and crystals can reach several millimetres. A pass several millimetres below the previous may therefore have to break more bonds than just those contained within the shear vane isolating ring. Following this argument it is logical for the torque reading to increase when the approach angle goes up. This theory goes some way to explaining the disproportionate peaks and troughs observed in some of the better profiles with low angle ratios.

The approach angle is by no means the only factor affecting the clarity of a profile. However it does seem to have a major impact on the results.

#### **7.3.7.2 Effect of different power levels and gears**

It appears that the power level does not have a huge impact on the clarity of the generated profile as long as the approach angle of the shear vane blades is

sufficiently low. Lower power levels have slower rotational speeds so a lower rate of penetration is required for better clarity.

Tests done in 2<sup>nd</sup> gear have higher rotational speeds so a lower power level was used. The no load speed is still greater than in any of the 1<sup>st</sup> gear tests (>100rpm) but it is also much more susceptible to changes in applied torque. On several occasions the shear vane came to a standstill on an especially hard layer. This was not believed to be a problem as the focus was on the weak layers not the strong layers.

#### **7.3.7.3 Correlation ratio C**

The ratios between snow probe strengths and shear frame strengths varied between 0.3 and 1. This shows that shear frame results were consistently higher than shear vane results as well as showing a large spread in the correlation ratio C. There appears to be a relationship between the helix pitch and the correlation ratio C. For example when the helix pitch is high (around 18mm) such as in the tests done on the 7/8/2007, the ratio C, between snow probe and shear frame results is very close. Conversely when the helix pitch is low (around 7mm) such as in tests done on 31/8/2007, the ratio C is also very low (around 0.4).

A balance seems to exist between increasing the helical pitch so as to increase the C ratio and decreasing the rate of penetration to increase the profile clarity.

#### **7.3.7.4 Vane Size**

Theoretically a larger shear vane would be less susceptible to small local variations but more susceptible to misalignment. The reverse would be true for small shear vanes. The results suggest that larger vanes give better profile clarity in soft snow. This follows on to suggest that shear vanes should be selected for size depending on snow density near the layer of interest.

## 8 Conclusions

The objective of this project was to validate the use of a rotational shear vane probe as a useful tool in avalanche safety as well as develop a simple robust mechanism to measure the torque.

These objectives have been achieved. A new system of measuring the torque from a rotating shear vane has been developed. The system has been taken through several cycles of design and testing. The design is robust and very reliable. No significant failures were encountered during testing.

The current model can produce a snow profile showing similar form to that of a conventional snow profile. This is easily repeatable. The profile clarity was found to be dependant on the approach angle, the helical pitch distance and the rate of penetration. It is believed that with further investigation into this dependency a far more accurate result can be achieved. Ideally a shear strength profile would be obtained from a test.

Work is continuing on the development of the probe. The addition of a rotation counter is currently believed to be the most vital development required to achieve greater accuracy. There is currently the possibility of forming a company around the snow probe with the potential for a patent application.

## **9 Future Research and Developments**

### **9.1 *Rotation Counter***

This would be a most useful addition to the snow probe. It would enable constant monitoring of the approach angle and enable implementation of an empirical correction system. This would significantly increase the accuracy of the output.

Further more this would greatly increase the accuracy of the torque measurements. Currently the two equations 5.1 and 5.2 are related by replacing the efficiency of the drill motor and the rotational velocity with a linear equation derived from a Prony brake test.

This relies on constant battery characteristics which is unlikely with such extreme temperature differences. One must therefore accept some error with this conversion. If the rotational speed were recorded the Prony brake test would only need to be used to determine an efficiency curve for the drill motor. This would in effect remove any variability associated with the battery and therefore increase the output accuracy.

This could be a relatively simple system similar to that used on a bicycle speedometer. A magnet or multiple magnets could be attached to a wheel which spins past a small solenoid. The changing magnetic field will create a signal with a frequency proportional to the wheels rotation.

### **9.2 *Depth Sensor***

Ideally a more accurate depth sensor would be used. The current 1cm resolution is greater than the size of some layers. However this can partially be corrected for by splining the depth vs time distribution to give a more continuous data stream.

The reflector is also less than ideal. A simple support could be added to hold the reflector above the snow during the calibration phase of a sample test. This would remove the error incurred by the operator holding the reflector during calibration.



**Figure 9.1 a simple addition to the existing reflector to make testing more accurate and easier.**

### **9.3 Calibration**

Some effort needs to be put into understanding why the prony brake test calibration curves are no longer straight. This may be as simple a problem as changing the program on the micro processor, however it may also be a hardware issue. This needs to be done by the technicians who built the circuits.

### **9.4 Industrial Design Aspects**

#### **9.4.1.1 Improved PDA user interface**

Currently the PDA is used as a data logger. Ideally the PDA unit would give real time results with all the processing being done out in the field. A simple wizard would allow the tester to input all the relevant probe characteristics and even select specific layers to get average shear strengths over several samples.

#### **9.4.1.2 Smaller Prototypes**

The current drill could easily be scaled down to a smaller version. 9V drills are readily available. It may also be possible to incorporate some or all of the circuits inside the drill housing.

#### **9.4.1.3 Added Utility**

One of the biggest problems mountainous regions are having at the moment is finding an easy way to collate data from many regions into a useful form. Much of the data is currently being noted down on paper. If the information is then to be transferred to a central location it must be digitalised. Most ski areas are reluctant to

make this extra effort since it is unlikely to benefit them. The snow probe could remove the need for the paper version by allowing all weather observations to be recorded on the PDA. For example:

- A temperature probe as a separate accessory to be place in the snow while shear testing us being done.
- Facility for weather observation, stomp depth etc. inputs on the PDA.

This would streamline all data collection making it easier for ski areas to look at historical data as well as simplify data sharing.

## 10 References

- Barnes, G. E. (2000). Soil Mechanics - Principles and Practice. London, MacMillian Press.
- Birkeland, K. W. (1995). "The Spatial Variability os Snow Resistance on Portential Avalanche Slopes." Journal of Glaciology **41**(137): 183-189.
- Birkeland, K. W., K. Kronholm, et al. (2004). "Changes in the shear strength and micro-penetration hardness of a buried surface-hoar layer." Annals of Glaciology **38**.
- Calding, L. and S. Odenstad (1950). "The Vane Borer." Proceedings Royal Sweedish Geotechnical Institute **No.2**.
- Cognar, S. (2007). Capacitec Snow Sonde. Avalanche Conference, Christchurch New Zealand.
- Conway, H. and J. Abrahamson (1984). "Snow stability index." Journal of Glaciology **30**(106): p321-327.
- Craig, R. F. (1995). Soil Mechanics. London, Chapman & Hall.
- Earl, W. M., H. Grey, et al. (1985). "Remote sensing of snow accumulation." Cold Regions Science and Technology **11**: 199-202.
- Evans, E. (2002). Development of a Rotational Shear Penetrometer. Mechanical Engineering. Christchurch, University of Canterbury: 55.
- Foehn, P. (2001). "Simulation of surface-hoar layers for snow-cover models." Annals of Glaciology **32**: 19-26.
- Jamieson, B. and C. D. Johnston (2001). "Evaluation of the shear frame test for weak snowpack layers." Annals of Glaciology **32**: 59-69.
- Johnson, J. B. and M. Schneebeli (1997). Snow Strength Penetrometer. United States.
- Keeler, C. M. and W. F. Weeks (1967). Some Mechanical Properties of Alpine Snow. US Army Cold Regions Research and Engineering Laboratory: 43.
- Keeler, C. M. and W. F. Weeks (1968). "Investigation into the mechanical properties of alpine snow-packs." Journal of Glaciology **7**(50): p253-271.
- Landry, C., K. Birkeland, et al. (2004). "Variations in snow strength and stability on uniform slopes." Cold Regions Science and Technology Snow And Avalanches **39**(2-3): 205-218.
- Logan, S., K. Birkland, et al. (2005). "Temporal changes in the spatial variability of shear strength and stability."

McClung, D. and P. A. Schaerer (1993). The Avalanche Handbook. Seattle, Mountaineers Books.

Perla, R. I. and M. J. Martinelli (1976). Avalanche Handbook. Washington DC, US Government Printing Office.

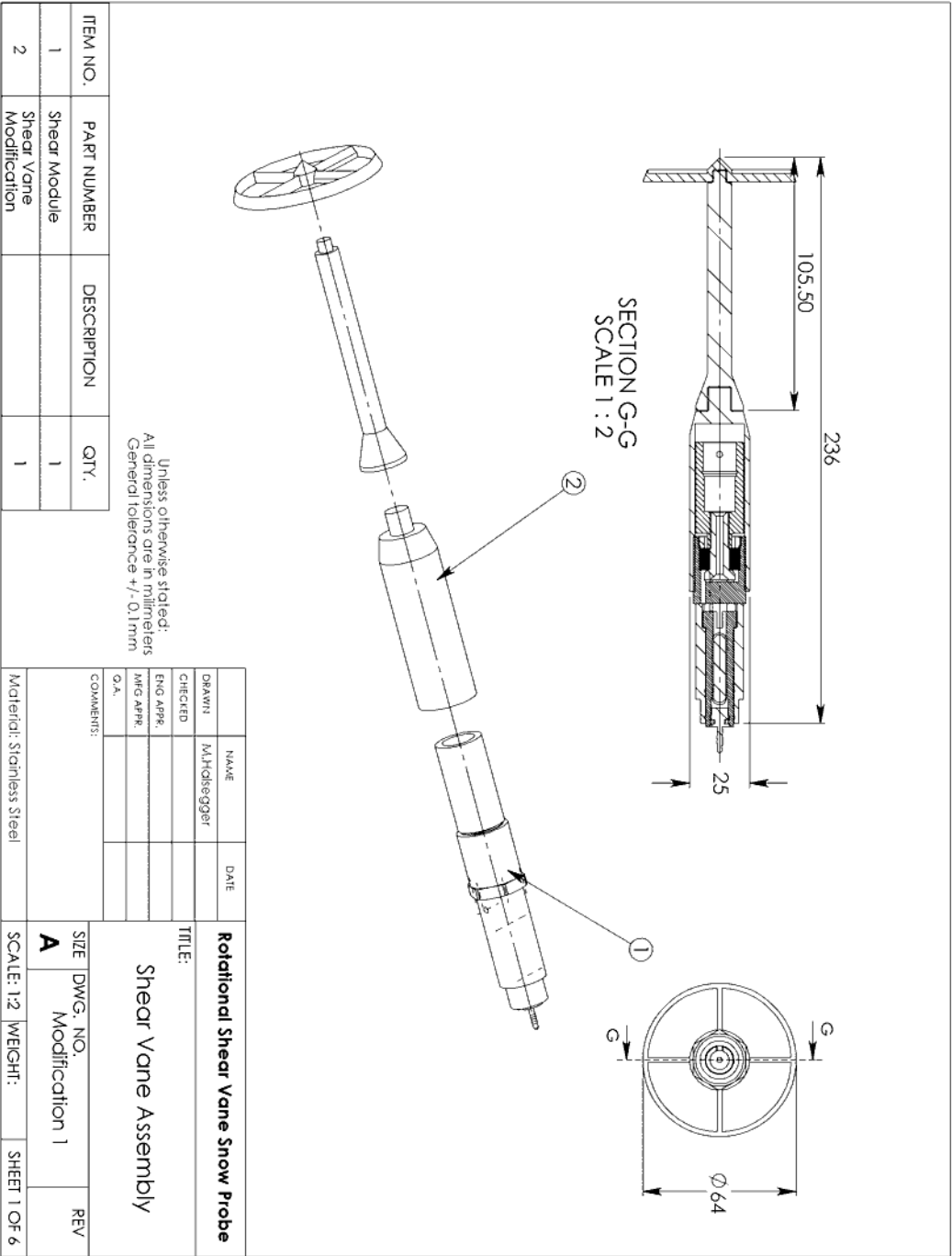
Schneebeli, M. and J. B. Johnson (1998). "A constant-speed penetrometer for high-resolution snow stratigraphy." Annals of Glaciology **26**: 107-111.

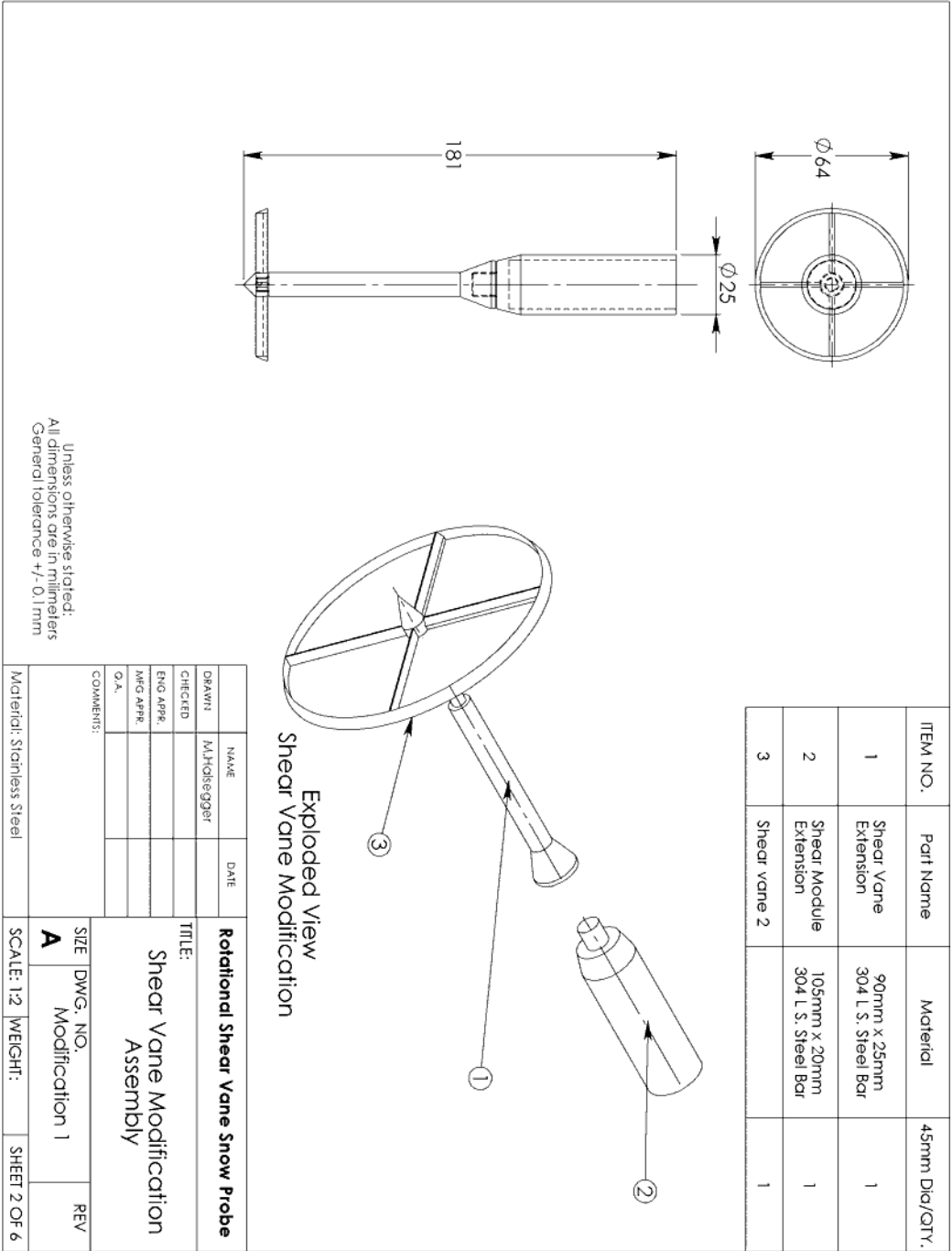
Schneebeli, M., C. Pielmeier, et al. (1999). "Measuring snow microstructure and hardness using a high resolution penetrometer." Cold Regions Science and Technology **30**(1-3): 101-114.

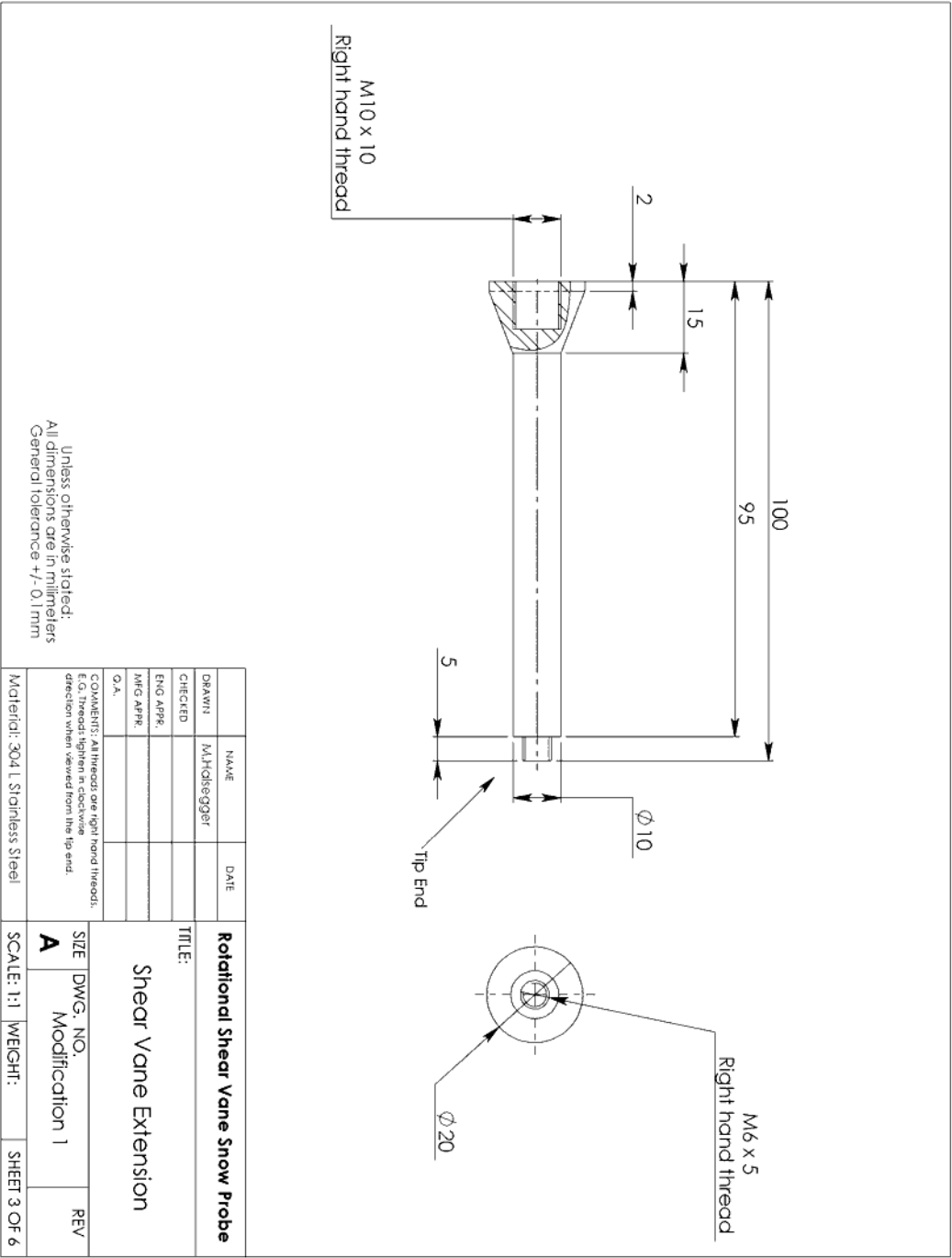
Schweizer, J., K. Kronholm, et al. (2006). "Spatial Variability - So What?" Unpublished.

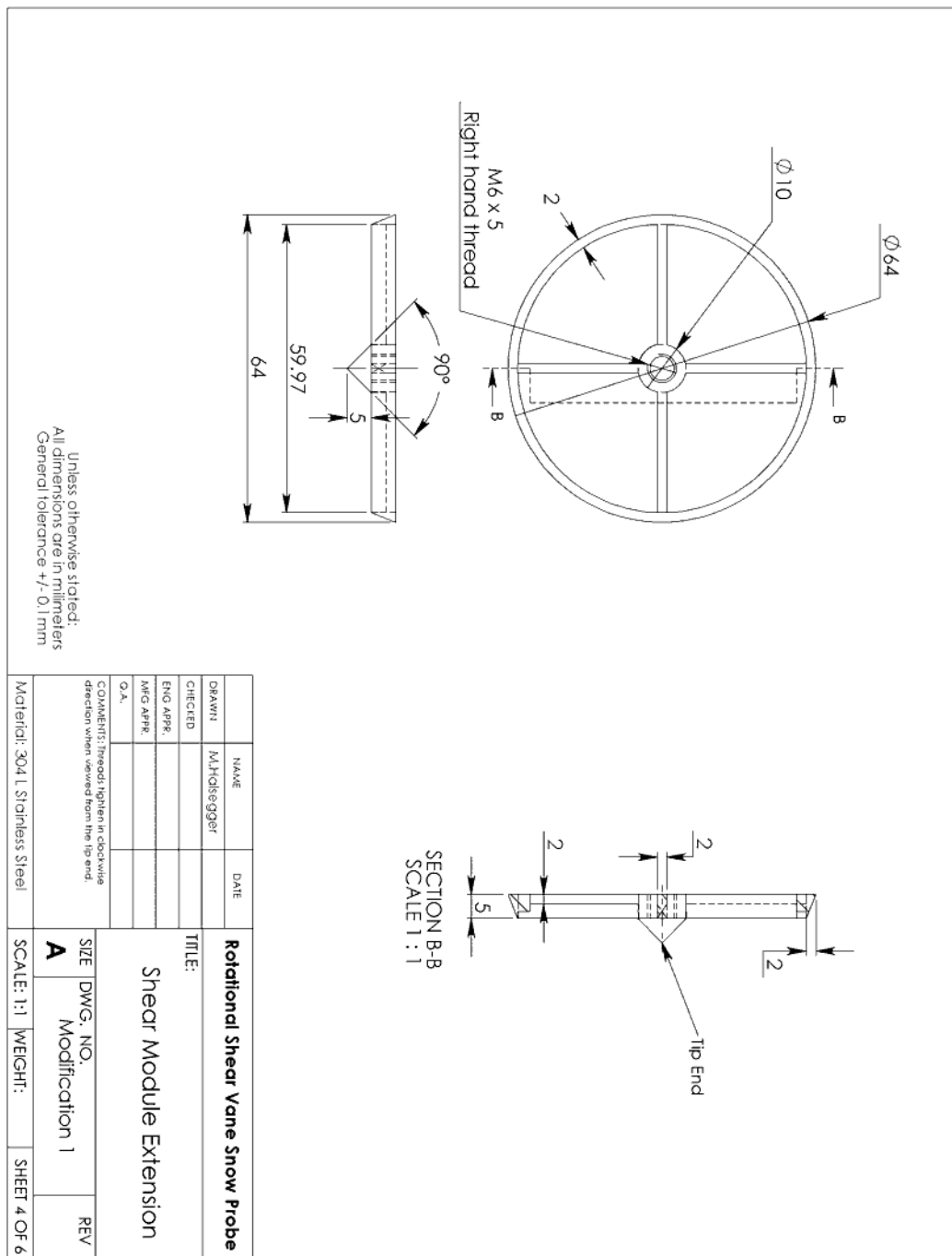


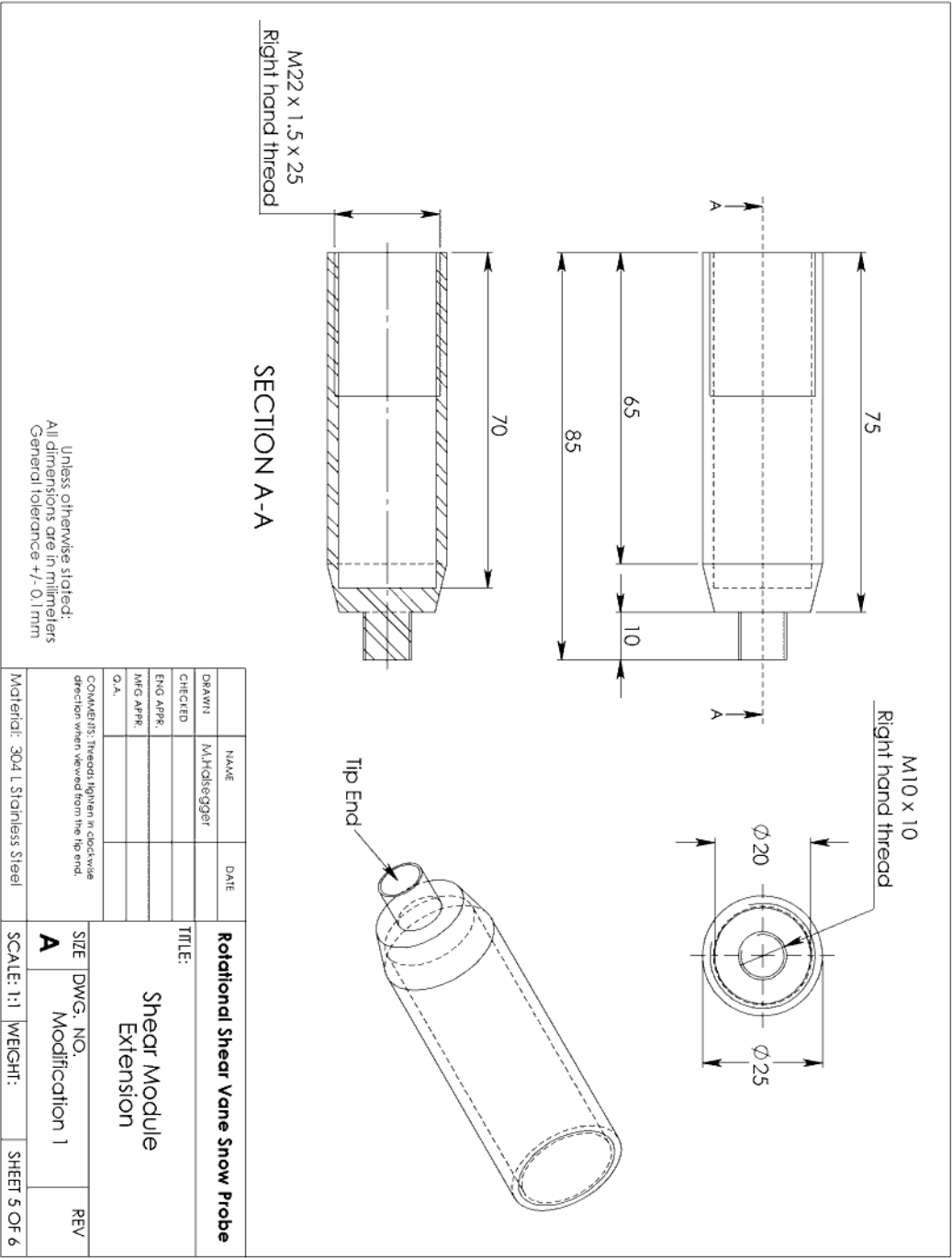
11 Appendix A: Prototype 1 Modification Drawings

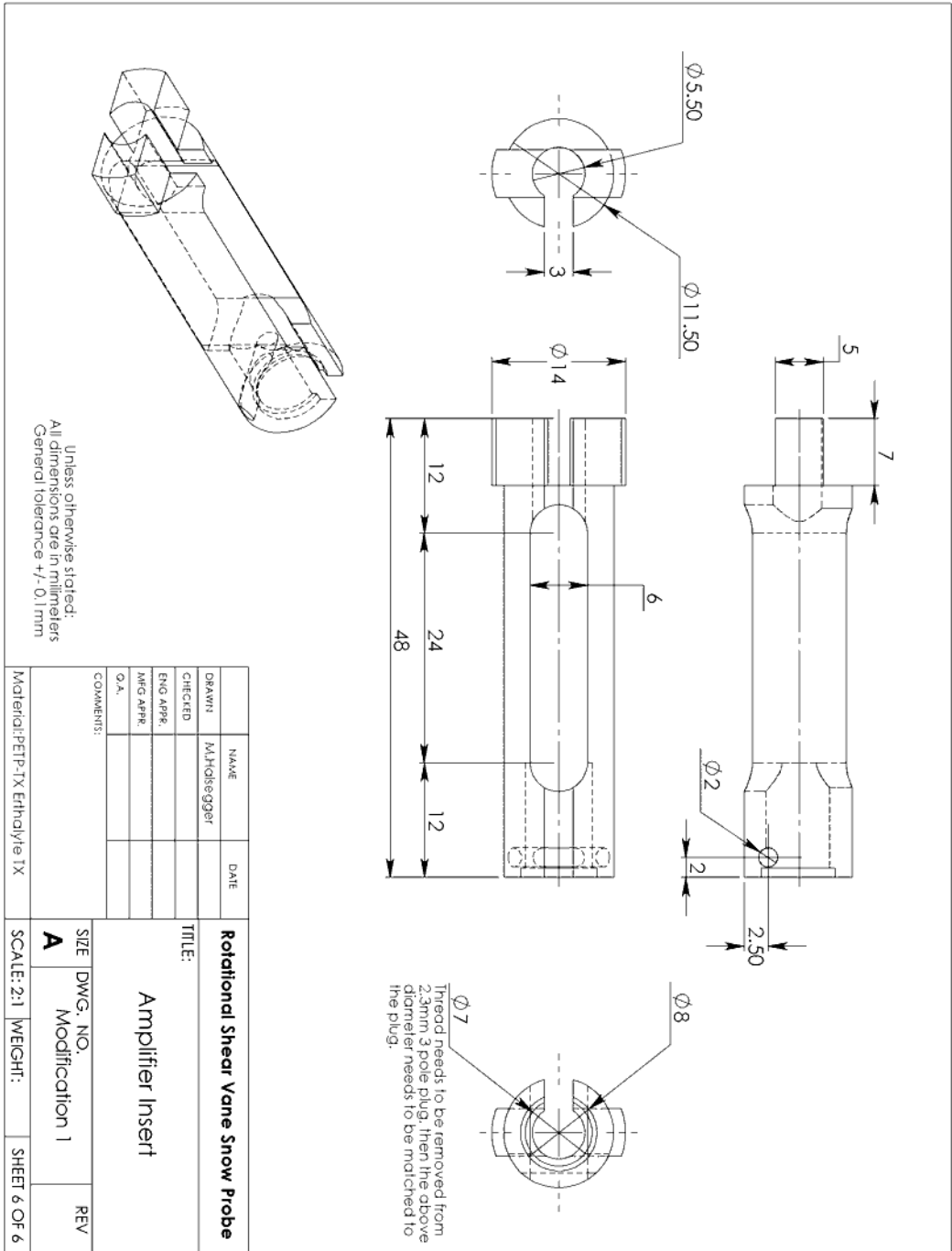


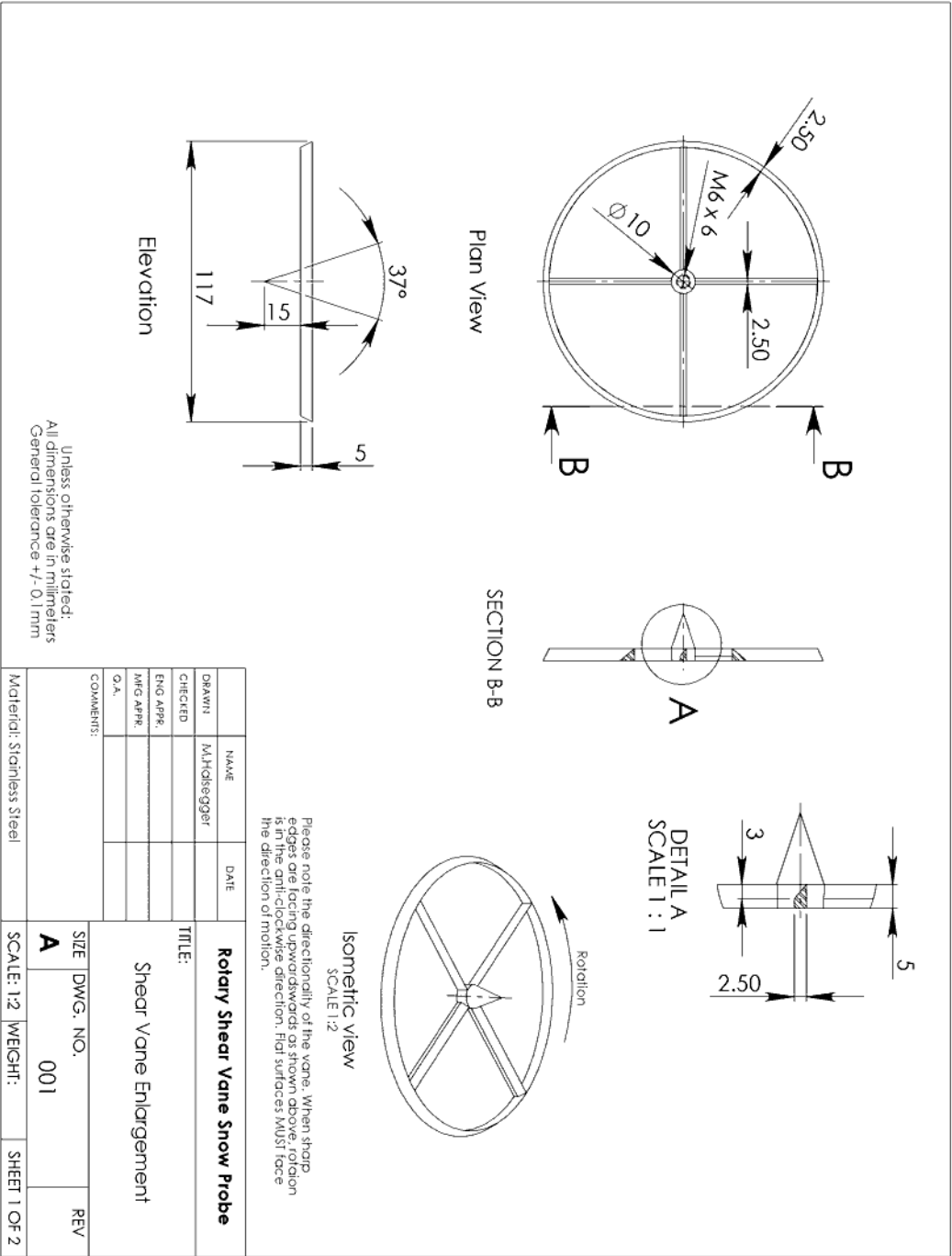


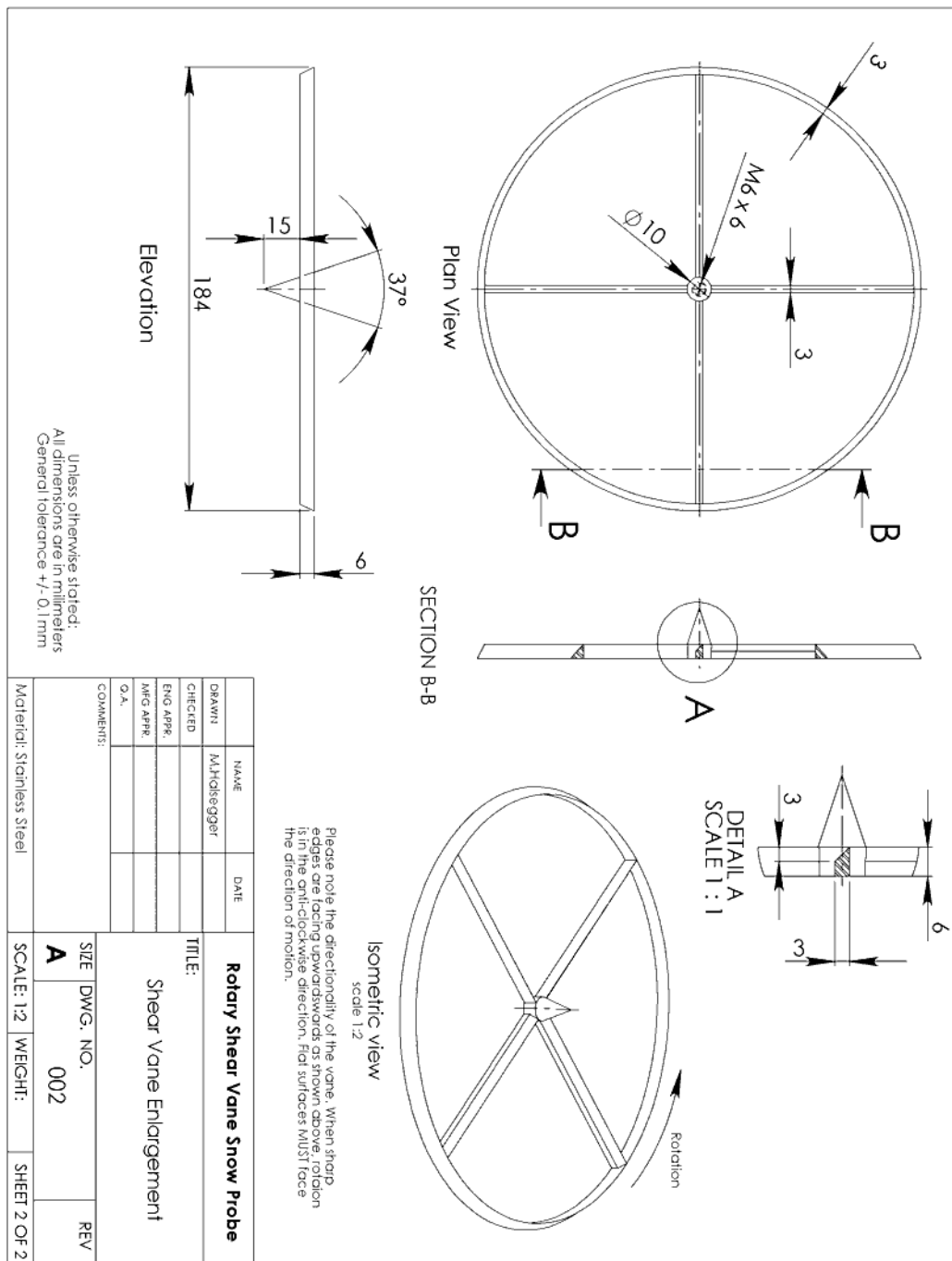














## **12 Appendix B: Electrical Diagrams**



## 13 Appendix C: Dell Axim PDA

### 13.1 *The Dell Axim X51v palm top*

The Dell Axim X51v, released late September 2005, featured Windows Mobile 2003 Second Edition with Windows Mobile 5.

The X51v featured:

- 3.7" VGA LCD screen with 16-Bit Colour and Portrait/Landscape Support
  - 3.7" VGA is around 2.22" x 2.96" = around 216.2162 pixels per inch
- Intel 2700G 3D multimedia accelerator with 16MB video RAM
- VGA-Out functionality (using an optional adapter cable), enabling the PDA to be connected to a monitor
- Built-In CompactFlash Type II expansion slot
- Built-In Secure Digital expansion slot
- Available Built-In 802.11b Wi-Fi Certification
- Standard Built-In Bluetooth 1.2 Compliance
- Long-range IrDA interface
- Up to 256MB Intel StrataFlash ROM with 64MB on-board RAM
- Microsoft Windows Mobile 5.0 software with Windows Media Player 10 Mobile (Upgradeable to Windows Mobile 6.0 with a downloaded ROM update)

The X51v has a VGA screen, a 624MHz processor, 256MB flash ROM.